(2)

David Taylor Research Center

Bethesda, Maryland 20084-5000

DTRC-87/SHD-1253-01 August 1988

Ship Hydromechanics Department
Research and Development Report

Vertical Plane Oscillation Experiments on a Series of Two-Dimensional SWATH Demi-Hull Sections

by

Christopher J. Hart
Robert O. Kiesow

DTRC-87/SHD-1253-01 Vertical Plane Oscillation Experiments on a Series of Two-Dimensional SWATH Demi-Hull Sections

MAJOR DTRC TECHNICAL COMPONENTS

CODE 011 DIRECTOR OF TECHNOLOGY, PLANS AND ASSESSMENT

12 SHIP SYSTEMS INTEGRATION DEPARTMENT

14 SHIP ELECTROMAGNETIC SIGNATURES DEPARTMENT

15 SHIP HYDROMECHANICS DEPARTMENT

16 AVIATION DEPARTMENT

17 SHIP STRUCTURES AND PROTECTION DEPARTMENT

18 COMPUTATION, MATHEMATICS & LOGISTICS DEPARTMENT

19 SHIP ACOUSTICS DEPARTMENT

27 PROPULSION AND AUXILIARY SYSTEMS DEPARTMENT

28 SHIP MATERIALS ENGINEERING DEPARTMENT

DTRC ISSUES THREE TYPES OF REPORTS:

1. **DTRC reports, a formal series,** contain information of permanent technical value. They carry a consecutive numerical identification regardless of their classification or the originating department.

2. **Departmental reports, a semiformal series,** contain information of a preliminary, temporary, or proprietary nature or of limited interest or significance. They carry a departmental alphanumerical identification.

3. **Technical memoranda, an informal series,** contain technical documentation of limited use and interest. They are primarily working papers intended for internal use. They carry an identifying number which indicates their type and the numerical code of the originating department. Any distribution outside DTRC must be approved by the head of the originating department on a case-by-case basis.

UNCLASSIFIED
SECURITY CLASSIFICATION OF THIS PAGE

REPORT DOCUMENTATION PAGE

1a. REPORT SECURITY CLASSIFICATION UNCLASSIFIED	1b. RESTRICTIVE MARKINGS
2a. SECURITY CLASSIFICATION AUTHORITY	3. DISTRIBUTION / AVAILABILITY OF REPORT Approved for public release; distribution is unlimited.
2b. DECLASSIFICATION / DOWNGRADING SCHEDULE	
4. PERFORMING ORGANIZATION REPORT NUMBER(S) DTRC - 87/SHD - 1253 - 01	5. MONITORING ORGANIZATION REPORT NUMBER(S)
6a. NAME OF PERFORMING ORGANIZATION David Taylor Research Center 6b. OFFICE SYMBOL (If applicable) Code 1562	7a. NAME OF MONITORING ORGANIZATION Naval Sea Systems Command
6c. ADDRESS (City, State, and Zip Code) Bethesda, MD 20084-5000	7b. ADDRESS (City, State, and Zip Code) Washington, D.C. 20362
8a. NAME OF FUNDING / SPONSORING ORGANIZATION NAVSEA 8b. OFFICE SYMBOL (If applicable) Code 55W3	9. PROCUREMENT INSTRUMENT IDENTIFICATION NUMBER
8c. ADDRESS (City, State, and Zip Code) Naval Sea Systems Command, NAVSEA 55W3 Washington, D.C. 20362	10. SOURCE OF FUNDING NUMBERS PROGRAM ELEMENT NO. 64567N; PROJECT NO.; TASK NO.; WORK UNIT ACCESSION NO. DN507113

11. TITLE (Include Security Classification)
Vertical Plane Oscillation Experiments on a Series of Two-Dimensional SWATH Demi-Hull Sections

12. PERSONAL AUTHOR(S)
Hart, Christopher J. and Kiesow, Robert O.

13a. TYPE OF REPORT	13b. TIME COVERED	14. DATE OF REPORT (Year, Month, Day)	15. PAGE COUNT
Final	FROM_____ TO_____	1988 June	133

16. SUPPLEMENTARY NOTATION

17. COSATI CODES			18. SUBJECT TERMS (Continue on reverse if necessary and identify by block number)
FIELD	GROUP	SUB-GROUP	SWATH; Two-dimensional Added Mass and Damping; Seakeeping

19. ABSTRACT (Continue on reverse if necessary and identify by block number)

Results of vertical plane oscillation experiments, conducted to determine the added mass and damping characteristics of a series of two-dimensional ~~(2-D)~~ demi-hull sections are presented. These sections represent variants of several Small Waterplane Area Twin Hull (SWATH) ship designs currently in development ~~by the U.S. Navy~~, including a fully offset strut, commonly referred to as the 'golf club.' Added mass and damping coefficients, along with radiated wave measurements, are presented for eight models, at two drafts and at least two amplitudes of oscillation. Comparisons between models illustrate the effects of lower hull geometry, strut offset, and strut thickness. Measured radiated wave data agree qualitatively with measured damping results, and are particularly interesting for the golf club hull forms where the radiated wave heights are asymmetric. Also presented are results of limited zero speed experiments on four models consisting of 3-D extensions added to the 2-D models. The coefficients are presented in the 2-D non-dimensionalization scheme, for comparative purposes. These results should provide information useful in the development and validation of SWATH seakeeping prediction programs for a range of hull forms.

20. DISTRIBUTION / AVAILABILITY OF ABSTRACT	21. ABSTRACT SECURITY CLASSIFICATION	
☐ UNCLASSIFIED/UNLIMITED ☒ SAME AS RPT ☐ DTIC USERS	UNCLASSIFIED	
22a. NAME OF RESPONSIBLE INDIVIDUAL Christopher J. Hart	22b. TELEPHONE (Include Area Code) 202-227-1554	22c. OFFICE SYMBOL Code 1562

DD FORM 1473, 84 MAR — 83 APR edition may be used until exhausted. All other editions are obsolete.

SECURITY CLASSIFICATION OF THIS PAGE
UNCLASSIFIED

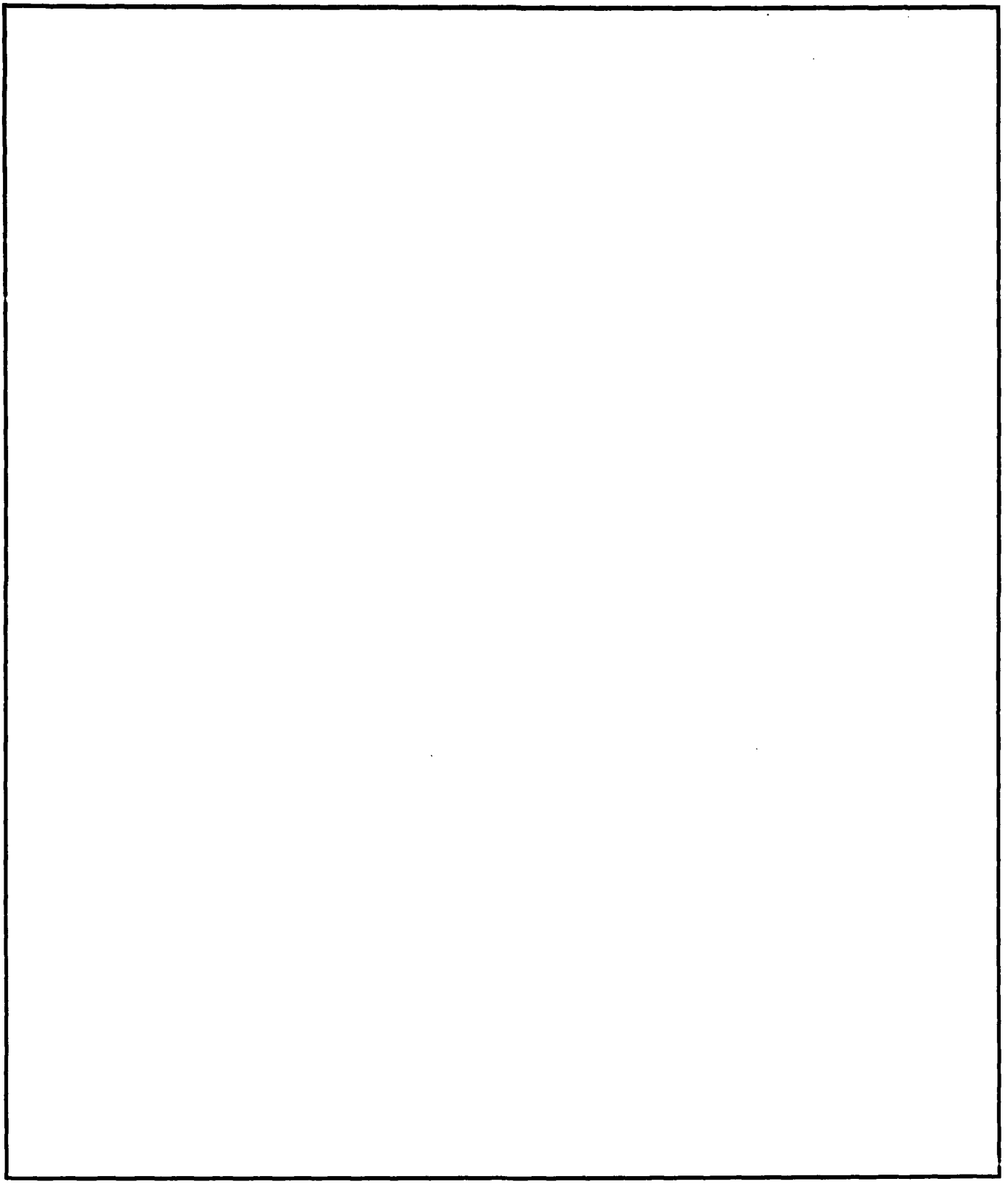

CONTENTS

CONTENTS (continued)

Page

FIGURES

FIGURES (continued)

Page

FIGURES (continued)

Page

FIGURES (continued)

Page

FIGURES (continued)

Page

FIGURES (continued)

Page

FIGURES (continued)

Page

TABLES

TABLES (continued)

Page

TABLES (continued)

Page

TABLES (continued)

Page

TABLES (continued)

Page

ABSTRACT

Results of vertical plane oscillation experiments, conducted to determine the added mass and damping characteristics of a series of two-dimensional (2-D) demi-hull sections are presented. These sections represent variants of several Small Waterplane Area Twin Hull (SWATH) ship designs currently in development by the U.S. Navy, including a fully offset strut, commonly referred to as the 'golf club.' Added mass and damping coefficients, along with radiated wave measurements, are presented for eight models, at two drafts and at least two amplitudes of oscillation. Comparisons between models illustrate the effects of lower hull geometry, strut offset, and strut thickness. Measured radiated wave data agree qualitatively with measured damping results, and are particularly interesting for the golf club hull forms where the radiated wave heights are asymmetric. Also presented are results of limited zero speed experiments on four models consisting of 3-D extensions added to the 2-D models. The coefficients are presented in the 2-D non-dimensionalization scheme, for comparative purposes. These results should provide information useful in the development and validation of SWATH seakeeping prediction programs for a range of hull forms.

ADMINISTRATIVE INFORMATION

This task was performed for and funded by the Naval Sea Systems Command, Code 55W3, in support of the Common Hull SWATH contract design effort under Program Element No.64567N, Task Area S1803536. This work was conducted at the David Taylor Research Center (DTRC)* under work unit number 1-1235-788-15. It was administered by the SWATH Office, DTRC Code 1235, of the Ship Systems Integration Department and carried out by the Special Ship and Ocean Systems Dynamics Branch, Code 1562.

INTRODUCTION

SWATH ships are of interest to the US Navy because of their markedly reduced motion characteristics in rough seas. The Navy's first SWATH ship class will be the T-AGOS 19, for which a construction contract was awarded in November 1986. The lower hull of the T-AGOS 19 has what are referred to as *"producible oval"* cross-sections, composed of semi-circular and flat components. Several

* Formerly the David W. Taylor Naval Ship Research and Development Center (DTNSRDC). The name was officially changed to David Taylor Research Center (DTRC) in September, 1987.

alternative lower hull cross-sections have been proposed for both the T-AGOS 19 class and other SWATH designs, including the Common Hull SWATH. Shipbuilder representatives on the T-AGOS 19 design team proposed a rectangular lower hull cross-section with radiused corners (referred to in this report as *Shipbuilders*, or *Radiused Rectangle*). Another SWATH configuration that has been considered for naval and oceanographic applications, has the strut positioned outboard of the lower hull centerline such that the outside edge of the strut is tangent to the outside edge of the lower hull (resembles the shape of a golf club). Referred to as the *Golf Club*, this configuration has been of interest to ship operators, since the offset strut might facilitate over-the-side operations. In order to assess the impact on seakeeping performance of these and other proposed lower hull and strut designs, the effects of these variations on the detailed hydrodynamic characteristics, such as *added mass* and *damping* , needed to be determined.

Therefore, experiments were conducted at the David Taylor Research Center on a series of eight models to study the effects of lower hull shape, strut thickness, strut offset, and draft on the two-dimensional vertical plane added mass and damping characteristics. In addition to the two-dimensional (2-D) tests, follow-on experiments were conducted on several 3-D hull sections, composed of adding 3-D extension pieces to the ends of the 2-D models. These tests involved several test-setups and conditions, including zero speed heave as well as some forward speed heave and pitch oscillations for some models. While the details and results of the 3-D experiments are being reported separately, the zero speed heave oscillation results are presented in this report in the same form as the two-dimensional data for comparative purposes. The oscillation data should provide information useful in the development and validation of SWATH seakeeping prediction programs for a range of hull forms.

DESCRIPTION OF MODELS

Eight models were tested, representing design variations of a two-dimensional single-hull cross section of the SWATH T-AGOS 19 hull form. These models, constructed of solid pine and built to a

1/30th scale, were designated A through H, as shown in Fig.1* . The *true ellipse* (A), the *full golf club* (G), and the *radiused rectangle* (H) were one piece models, while the remaining models (B-F) were of two piece design. The *semi-circle* (lower hull) variations (B,C and D) consisted of a common lower hull onto which either a full strut or a thin strut was vertically mounted. The *half golf club* sections (E and F) were similar in that they also shared a common portion of the lower hull, except that both the full strut and the thin strut included a section of the lower hull and were attached horizontally (see Fig. 1).

The models were all 5 ft (152.4 cm.) in length and were geometrically similar in several other dimensions including: major and minor axes of all lower hulls, strut height and strut thickness (depending on which of two struts), the overall model height, and the design draft. Principal dimensions common to all models are shown in Fig. 2. Table 1 provides additional characteristics of the individual models, as they were tested. As shown in Fig. 2, there were essentially three different lower hull shapes: the *true ellipse* (A), the *semi-circle with flats* (models B-G), and the *shipbuilder's* or *radiused rectangle* (H). A fourth lower hull configuration, model (C), consisted of model (B) with the addition of a bilge keel. The bilge keel ran the length of the bilge radius, and had the following model scale dimensions: 0.75 in (1.91cm) width, 0.225 in.(0.57 cm) base, and 5 ft.(152.4 cm.) length.

The effects of strut thickness and offset were investigated on the SWATH T-AGOS-like lower hull (semi-circle with flats) using models (D-G). The strut thickness on both *thin-strut* models (D and F) was equal to half the thickness of the full strut (Fig.2). On model (D), the thin strut was positioned along the center of the model. The strut centerline positions for the half-golf club models E and F, were offset 1.35 in (3.43 cm) and 1.8 in (4.6 cm) outboard of the lower hull centerline, respectively. These offsets correspond to a position halfway between the lower hull centerline and the strut centerline of a full golf club design (of the same strut thickness), hence the term *half-golf club*.

* Detailed model drawings are on file as SWATH T-AGOS R&D Models, NAVSEA Drawing # 55W32-9294, pps 1-3.

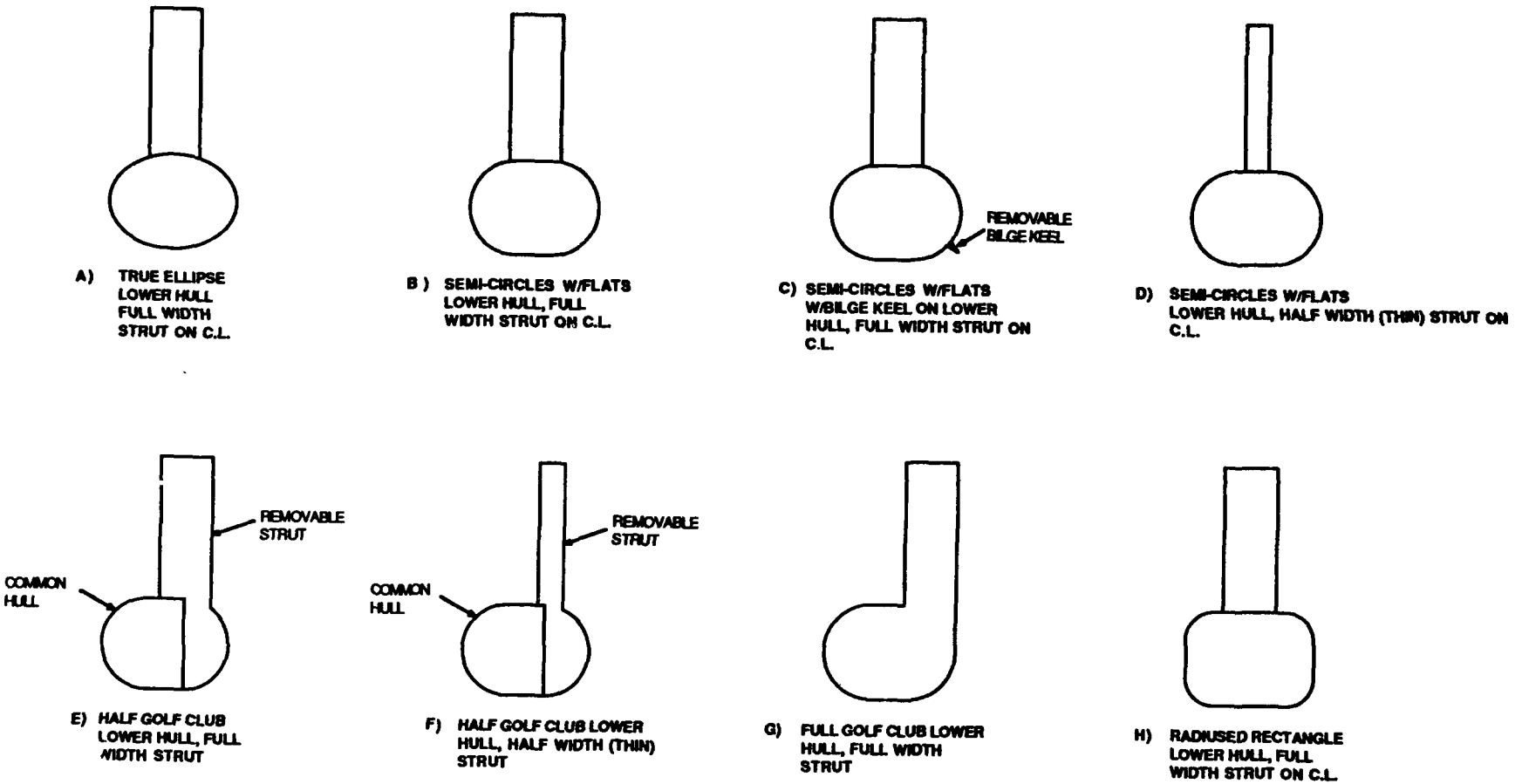

Fig. 1. Cross-sections of the two-dimensional models tested.

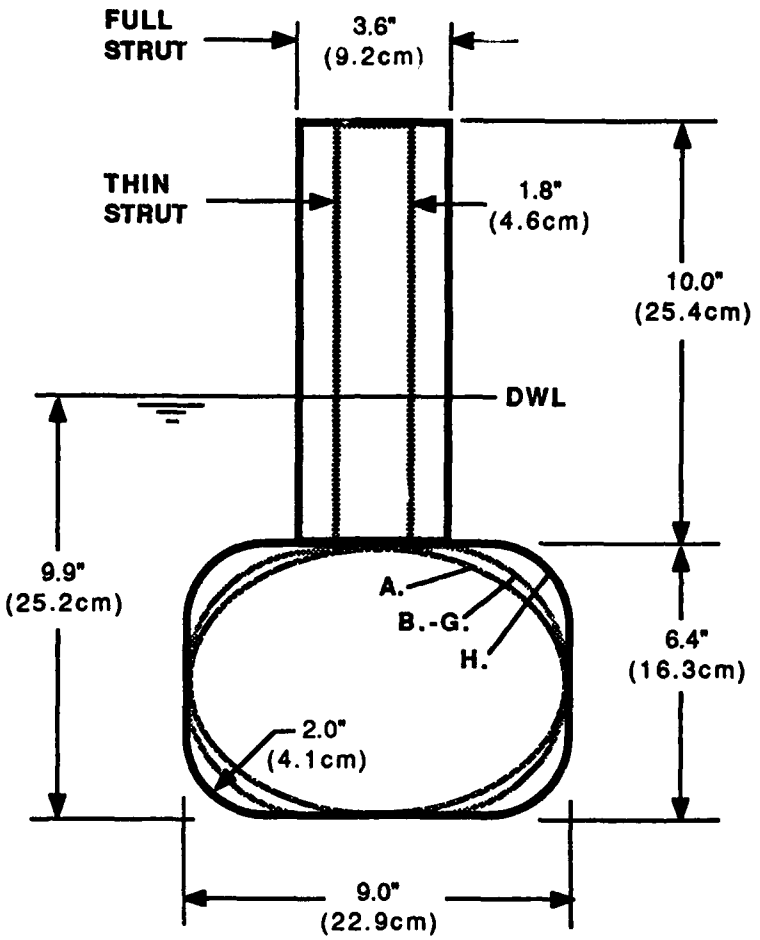

Fig. 2. Common dimensions of model cross-sections.

Table 1. Model characteristics (a) in English units, (b) in SI or metric units.

Table 1a. English units.

Model	Name	Design Displacement lbs.*	Deep Draft Displacement lbs	Sectional Area at Design Draft sq.in.	Waterplane Area calc.*, sq. in.	Restoration Coefficient calc.*, lbs/ft	Restoration Coefficient Measured,lbs/ft
A	True Ellipse	125.9	133.8	58.2	216.0	93.4	95.2
B	Semi-Circle,Full Strut	132.8	140.8	61.4	216.0	93.4	96.5
C	Semi-Circle, w/ Bilge Keel	133.1	141.2	61.5	216.0	93.4	96.5
D	Semi-Circle,Thin Strut	119.1	123.1	55.1	108.0	46.7	48.1
E	Half Golf Club	133.4	141.3	61.7	216.0	93.4	94.8
F	Half Golf Club, Thin Strut	119.5	123.5	55.3	108.0	46.7	48.4
G	Full Golf Club	137.5	145.5	63.6	216.0	93.4	95.8
H	Shipbuilder's (rad. rectangle)	144.3	152.3	66.8	216.0	93.4	96.0

**Calculated using model dimensions*

Table 1b. SI units.

Model	Name	Design Displacement kg*	Deep Draft Displacement kg	Sectional Area at Design Draft sq.cm.	Waterplane Area calc.*, sq.cm.	Restoration Coefficient calc.*, kg/m	Restoration Coefficient Measured,kg/m
A	True Ellipse	57.1	60.7	375.7	1393.5	139.0	141.7
B	Semi-Circle,Full Strut	60.2	63.9	396.3	1393.5	139.0	143.6
C	Semi-Circle, w/ Bilge Keel	60.4	64.0	397.3	1393.5	139.0	143.6
D	Semi-Circle,Thin Strut	54.0	55.8	355.4	696.8	69.5	71.6
E	Half Golf Club	60.5	64.1	398.1	1393.5	139.0	141.0
F	Half Golf Club, Thin Strut	54.2	56.0	356.6	696.8	69.5	72.1
G	Full Golf Club	62.4	66.0	410.4	1393.5	139.0	142.6
H	Shipbuilder's (rad. rectangle)	65.5	69.1	430.7	1393.5	139.0	142.8

Calculated using model dimensions

EXPERIMENTAL SET UP AND TEST PROCEDURE

Tests were conducted at The David Taylor Research Center on Carriage 5 with the carriage positioned at mid-station in the High Speed Basin.* The High Speed Basin is 2968 ft.(904 m) in length, 21 ft.(6.4 m) wide, and 16 ft.(4.9 m) deep, except for a *shallow water* section 1169 ft.(356 m) long at the West end with a depth of 10 ft.(3 m). A sketch of the experimental set-up is shown in Fig.3a. The Mark II oscillator,† equipped with a scotch yoke was used to provide a forced sinusoidal heaving motion for the various 2-D SWATH models tested. The oscillator was mounted to an "A" frame, which in turn was mounted to the vertical tow rails on Carriage 5. A power hoist on the vertical rails allowed the entire oscillator/A-frame assembly to be raised and lowered to adjust the waterlines for the various draft conditions tested. The oscillation frequency was varied by changing the voltage input to the oscillator's motor, and ranged from 1 to 14 radians per second. The oscillation amplitudes ranged from .25 to 1.5 inches (0.64 to 3.81 cm) and were changed by adjusting the motion of the crank inside the scotch yoke mechanism.

* For more details on either the High Speed Basin or Carriage 5 see Besch, P.K. and Callanen, S. E., "Ship Performance Department Facilities Handbook," DTRC Technical Memorandum, SPD-TM-15-83-137 (Mar 1983)

† For details on the Mark II vertical oscillator see DTRC Reference Drawings E-1127-1 through -5.

To maintain a two dimensional flow during oscillation, end plates were fashioned and mounted to the main aluminum channel, at the base of the oscillator shaft (see Fig.3a and 3b). These plates were designed to minimize the fluid flow around the ends of the models and to prevent transverse wave reflections in the basin. Although they oscillated with the models, the end plates were mounted above the gage assembly and sufficiently spaced apart from the ends of the models (≈0.25 in or 0.64 cm) so as not to interfere with force measurements. The end plates also channeled the propagating waves to two wave probes positioned 3.5 ft.(106.7 cm.) from either side of the centerline of the model. The model itself, was positioned transversely in the basin, allowing the waves to propagate towards the ends of the basin and thus effectively preventing any reflected wave interference during data collection. The effectiveness of the end plates can be seen in the photograph (Fig.4) of model G during oscillation test.. It should be noted that the golf club models and bilge keel (model C) were oriented in the tank such that the *inboard* side of the hull faced toward the East end of basin (as shown for model G, in Fig 3a). And therefore, the West side of the model was the side to which the strut was offset and the side with the bilge keel (corresponding to *outboard* if both hulls were present). This is only significant to the radiated wave height data for the asymmetric hull forms.

The vertical forces were measured using a pair of four inch *block gages* ganged together, as shown in Fig. 3b. A 200 lb capacity block gage (Z1) was positioned directly below the oscillator shaft, and a 50 lb capacity block gage (Z2) was positioned directly above the center of the model. The purpose of using two gages was to provide better resolution of the force measurements over the broad range of test conditions (i.e., different models, drafts, amplitudes, frequencies...). Appropriate ballast weights were added to each model, as needed, to achieve the proper displacement for the design or the deep draft test conditions.

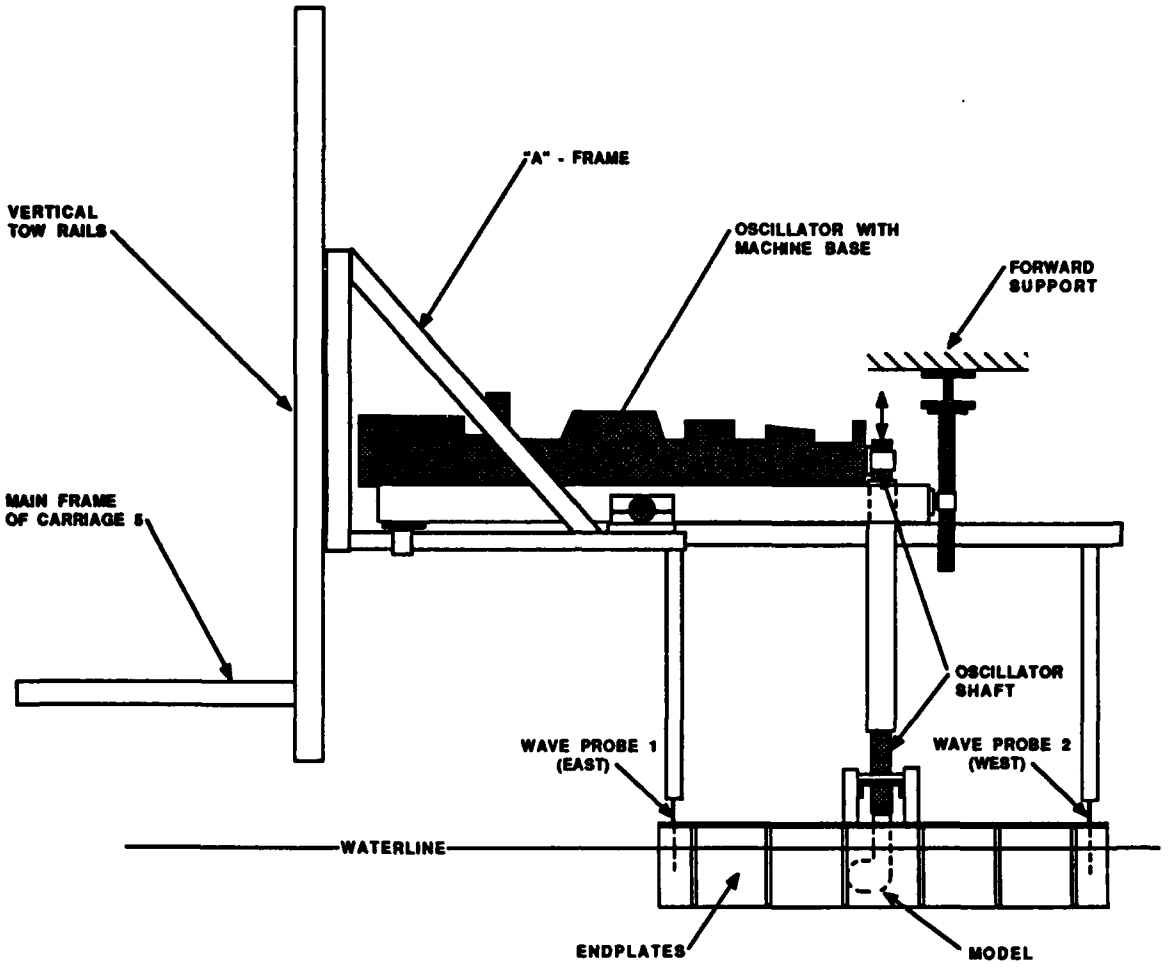

Fig. 3a. Mark II Oscillator and model set-up.

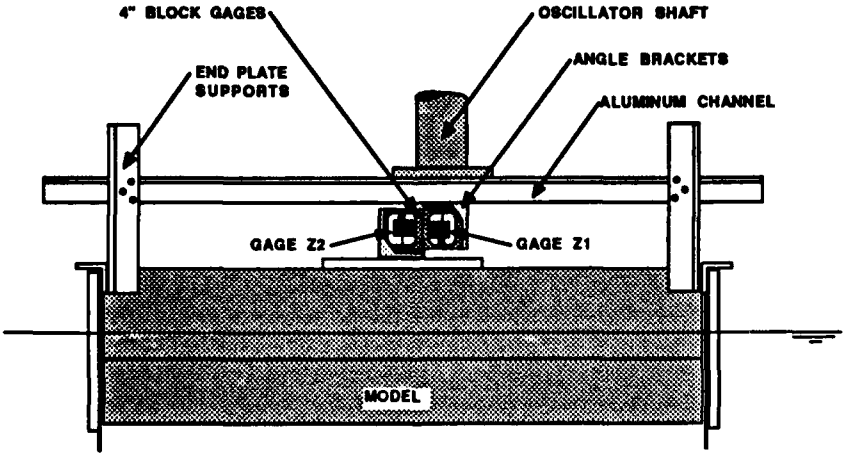

Fig. 3b. Block gage and end plate set-up.

Fig. 3. Test set-up for two-dimensional oscillation experiments.

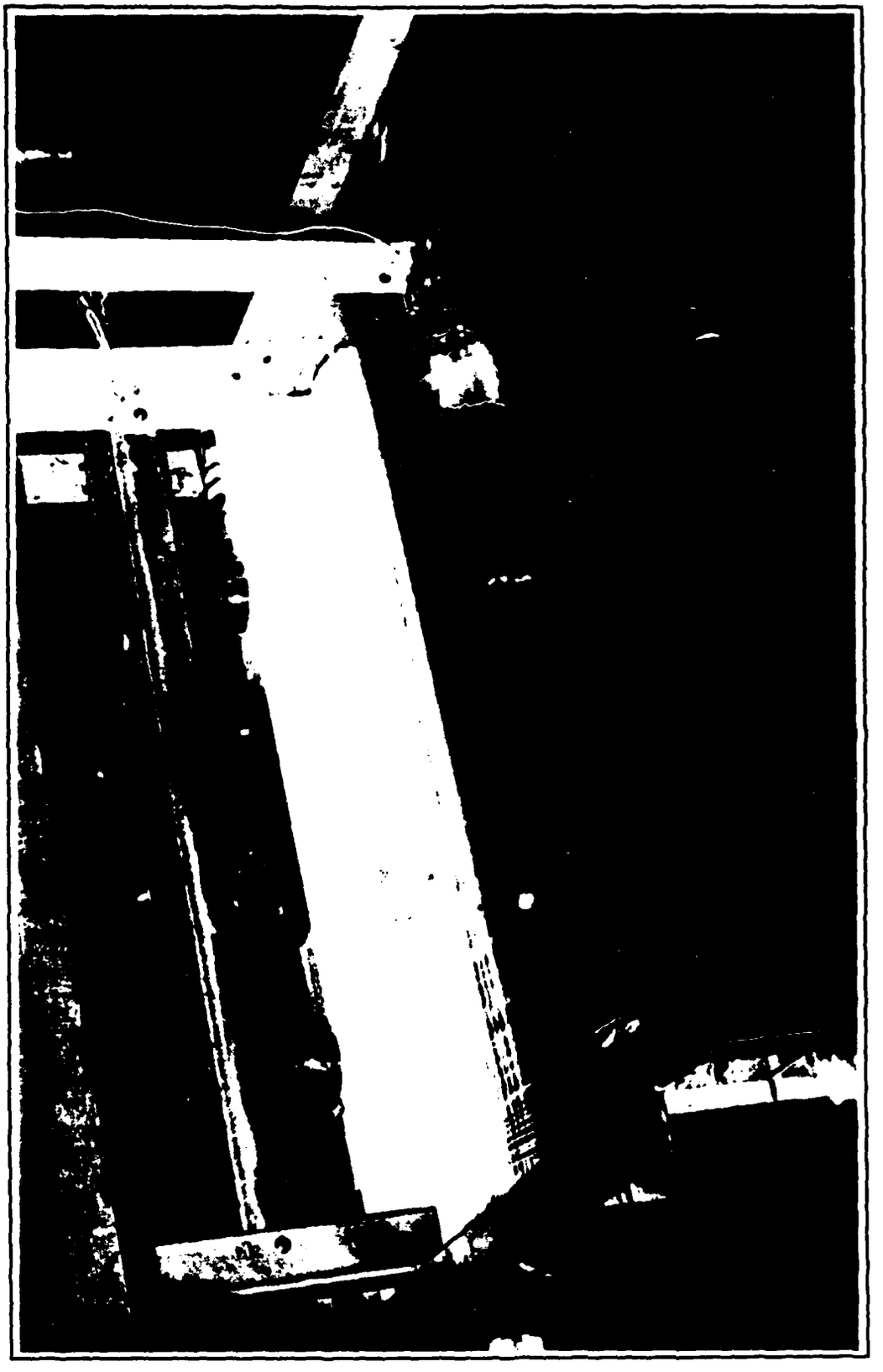

Fig. 4. Photograph of model G, full golf club (run#537) deep draft, 0.5 inch (1.27 cm) amplitude, at a model frequency of 10 radians/second.

TEST PROGRAM

Presented in Table 2 is an overall test matrix of the various combinations of drafts and amplitudes for which oscillation tests were conducted on each of the eight models. All models were tested at two drafts corresponding to a design (T–AGOS equivalent) draft of 9.9 in (25.2 cm) or 24.75 ft (ship scale), and a deep draft of 10.9 in (27.7 cm) or 27.25 ft (ship scale). Oscillations at each draft were also performed at various amplitudes to provide a measure of the linearity of the response. Typically, two oscillation amplitudes (0.5 and 1.0 in., model scale) were investigated. Additional drafts and amplitudes were tested on some models, as noted in Table 2. For each model at each test condition listed, oscillations were typically performed at ten discrete frequencies ranging from 1 to 14 rad/sec. model scale. This corresponds to a full scale frequency range of 0.2 to 2.6 rad/sec, and was chosen to represent reasonable encounter frequencies of a ship traveling at speeds between 0 and 10 knots. Static heave tests were also conducted on each model to determine the heave restoration coefficient (i.e. to verify calculated waterplane areas).

Table 2. Matrix of test conditions.

Model	Name	OSCILLATION AMPLITUDES, Inches (cm)					
		DESIGN DRAFT			DEEP DRAFT		
		0.5 (1.27)	1.0 (2.54)	1.5 (3.81)	0.5 (1.27)	1.0 (2.54)	1.5 (3.81)
A	True Ellipse	X	X		X	X	
B	Semi-Circle,Full Strut*	X	X	X	X	X	
C	Semi-Circle, w/ Bilge Keels	X	X		X	X	
D	Semi-Circle,Thin Strut	X	X		X	X	
E	Half Golf Club**	X	X		X	X	
F	Half Golf Club, Thin Strut	X	X		X	X	
G	Full Golf Club	X	X	X	X	X	X
H	Shipbuilder's (rad. rectangle)	X	X		X	X	

** Amplitude of .25" was also tested at design draft*
***Also tested at 1" shallow draft, with .5"amplitude*

DATA COLLECTION AND REDUCTION

A list of the specific measurements, including the location, calibration factor, and type of transducer used in data collection is given in Table 3. The selection of the force range for the two block gages was based on predictions from the SWATH Seakeeping Evaluation Program. An Analogic 15 bit

analog–to–digital (A–D) converter and an Interdata Model 70 computer were used to digitize and record time histories of all channels to magnetic tape at a rate of 60 samples/channel/second. Analog signals were filtered prior to digitizing using 15 hz, 6 pole Butterworth low pass filters, and were monitored throughout the test using an analog strip chart recorder. At each test condition, 10 oscillations were recorded and

Table 3. Measurement Transducers.

Channel	Measurement	Transducer	Calibration units/volt	Location
1	Heave Displacement	String Potentiometer	.4 in/v (1 cm/v)	oscillator shaft
2	Heave Force, Z1	200 lb cap. 4"Block Gage	40 lb/v (178 N/v)	4 in. off longitudinal center
3	Heave Force, Z2	50 lb. cap. 4"Block Gage	5 lb/v (22.2 N/v)	longitudinal center
4	Radiated Wave Height 1	Resistance Wire Probe	.7 in/v (1.8 cm/v)	3.5 ft. from model
5	Radiated Wave Height 2	Resistance Wire Probe	.7 in/v (1.8 cm/v)	3.5 ft. from model

harmonic analysis provided the heave force amplitude and phase, from which the hydrodynamic coefficients were determined as follows.

The equation of motion for pure, uncoupled heave is given by:

$$a\ddot{z} + b\dot{z} + cz = F(t) \qquad [1]$$

where a = virtual mass = M+m

M = displaced mass of the model,

m = hydrodynamic or added mass,

b = damping coefficient (dimensional),

c = restoration or spring constant,

and $\ddot{z}$, $\dot{z}$, z = heave acceleration, velocity and displacement, respectively.

F(t) = the force required for the oscillator to impose harmonic heave motion on the model. This motion can be described in the positive z - direction as follows:

$$z = z_0 \cos(\omega t)$$

$$\dot{z} = -z_0 \omega \sin(\omega t) \qquad [2]$$

$$\ddot{z} = -z_0 \omega^2 \cos(\omega t)$$

where

z_0 = heave amplitude

ω = frequency in radians/second.

Since the magnitude and phase of the heave force can be determined by harmonic analysis, the hydrodynamic coefficients can be determined by separating the heave force into *in–phase* and *out–of–phase* force components;

$$F(t) = F_{z_0} \cos(\omega t + \varepsilon) \qquad [3]$$

where:

F_{z_0} = heave force amplitude, and

ε = phase angle between motion and response.

By expanding Eq. 3 and separating into sine and cosine terms:

$$F(t) = (F_{z_0} \cos \varepsilon) \cos(\omega t) - (F_{z_0} \sin \varepsilon) \sin(\omega t) \qquad [4]$$

or

$$F(t) = F_{in} \cos(\omega t) - F_{out} \sin(\omega t) \qquad [5]$$

where the in–phase and out–of–phase force components are defined as:

$$F_{in} = F_{z_0} \cos \varepsilon \qquad \text{(in–phase component)} \qquad [6]$$

$$F_{out} = F_{z_0} \sin \varepsilon \qquad \text{(out–of–phase component).}$$

Substituting Eqs. 5 and 2 into Eq. 1; and separating sine and cosine terms, the acceleration and velocity dependent coefficients, a and b can be solved for, such that:

$$a = \frac{F_{in} - cz_0}{(-z_0 \omega^2)} \qquad [7]$$

and

$$b = \frac{F_{out}}{z_o \omega} \quad . \qquad [8]$$

While the restoration coefficient c, for a wall sided body can be calculated from,

$$c = \rho \, g \, A_{wp} \qquad [9]$$

where ρ = water density

g = gravitational constant (=32.155 ft/s^2 or 9.801m/s^2 at DTRC)

and A_{wp} = waterplane area,

the values of c obtained from static displacement tests were used in the calculations, in order to improve accuracy (since model waterplane areas were slightly higher than design). The values of c determined by both methods are included in Table 1.

The hydrodynamic *added mass* and *damping* coefficients α and δ, were determined from Eqs. 7 and 8 and nondimensionalized as follows:

$$\alpha_{1,2} = \frac{a - (M_{1,2})}{M} \qquad [10]$$

and $$\delta_{1,2} = \frac{b}{(M\omega)} \qquad [11]$$

where the subscripts 1 and 2 refer to the data based on force measurements from the Z1 and Z2 gages, respectively, and

M_1, M_2 = mass of model and test apparatus as seen by the Z gages (Note: $M_1, M_2 \neq M^*$).

The measured radiated waves heights from probes 1 and 2 were divided by the heave oscillation amplitude to define *radiated wave transfer functions* , TF1 and TF2, respectively. The coefficients and transfer functions were plotted versus a *nondimensional frequency parameter* , $\frac{\omega^2 B}{2g}$ or $\frac{kB}{2}$ where:

---

* During the tests, ballast weights were added to the models to make the test apparatus weight, M1 (as seen by the Z1 Gage), equal to model displacement. However, since calculations of model displacement at the time of tests were preliminary, slight differences may be observed between M1 and M (in the Appendices), due to final corrections to the model displacements.

k= wave number, and

B= *beam* or *breadth* of the lower hull cross section.

This nondimensionalization of α, δ, and *frequency* follows the notation used in several previous 2-D oscillation experiments conducted at DTRC, such as those performed by Jones* and Stahl†.

PRESENTATION AND DISCUSSION OF RESULTS

All nondimensional added mass and damping coefficients, along with the radiated wave transfer functions are presented in Appendices A-H, for models A-H respectively. The results are given in both graphical and tabular form for all drafts and oscillation amplitudes tested. Each appendix is organized as follows. Plots of $\alpha_{1,2}$ (alpha1, and alpha2), $\delta_{1,2}$ (delta1 and delta2) and TF1 and TF2 are presented versus kB/2 on a single page for each combination of draft and amplitude tested. The plots are followed by the corresponding data presented in tabular form.

It should be noted that not all data points were plotted. For some test conditions, data were taken over a greater frequency range. Although all data are included in the tables, coefficients at the highest and lowest frequencies (kB/2>1.2, kB/2<.02) were left off of the plots due to scatter/uncertainty. At the low frequency end (kB/2<.02), the uncertainty is due to the fact that the measured heave force is predominantly the restoration or buoyant force, and the inertial and hydrodynamic components of the measured forces are small. At the high frequency end (kB/2>1.2) the uncertainty is due to observations made during the test, that transverse wave reflections were building up between the end plates which may have adversely affected the results. Also note that in the appendices, some of the α_2 and δ_2 coefficients do not extend as far out in the frequency range as α_1 and δ_1. This is *not* due to an uncertainty problem, but rather is due to the fact that the heave forces exceeded the maximum load capacity of the Z2 gage (since it is the more

* Jones, H. D., "Experimental and Theoretical Comparison of Added Mass and Damping of Two-dimensional Twin Hull Shapes," DTRC Test & Evaluation Report 348-H-06 (Dec 1970)

† Stahl, R., "Experimental Determination of Heave Added Mass and Damping of Two-dimensional Bulbous Cylinders at the Free Water Surface," DTRC Ship Performance Dept. Evaluation Report 516-H-01 (Mar 1973)

sensitive of the 2 gages). Details of the various sources of error and measurement uncertainty are discussed further in the *Experimental Accuracy* section of the report.

While it was not practical to cross–plot all of the combinations of results (models, drafts and amplitudes), several cross-plots of the various model results are presented in the following sections to illustrate the major trends in the data. These major trends are given in Figs. 5 to 9 and discussed in the following sub-sections:

- Effects of Amplitude and Draft (comparing models B and G)
- Effects of the Lower Hull Shape (comparing models A, B, C and H)
- Effects of the Strut Offset (comparing models B, E and G)
- Effects of the Strut Thickness (comparing models B, D and F).

The coefficients alpha1 and delta1 are used in the cross–plots since they cover the full frequency range and agreement between Z1- and Z2-based coefficients is good throughout the frequency range.

EFFECTS OF AMPLITUDE AND DRAFT

The effects of oscillation amplitude on added mass and damping are illustrated in Fig. 5a for model (B), the semi-circle with flats, and in Fig. 5b for model (G), the full golf club. For both models the added mass coefficients are quite linear while the damping coefficients exhibit some dependence on the amplitude of oscillation. The damping coefficient for model B is clearly non-linear with amplitude, however the magnitude is relatively small in comparison with the golf club or thin strut models.

Figures 6a and 6b present the variation of added mass and damping coefficients with *draft* for models B and G at an oscillation amplitude of 1.0 in.(2.54 cm). Figure 6a shows that for model B, an increase in draft reduces both the non-dimensional added mass and damping coefficients over the frequency range. The reduction of the added mass is more significant at the low frequency end, while the reduction in damping is more pronounced at higher frequencies. The decrease in the nondimensional added mass, in this case, is approximately equal to the increase in mass at the deep draft. Therefore, the *dimensional* added mass does not appear to be significantly affected by draft. The reduction in damping

(dimensional), on the other hand, appears to be more significant, and may be due partly to the lower wavemaking at the higher frequencies (see wave TF's in App.B).

Model G, tested at 3 drafts, was the only model tested at a shallow draft condition. Figure 6b shows that the effect of decreasing draft is to increase the added mass at low frequency but reduce it at high frequency. This trend is similar to the comparison of a golf club to non-golf club section at the same draft (see Fig.9). The damping increased with decreasing draft over the frequency range. The large damping at shallow draft is expected due to increased wave making at the free surface. This can also be confirmed by observing the radiated wave height transfer functions (given in Appendices).

EFFECTS OF LOWER HULL SHAPE

Added mass and damping coefficients are presented in Fig. 7 for the true ellipse (A), semi-circle (B), the semi-circle with bilge keel (C) and the radiused rectangle (H), to illustrate the effects of lower hull shape. Note that while the strut shape and overall dimensions are the same for each model, the actual displacements vary between them by nearly 13%. Since the hydrodynamic coefficients are nondimensionalized by displaced mass, this should not significantly affect comparisons between the models (i.e. the trends cited below are consistent for the dimensional coefficients, as well).

The models A, B and H exhibit expected trends, with the ellipse having lowest added mass and damping (over most of the frequency range), and the shipbuilder's (model H) having the largest (not counting model C). It should be noted that model C,* the semi-circle w/bilge keel, has the largest added mass and damping coefficients of the four non-golf club hull forms. As can be seen in Fig. 7, the addition of the bilge keel to model B significantly raised the added mass and damping over the entire frequency range. The magnitude of the differences between the various lower hull shapes, however, are small by comparison to the golf club hull forms.

* A further discussion of the bilge keel (model C) results is given in the section on *Radiated Wave Damping*.

EFFECTS OF STRUT OFFSET

The effects of strut offset are illustrated in Fig. 8 which presents the added mass and damping coefficients for models B (semi-circle), E (half golf club), and G (full golf club) at design draft for a 1 inch oscillation amplitude. Increasing the strut offset appears to raise the added mass at the low frequencies, while providing a lower added mass at the higher frequencies. As mentioned earlier, this characteristic is similar to what was observed in draft variations of model G (see Fig. 6b). The damping increases with increased strut offset over the entire frequency range.

Illustrated in Fig. 9 is the effect of moving a *thin strut* from the lower hull centerline (model D) to a half golf club position (model F). Note that the magnitudes of added mass and damping due to strut offset are greater for the thin strut at the half golf club position than for a full thickness strut at the full golf club position.

EFFECTS OF STRUT THICKNESS

In Fig. 9, the effects of strut thickness on added mass and damping characteristics are illustrated by comparing models (B) semi-circle and (D) thin strut semi circle. Halving the strut thickness raises both the added mass and damping characteristics over the entire frequency range. Unlike the golf club hull forms, the increase in added mass occurs over the entire frequency range and not just at low frequencies.

In summary, it should be recognized that the use of these data can be complex, and care should be taken in interpreting the results in both dimensional and nondimensional forms. Also, since not all data were cross-plotted, the trends illustrated above may not hold for all of the different oscillation amplitude and draft test conditions. However, since all data are provided in the appendices, comparisons of particular interest can readily be made.

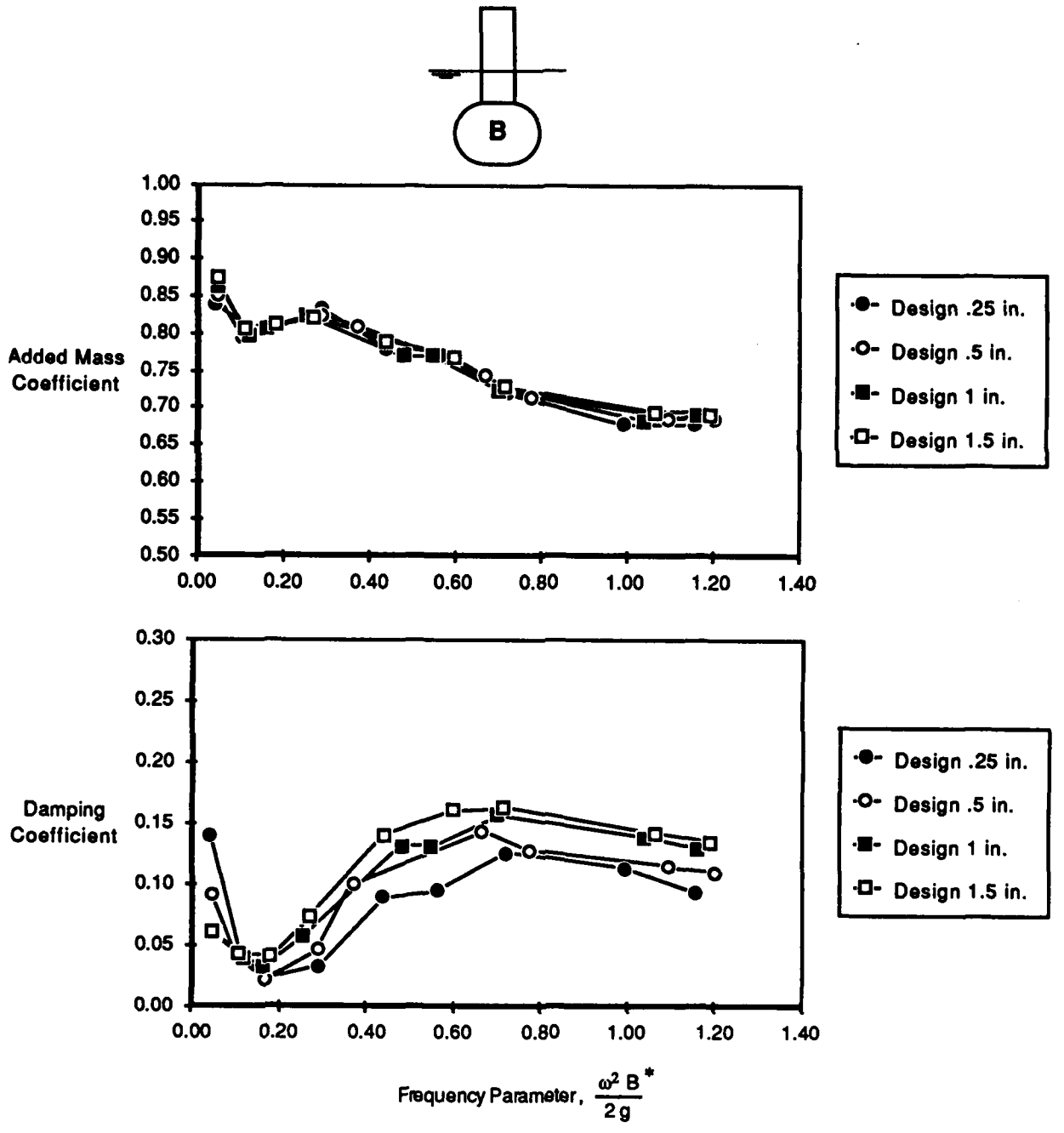

Fig. 5a. Amplitude variation for model B, at design draft.

Fig. 5. Effects of oscillation amplitude on added mass and damping, for models B and G.

*Note: B= *breadth* or *beam* of lower hull.

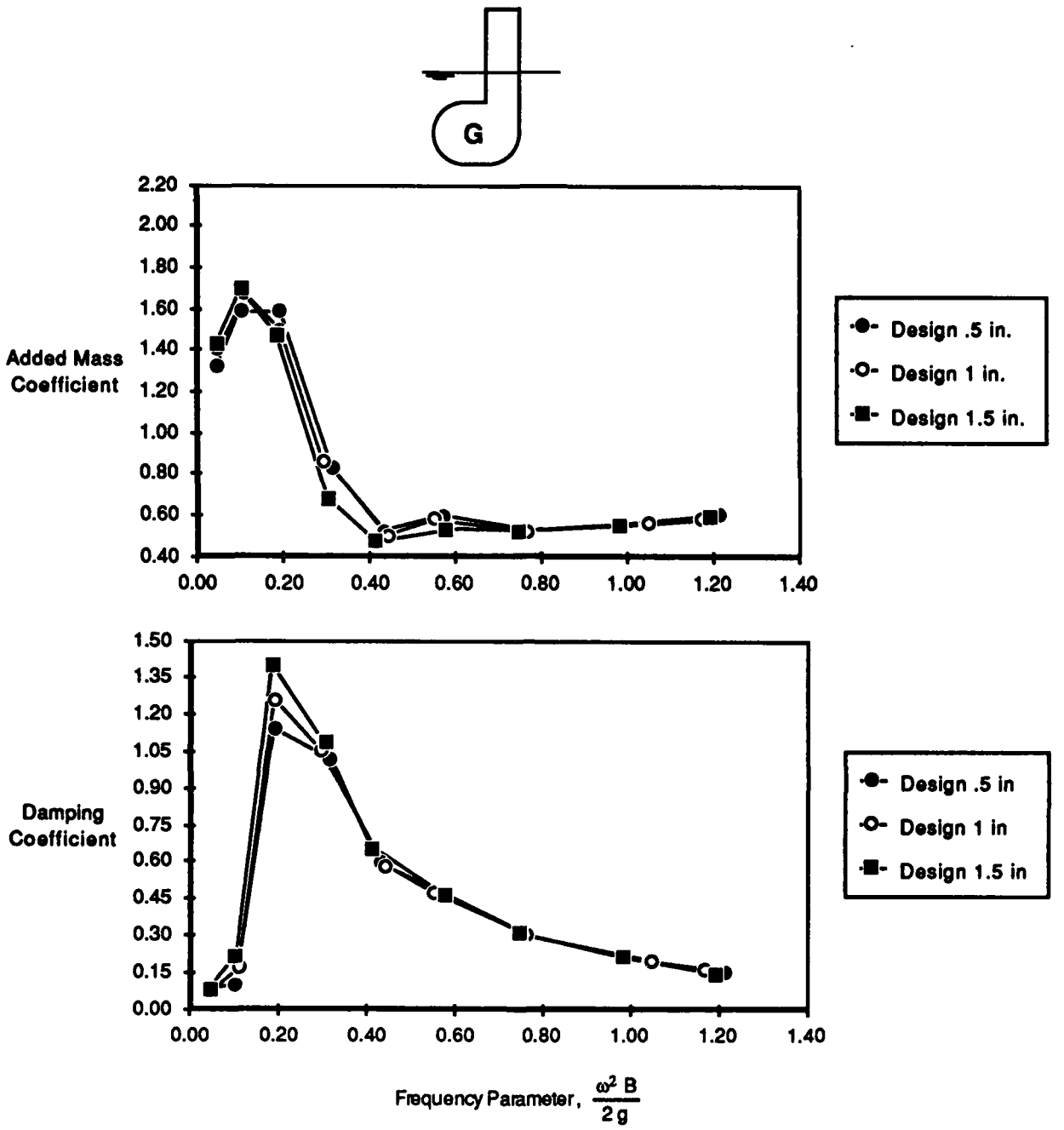

Fig. 5b. Amplitude variation for model G, at design draft.

Fig. 5. (continued)

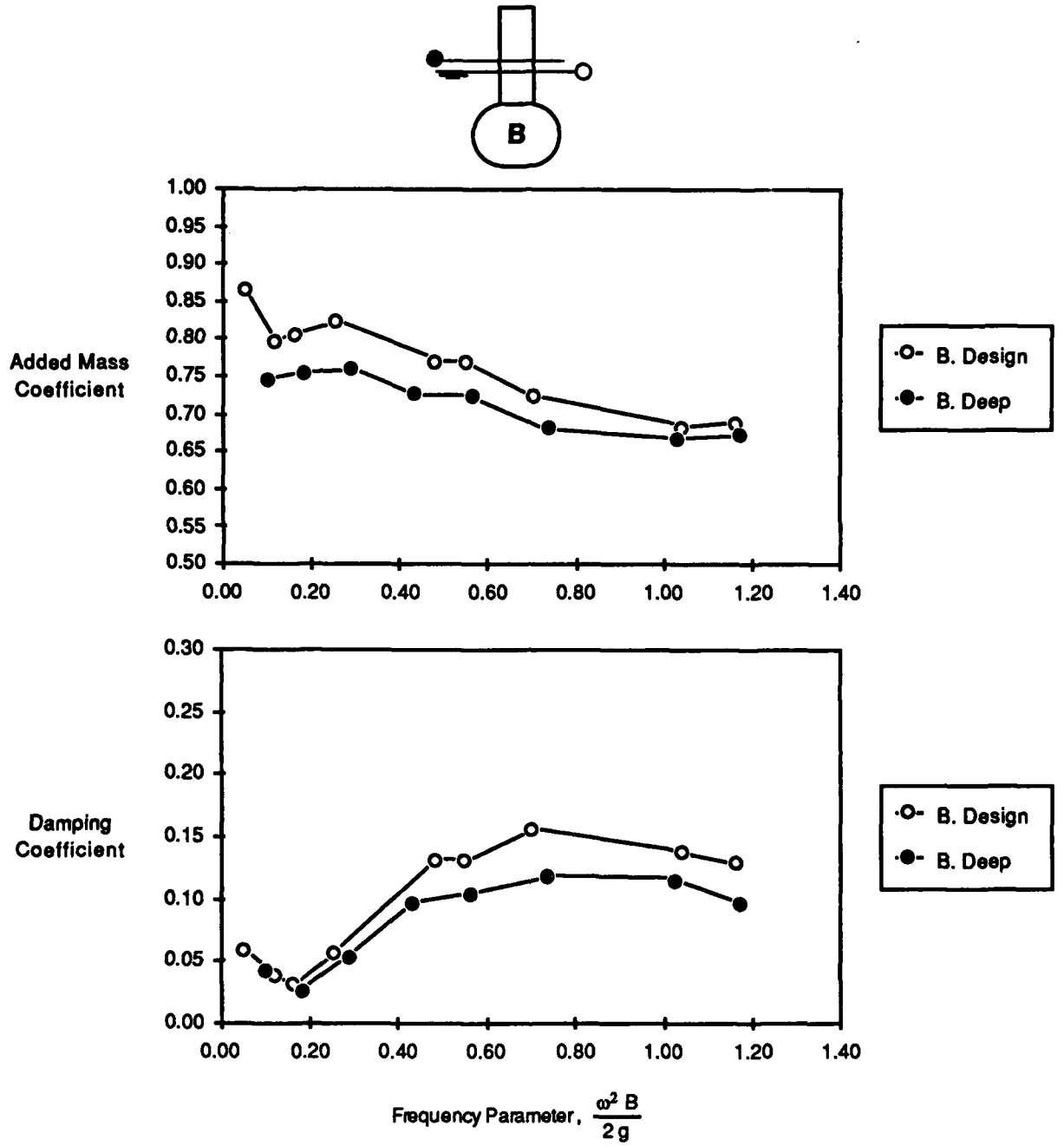

Fig. 6a. Draft variation for model B, at 1.0 inch (2.54 cm) amplitude of oscillation.

Fig. 6. Effects of draft on added mass and damping for models B and G.

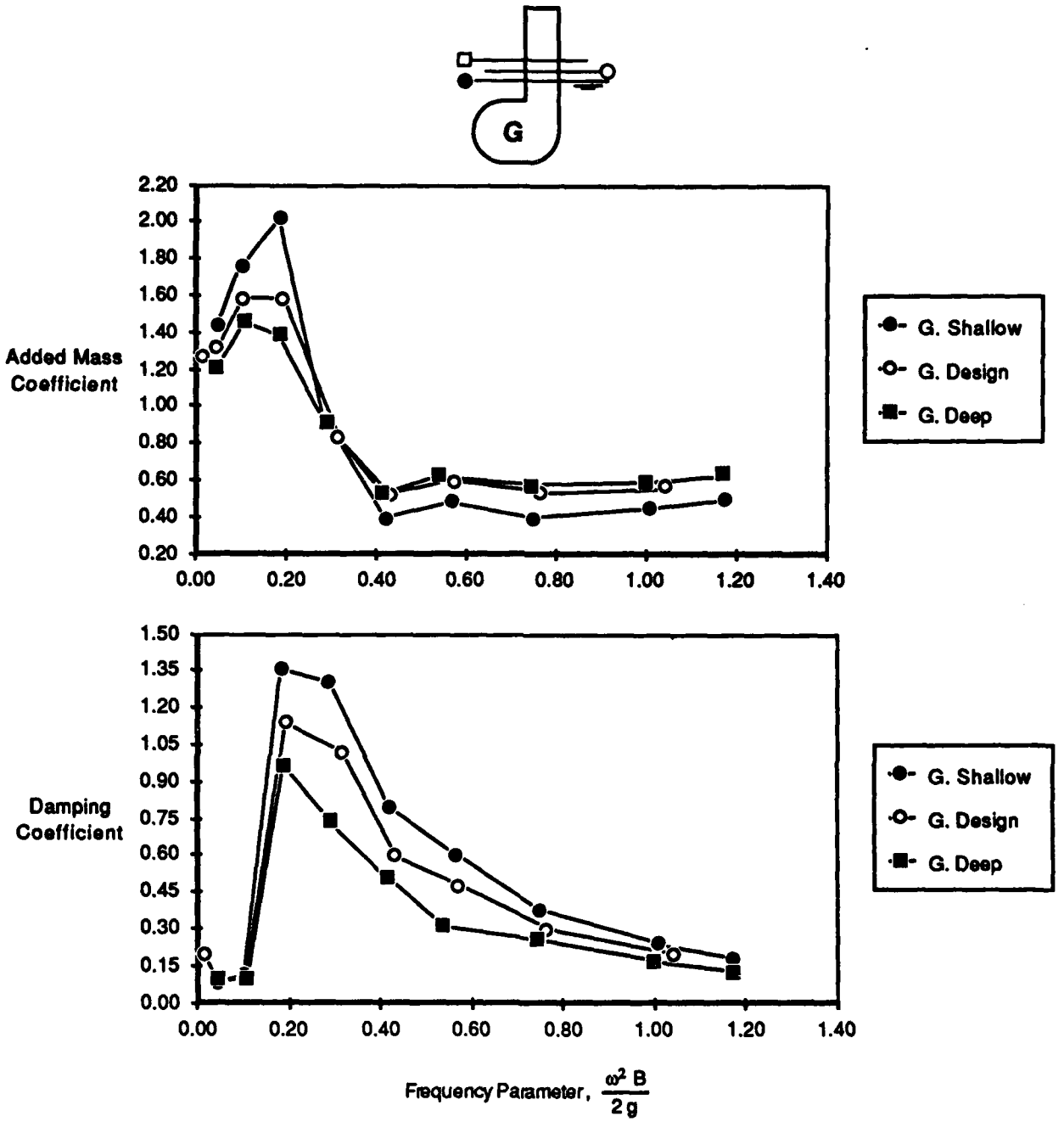

Fig. 6b. Draft variation for model G, at 0.5 inch (1.27 cm) amplitude of oscillation.

Fig. 6. (continued)

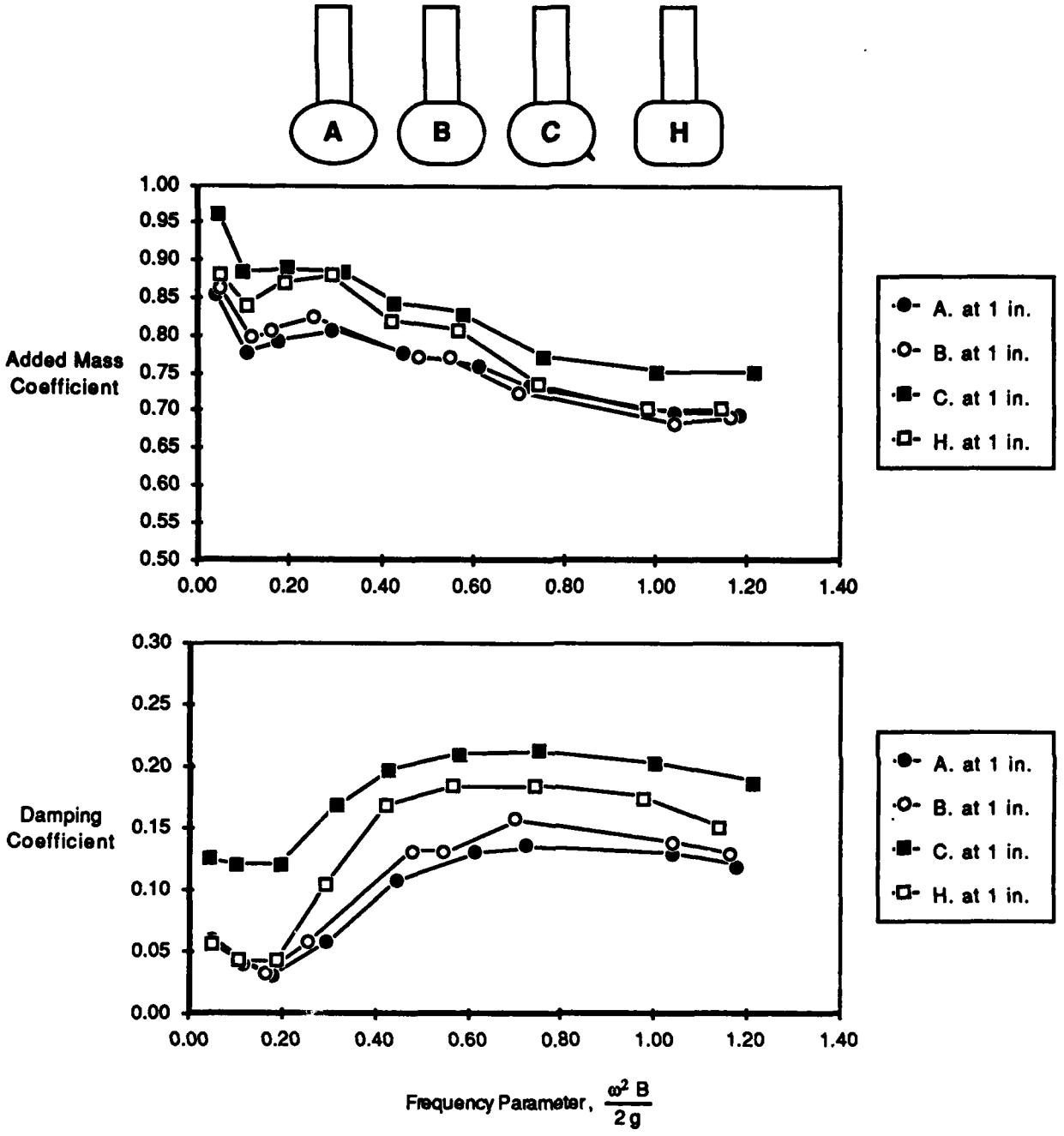

Fig. 7. Effects of lower hull shape and bilge keel on added mass and damping as shown by models A, B, C, and H at design draft, 1.0 inch (2.54 cm) oscillation amplitude.

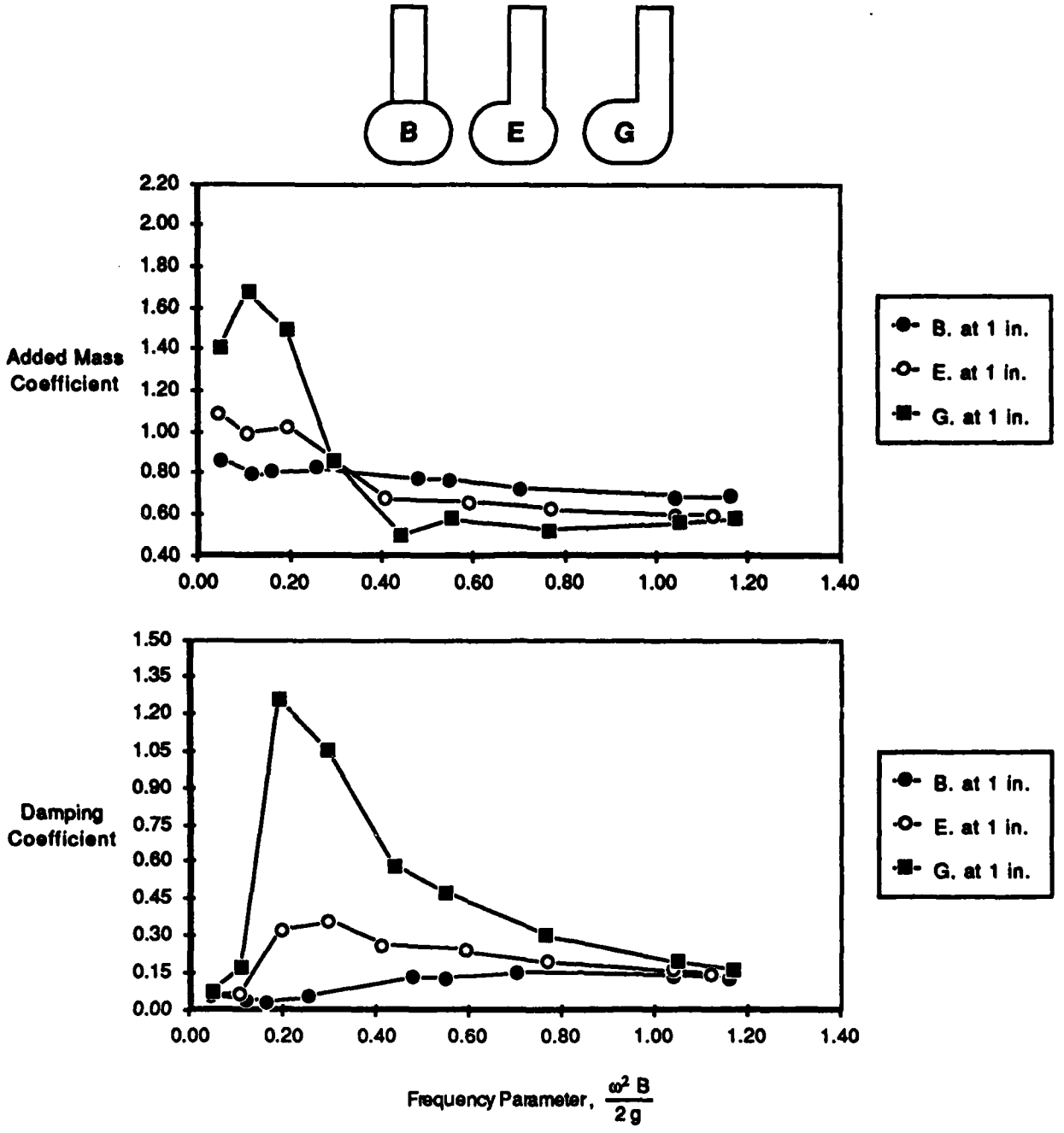

Fig. 8. Effect of strut offset on added mass and damping as shown by models B, E and G at design draft, 1.0 inch (2.54 cm) oscillation amplitude.

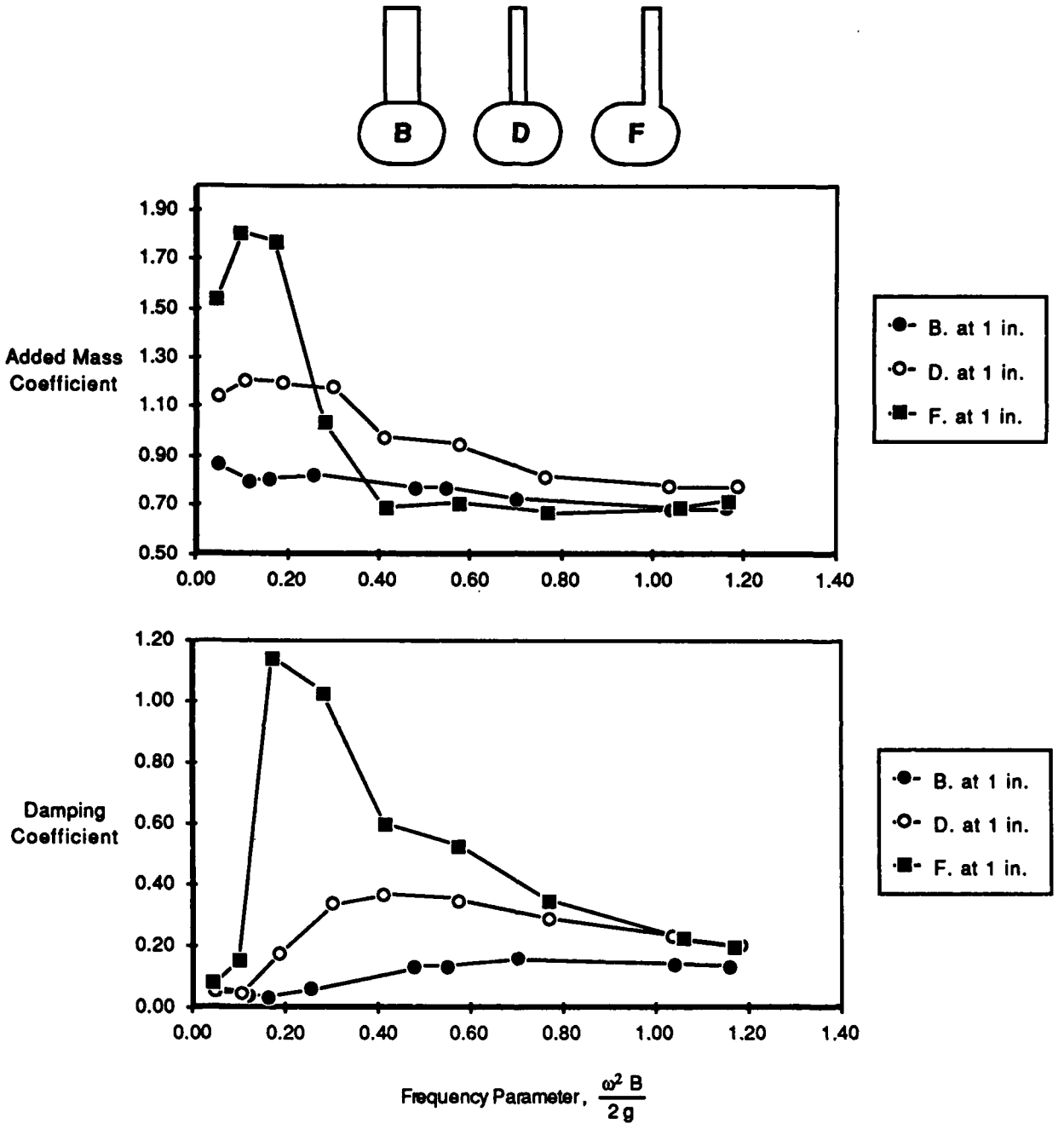

Fig. 9. Effects of strut thickness (and thin strut offset) on added mass and damping as shown by model B, D and F, at design draft, 1.0 inch (2.54 cm) oscillation amplitude.

RADIATED WAVE DAMPING

According to J.N. Newman[1] in *Marine Hydrodynamics* it can be shown from energy conservation

> *"...that the damping coefficient of a two dimensional body symmetrical about x=0 is related to the amplitude Ai of the far-field waves, generated by its motion, by the [following] equation"*

$$B_{ii} = \frac{\rho g^2}{\omega^3}\left(\frac{A_i}{\xi_i}\right)^2 \qquad [12]$$

where ξ_i = heave amplitude, and B_{ii} is in units of force per unit length per unit velocity.

This equation can be derived by equating the wave energy per unit time of the propagating waves to the average work per cycle to oppose the pressure force, and the wave damping can be solved for, as follows:

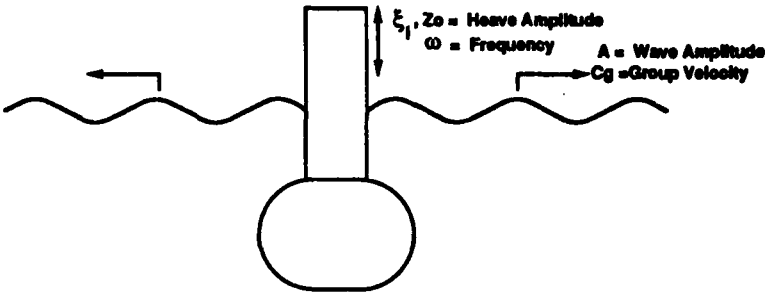

Fig. 10. Radiated waves from vertical oscillation of a two-dimensional body.

The *energy* per wave, E, can be expressed as

$$E = \frac{1}{2}\,\rho\, g\, (A)^2 \text{ and} \qquad [13]$$

the wave energy per unit time (per side of model), $\dot{E}$ is given by

$$\dot{E} = \frac{1}{2}\,\rho\, g\, (A)^2\, (Cg) \qquad [14]$$

and Cg is the wave *group velocity*, defined as

$$Cg = \frac{1}{2}\,\frac{g}{\omega}\,. \qquad [15]$$

The *average work* per cycle ,W, to oppose the pressure force on the model is given by

$$W = \frac{1}{2}\,\omega^2\, b_{wave}\, (z_o)^2 \qquad [16]$$

Therefore, by equating the energy per unit time of the waves propagating in both directions (2.0 times $\dot{E}$, Eq. 14) with average work per cycle (Eq. 16), an expression for wave damping can be obtained in terms of the amplitude ratios (previously defined as radiated wave transfer functions),

$$b_{wave} = \frac{\rho g^2}{\omega^3} \frac{1}{2}\left(TF1^2+TF2^2\right) \quad \text{[per unit wavelength].} \qquad [17]$$

Multiplying by model length, L, and non-dimensionalizing by $M\omega$, the wave damping coefficient is:

$$\delta_{wave} = \frac{\rho g^2 L}{M\omega^4} \frac{1}{2}\left(TF1^2+TF2^2\right) \quad \text{[referred to as } \textit{wave damping} \text{ in the figures].} \qquad [18]$$

A comparison is presented in Fig. 11 to Fig. 18 between the calculated wave damping based on the radiated wave transfer functions (Eq. 18) and the total measured damping (Eq. 11) for models A-H. The comparison is quite good with the wave damping providing a *qualitative* verification of the damping results; independent of the measured forces. Theoretically, the primary difference between the two curves should be a measure of the viscous component of damping. However, the wave damping curve for some models exceeds the measured *total* damping, mostly at low frequencies (near the peaks) such as in Figs. 14-17 (thin strut and golf club models). This is most likely due to the fact that at these frequencies, the radiated waves can hardly be considered to be measured in the *far field*. For example, at nondimensional frequency parameters of 0.5 and 1.0, the corresponding wavelengths (model scale) are 4.8 and 2.4 ft, respectively, where the wave probes were only 3.5 ft away from model. At the high frequency end, the difference between the two curves may very well provide a *quantitative* breakdown of the wave making and viscous components of damping. This, however, cannot be said with certainty since the waves were not really measured in the *far field*. Still, the radiated wave information does provide a comparative measure of the energy lost to wave generation, between the different models under the same test conditions. The radiated wave data may also be useful at some point in studying wave interactions between the hulls of twin hull configurations. While the calculation of a wave damping coefficient was limited to those presented in Figures 11 through 18, all radiated wave transfer functions are provided in the appendices for each model and test condition.

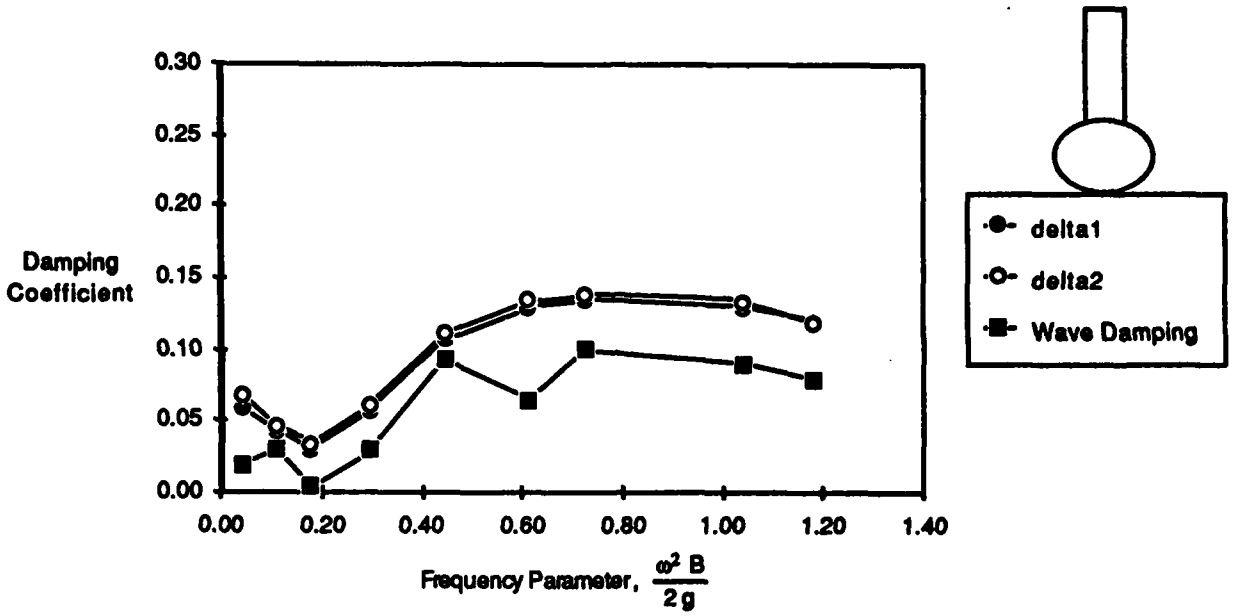

Fig. 11. Comparison of the damping coefficients calculated from the force measurements (delta1, delta2) and radiated waves ("Wave Damping") for model A, at design draft, and 1.0 inch (2.54 cm) amplitude.

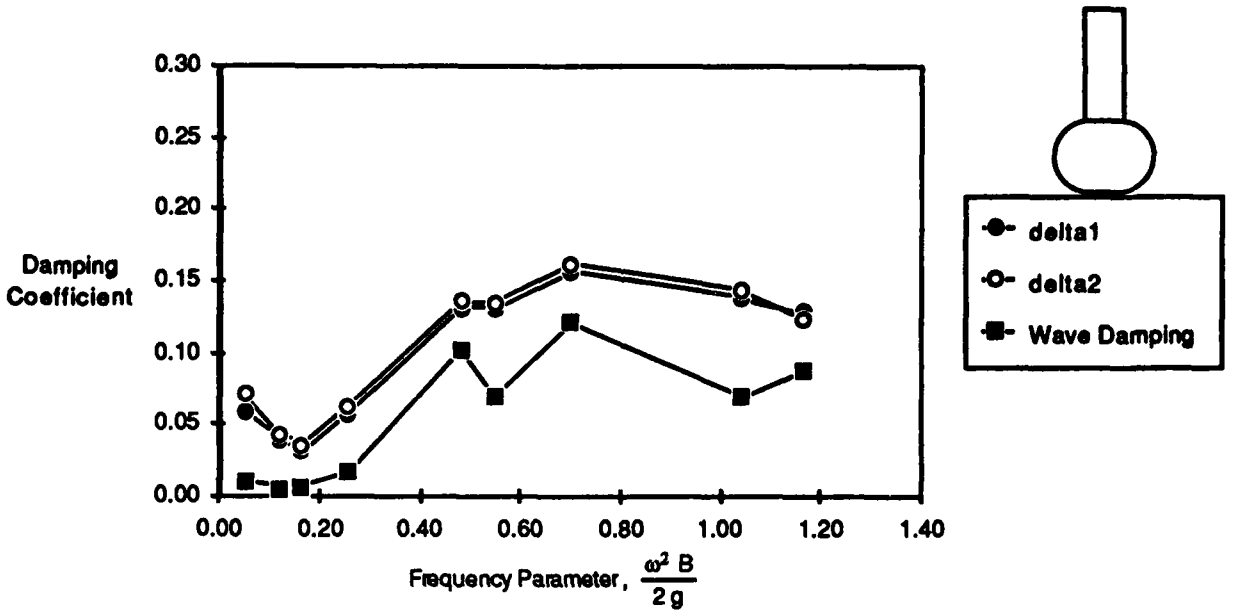

Fig. 12. Comparison of the damping coefficients calculated from the force measurements (delta1, delta2) and radiated waves ("Wave Damping") for model B, at design draft, and 1.0 inch (2.54 cm) amplitude.

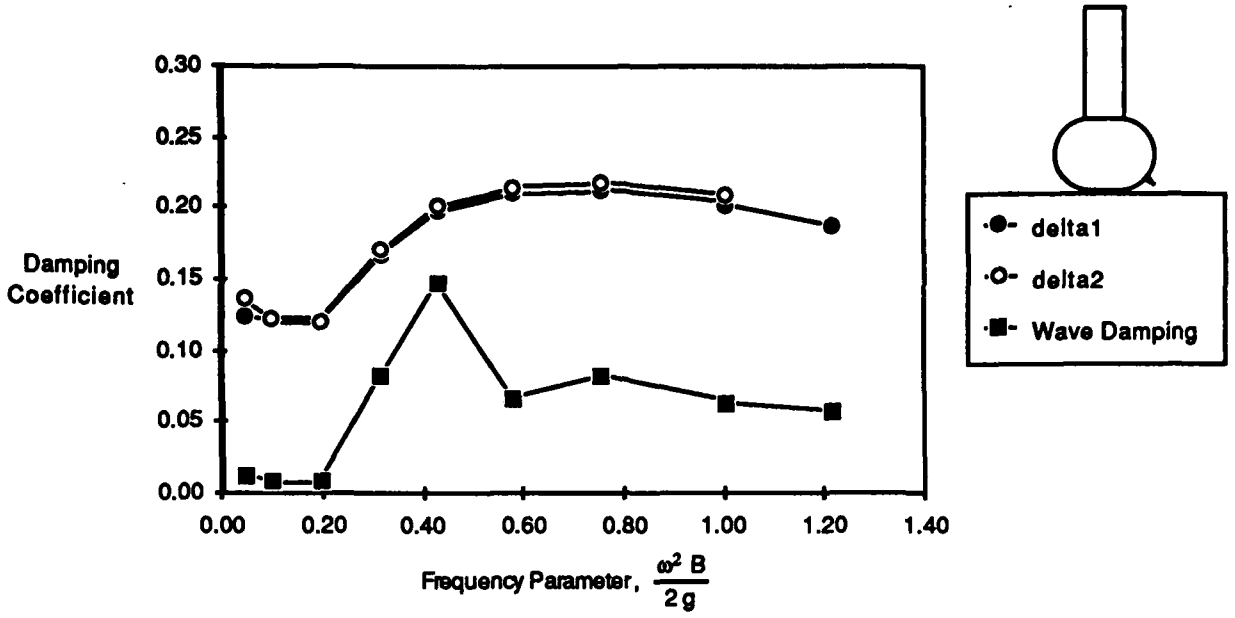

Fig. 13. Comparison of the damping coefficients calculated from the force measurements (delta1, delta2) and radiated waves ("Wave Damping") for model C, at design draft, and 1.0 inch (2.54 cm) amplitude.

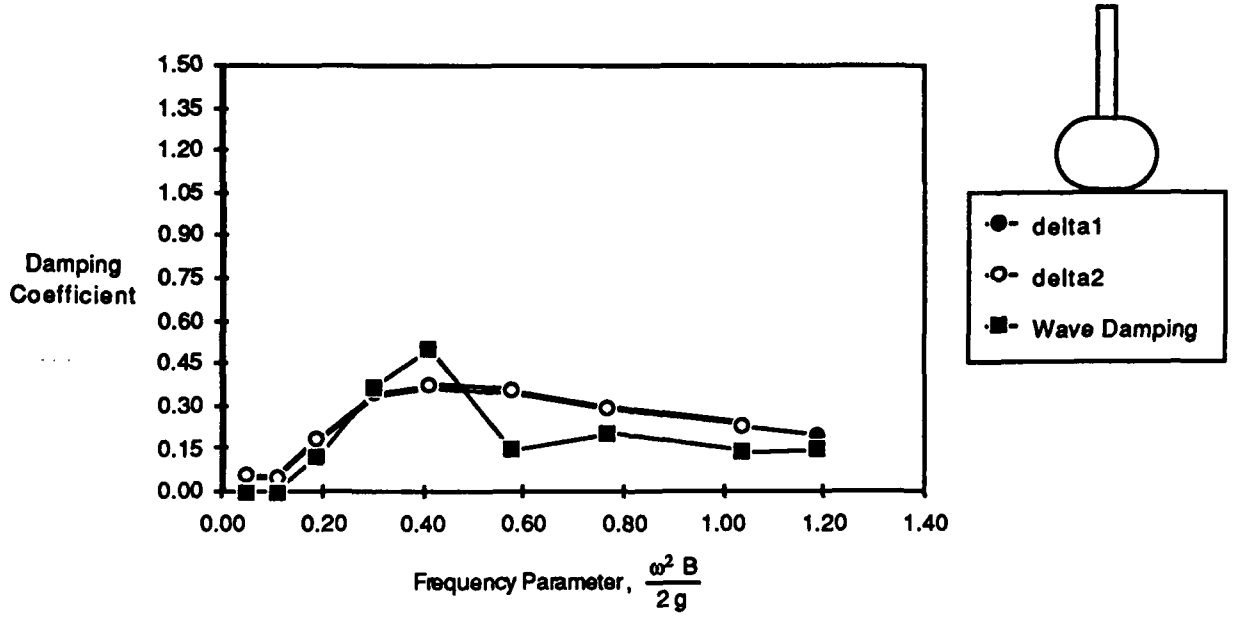

Fig. 14. Comparison of the damping coefficients calculated from the force measurements (delta1, delta2) and radiated waves ("Wave Damping") for model D, at design draft, and 1.0 inch (2.54 cm) amplitude.

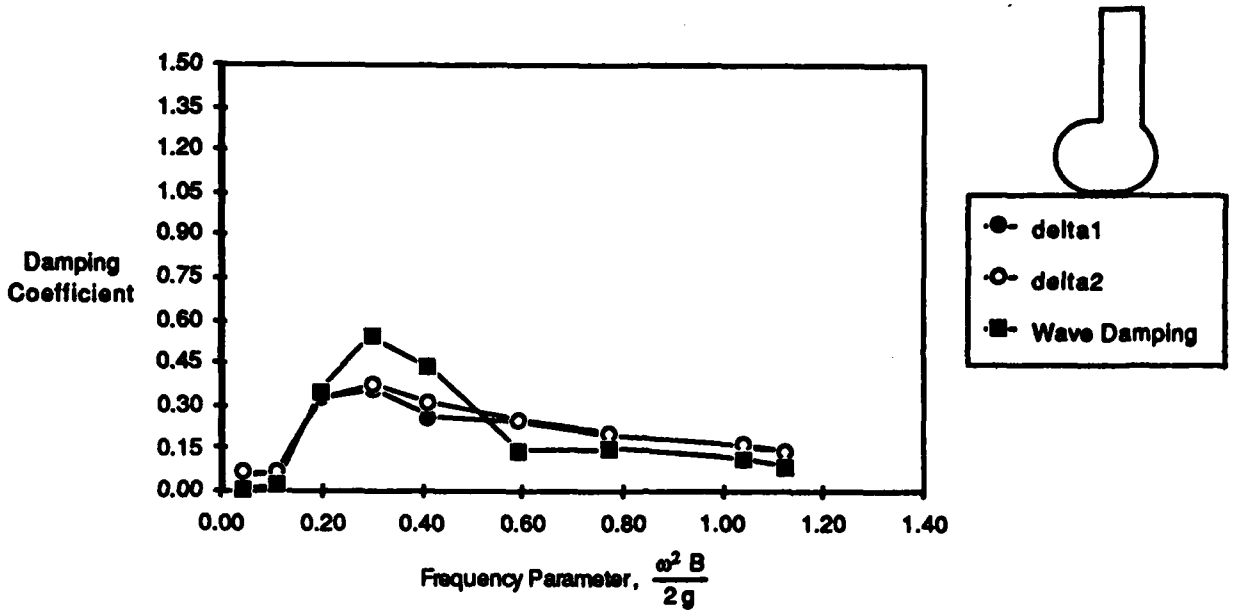

Fig. 15. Comparison of the damping coefficients calculated from the force measurements (delta1, delta2) and radiated waves ("Wave Damping") for model D, at design draft, and 1.0 inch (2.54 cm) amplitude.

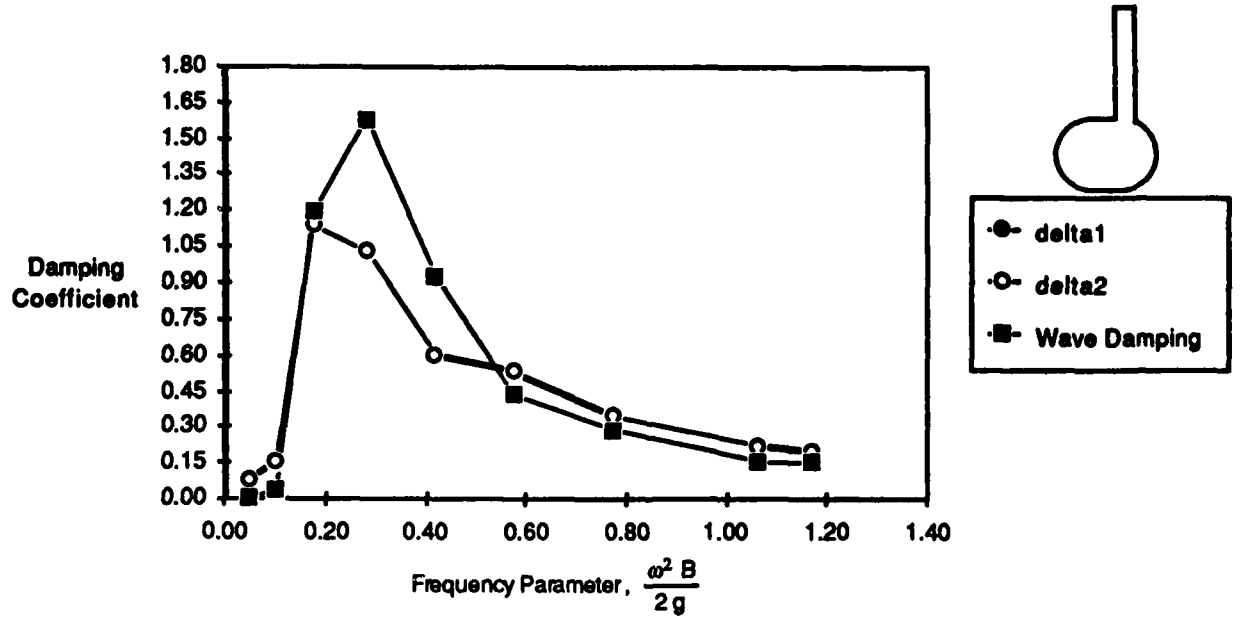

Fig. 16. Comparison of the damping coefficients calculated from the force measurements (delta1, delta2) and radiated waves ("Wave Damping") for model E, at design draft, and 1.0 inch (2.54 cm) amplitude.

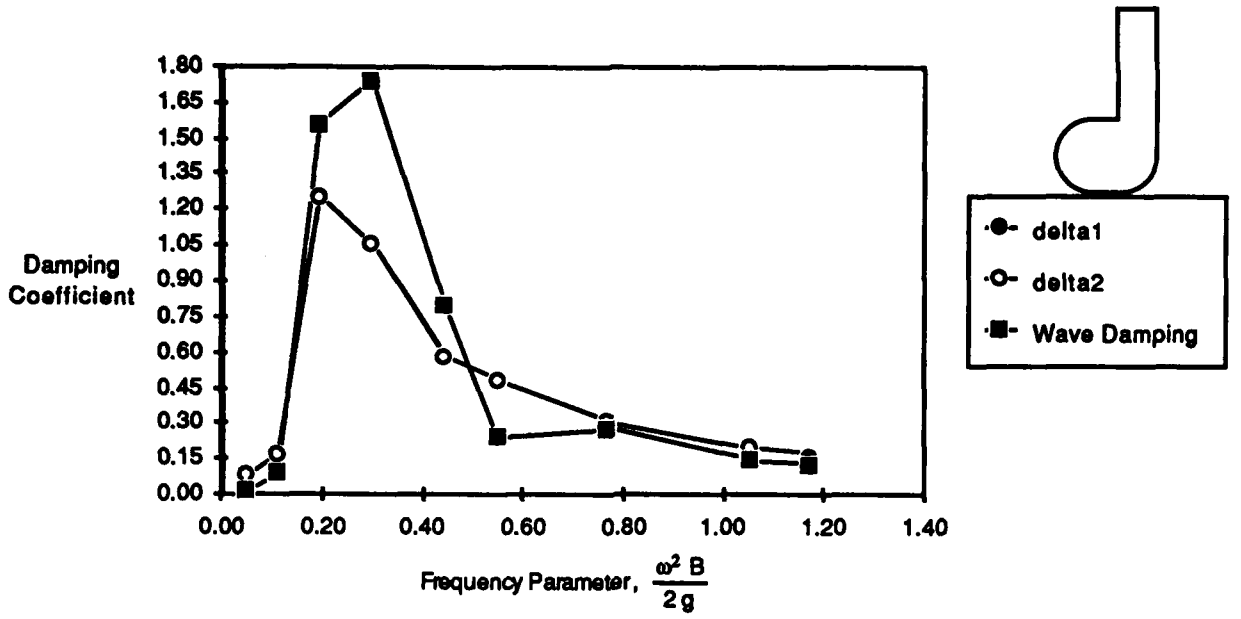

Fig. 17. Comparison of the damping coefficients calculated from the force measurements (delta1, delta2) and radiated waves ("Wave Damping") for model F, at design draft, and 1.0 inch (2.54 cm) amplitude.

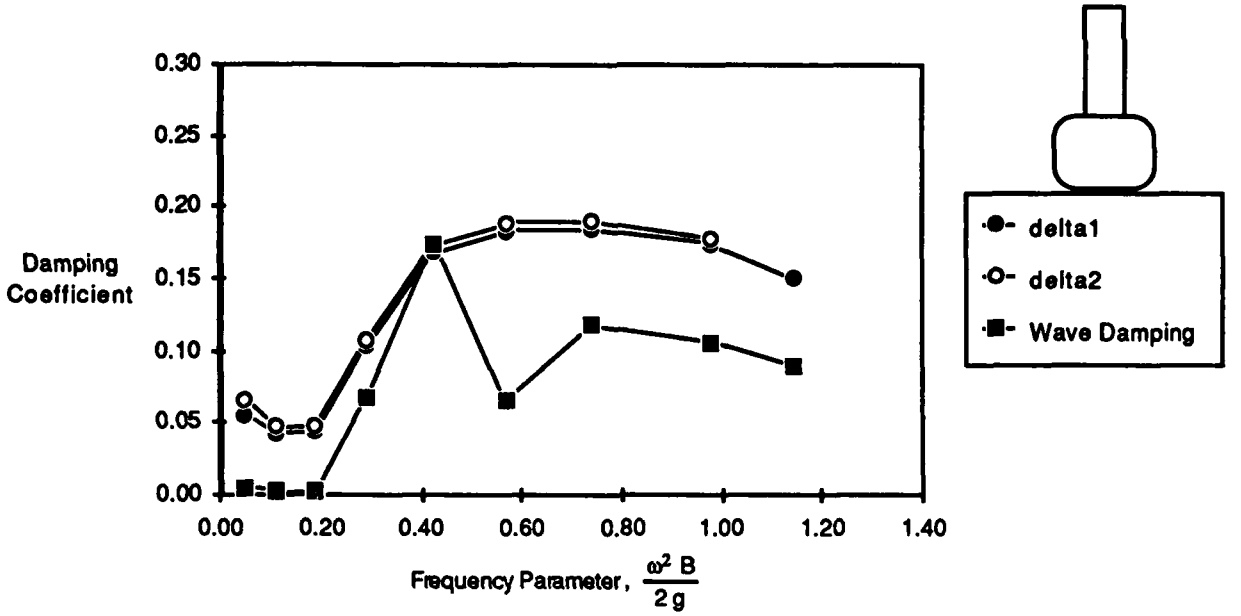

Fig. 18. Comparison of the damping coefficients calculated from the force measurements (delta1, delta2) and radiated waves ("Wave Damping") for model G, at design draft, and 1.0 inch (2.54 cm) amplitude.

One example of the use of the wave data is shown in Fig. 19, where a comparison between the *wave damping* and measured *total damping* is presented for the models B and C, to compare the damping effects of a bilge keel. This figure shows that the effect of adding a bilge keel to model B was to significantly increase the total damping while hardly affecting the wavemaking component of damping. This implies (or verifies) that the increase in damping is due to viscous effects, as would be expected for a bilge keel.

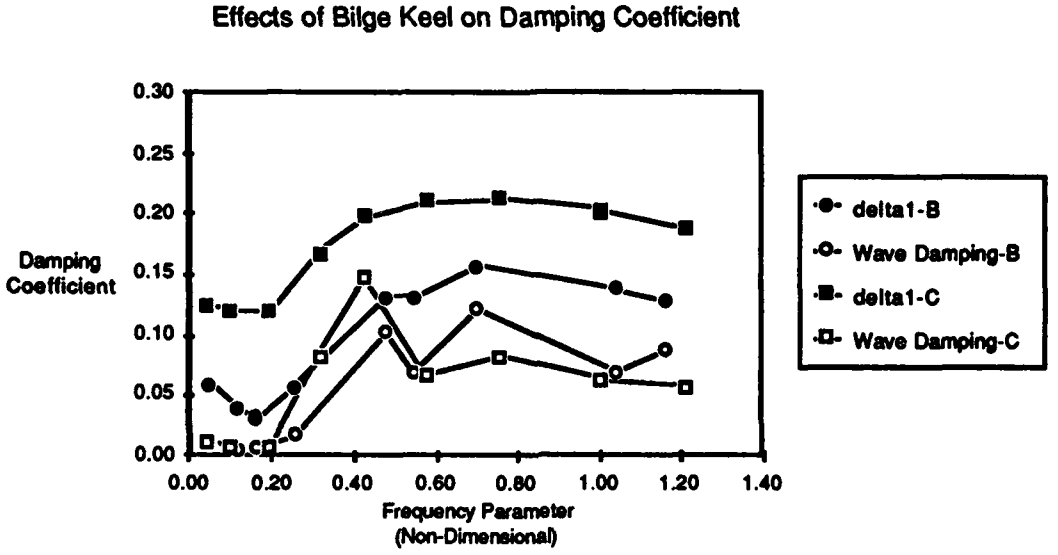

Fig. 19. Comparison of the damping coefficients calculated from the force measurements and radiated waves for models B and C to show the effects of the bilge keel on damping coefficients.

The main purpose of presenting the radiated wave results in the form of a damping coefficient is that, whether it be viewed as *quantitative* or *qualitative*, the positive agreement between the two sources of damping results is encouraging, in that, the wave measurements provide a completely independent confirmation of the trends and magnitudes of the damping characteristics for the series of models tested, thereby giving greater confidence in the results.

THREE-DIMENSIONAL OSCILLATION TESTS AT ZERO SPEED

Vertical plane oscillation experiments were conducted at a limited number of test conditions on models B and G, modified with additional bulbous sections added to each end of the 2-D models, to produce SWATH-like (3-D) hull sections. Figure 20 shows the general geometry of the end pieces, with the equations for the parabolic fairing of the strut and lower hull sections.

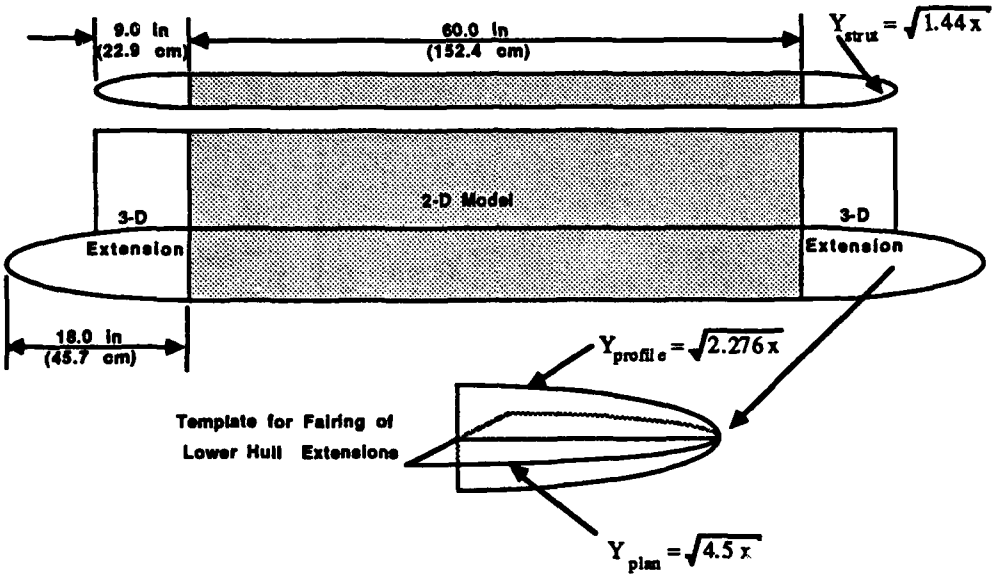

Fig. 20. Model geometry for the three-dimensional hull/strut extension pieces on models I, J, K and L.

Four configurations were tested at zero speed and designated with the letters I, J, K, and L. Models I and J are the three dimensional versions of models B and G, respectively (i.e. single hull), and with the construction of a second 3-D golf club hull, a twin hull 3-D golf club model was tested at two strut/hull spacings, designated as models K and L. The hull spacing for model K was 32 inches (81.28 cm) model scale, and corresponds to a golf club version of the T-AGOS 19 with a waterline beam of 80 ft (24.4 m). Model L, with a hull spacing of 27 inches (68.58 cm) model scale, was referred to as the *narrow* twin-hull golf club. The zero speed experiments were conducted on the same tow rig as shown in Fig.3, without the end plates. Also, heavier block gages were used; the 200 lb and 50 lb gages were replaced with 500 lb

and 200 lb capacity gages, respectively. The zero-speed 3-D results for models I, J, K, and L are presented in Appendices I, J, K, and L. The three-dimensional oscillation tests required two additional test set-ups for forward speed oscillations in heave and pitch; which required additional gages, analysis, and nomenclature. The details of these 3-D oscillation experiments are being reported separately. However, the zero speed coefficients for heave are presented in this report in the same format as the 2-D results for comparative purposes.

EXPERIMENTAL ACCURACY

The quality of the results of any experiment is dependent on the ability to accurately model and measure the required parameters. Even after all known corrections and calibrations have been applied, it is an excepted fact that all measurements have errors. Presented below are estimates of the known sources of experimental error, and some explanation of the effects on the final results. References 2 and 3 present a methodology which is becoming a standard for the estimation and reporting of measurement uncertainty. The types of error are typically categorized as *systematic* (B-*bias* or *fixed*) error, which for this project was generally based on judgement, and *random* or *precision* (S-precision) error estimated from statistical data. The sources of bias and precision errors are usually identified and estimated in each of the following four areas:

1. Calibration Errors
2. Data Acquisition Errors
3. Data Reduction Errors
4. Errors of Technique

This methodology, however, was not readily applicable to an oscillation type experiment*, due to the large amount of data acquired at independent test conditions and the frequency dependent nature of the

*A good presentation of the experimental accuracy of an oscillation experiment is given by O'Day and Jones[4].

experiments. Therefore, a somewhat simplified approach is presented here to quantitatively evaluate only the measurement uncertainty associated with the basic calibration and data acquisition errors of the transducers, followed by a more qualitative approach to the data reduction and technique errors.

CALIBRATION AND DATA ACQUISITION ERRORS

Table 4 presents estimates of the various sources of bias (B) and precision (P) error associated with calibration and data acquisition errors for each data channel, propagated to a calculation of the measurement uncertainty using the 95% and 99% confidence models (Ref. 2). The instrument calibrations were performed through the electronics and signal conditioning to exchange large bias of an uncalibrated transducer with the smaller precision error associated with applying a reference standard. For each data channel, the precision index was estimated using the standard deviation (S) about a least squares linear fit to the calibration data, given by

$$S^2 = \frac{\sum_i (y_i - b - mx_i)^2}{N-2}, \text{ for linear regression, } y=mx+b. \qquad [19]$$

Bias errors, listed as *cal bias* in Table 4, were estimated as the propagation of the cal standard from a known traceable reference standard. For the heave amplitude (Channel 1), a precision mechanical vernier on the oscillator was used to set heave to within .001 in (.0025 cm) for each test condition. The string pot measurement however, was less accurate with typical deviations between the vernier setting and the readout of approximately ±0.02 in (.05 cm). Since harmonic analysis of the data was performed using the string pot readings, heave accuracy is based on the string pot rather than the vernier. The two DTRC manufactured Block gages, with an estimated accuracy of 0.02% of full scale range, were selected to provide maximum resolution over a dual range of expected forces. For the 200 lb gage (Z1) this translates into ±0.04 lbs, and for the 50 lb (Z2) gage, ±0.01 lbs (listed as *transducer* error in Table 4.). The block gages were calibrated using a set of precision ground weights, both at the beginning and end of the experiment to check for any drift or changes in the calibration (also a measure of the bias error). Also, in-

place checks monitored the calibration throughout the testing, as ballast weights were repeatedly placed on models.

As mentioned, since calibrations were conducted through signal conditioning electronics, the primary sources of data collection (acquisition) errors listed in Table 4 were estimated to be from transducer error (based on manufacturer's specs), and the A/D conversion errors (expressed in engineering units). The A-D error for 15 bit conversion , at a full-scale range of ±10 volts, translates into a resolution of $20/2^{15}$ or ±.0006 volts. The corresponding bias errors are listed in engineering units for each channel in Table 4.

Table 4. includes estimates of measurement uncertainty for each transducer using the models for 99% and 95% confidence levels given in Eq.s 20 and 21, respectively (see Ref. 2 for details).

$$UADD = B + t\,S\ , \qquad \text{[99\% Confidence Model]} \qquad [20]$$

where t, the students t value, is function of degrees of freedom, and for large samples (N>30), t = 2.

$$URSS = \sqrt{[B^2 + (tS)^2]} \qquad \text{[95\% Confidence Model]} \qquad [21]$$

Table 4. Sources and estimates of experimental error for the measurement transducers (in English units).

	Channel 1 Heave, In		Channel 2 Z1-Gage, lb		Channel 3 Z2-Gage, lb		Channel 4 Wave Probe1,In		Channel 5 Wave Probe2,In	
ERROR SOURCE	B	S	B	S	B	S	B	S	B	S
Calibration										
Pre-cal		0.006		0.301		0.240		0.031		0.039
Post-cal				1.140		0.158				
Cal Bias	0.020		0.200		0.040		0.050		0.050	
TCal RSS	0.020	0.006	0.200	1.179	0.040	0.287	0.050	0.031	0.050	0.039
Data Collect										
Transducer	0.010		0.040		0.010		0.050		0.050	
A/D Convert	0.000		0.024		0.003		0.000		0.000	
TDCol RSS	0.010	0.000	0.047	0.000	0.010	0.000	0.050	0.000	0.050	0.000
UNCERTAINTY INTERVALS										
Total RSS	0.022	0.006	0.205	1.179	0.041	0.287	0.071	0.031	0.071	0.039
UADD-99%	0.035		2.564		0.616		0.133		0.149	
URSS-95%	0.026		2.367		0.576		0.094		0.105	

DATA REDUCTION AND TECHNIQUE ERRORS

The data reduction and analysis involved many techniques and subsequent opportunities for introducing errors which are not easily estimated or reduced to a single value of uncertainty. Harmonic analysis, in addition to yielding the fundamental response amplitudes, provided a measure of the quality of sinusoidal oscillation. In general, harmonic analysis performed on an average of 10 cycles per test condition, had the effect of filtering unwanted background noise. Also, any non-zero mean offset in the gage readings from one test condition to another are effectively eliminated, since the harmonic amplitudes are based on the peaks without regard to the mean (small offsets in the gage zeros can be a major problem in the precision of steady force measurements). For these tests, the motion of the oscillator was very nearly a pure sinusoid, with typically 99% of the mean-square energy of the heave motion signal in the first harmonic. From analysis output of minimum, maximum, and average values of amplitude and period, the maximum variations over 10 cycles were typically less than ±0.002 in (.005 cm) and ±0.02 sec, respectively. The magnitudes of the force signals were generally much larger than the background noise with typically 95-98% of the total energy contained in the first harmonic, and in the worse case (at low amplitude, low frequency test conditions ,i.e. low forces), the mean square energy was still greater than 50% of the total.

Once the forces are resolved into in-phase and out-of-phase components, the added mass and damping calculations are a function of many more factors, including basic measurements of model mass and hydrostatic restoration coefficients, as well as, the frequency dependence of the calculations. Models and gage hardware were weighed prior to carriage tests using a National Controls (NCI) Model 5785 electronic platform scale, with an overall range and accuracy of 200±0.02 lbs. While the hydrostatic restoration coefficient, C, could be calculated from Eq. 9, the measured values were used in calculations to improve accuracy, since the measured values account for the slight variations in model waterplane areas.

The calculation of the final results involves the accuracy of the measured forces, the hydrostatic restoration coefficients and the various model masses. Therefore, accuracy is to a large degree, a function of the relative balance between the components over the frequency range. At low frequency the results are driven by the hydrostatic effects. Since the inertial force is only a small part of the in-phase component, the accuracy of both the mass and restoration coefficient measurements would affect bias as well as increase the expected scatter of the data at low frequency. An increase in scatter at the lowest frequency was observed in the data during these tests. At high frequency the results are driven mainly by the inertial effects, and therefore the accuracy of the added mass is considered to be best, in this range. In the intermediate range, hydrostatic and inertial terms tend to cancel, and the most accurate damping is typically expected in this range.

One of the measures of accuracy of an experiment is the repeatability of specific test conditions. While few identical runs were specifically repeated, data taken at various amplitudes of oscillation and drafts, for similar models, exhibit trends which are smooth and consistent both in the linearity and the repeatability (i.e. degree of scatter) of the results. Figure 21 presents a comparison of the reported data for model A, at the design draft, 0.5 in (1.27 cm) amplitude test condition, with a repeated data set taken later in the experiment. This combination of model and amplitude represents a test condition with one the lowest total force outputs. Also, since the force data presented is for the less sensitive, Z1 gage, this comparison provides a conservative example of the test repeatability. The variation between the two sets of force data in Fig. 21 are slight, and based on typical variations between the force outputs of gages Z1 and Z2, do not appear to be significant.

Taken together, the repeatability of test results, the positive agreement between redundant force measurements, and the additional qualitative agreement between damping calculations from the measured radiated waves and force measurements (as previously discussed); provide a significant measure of confidence in results presented.

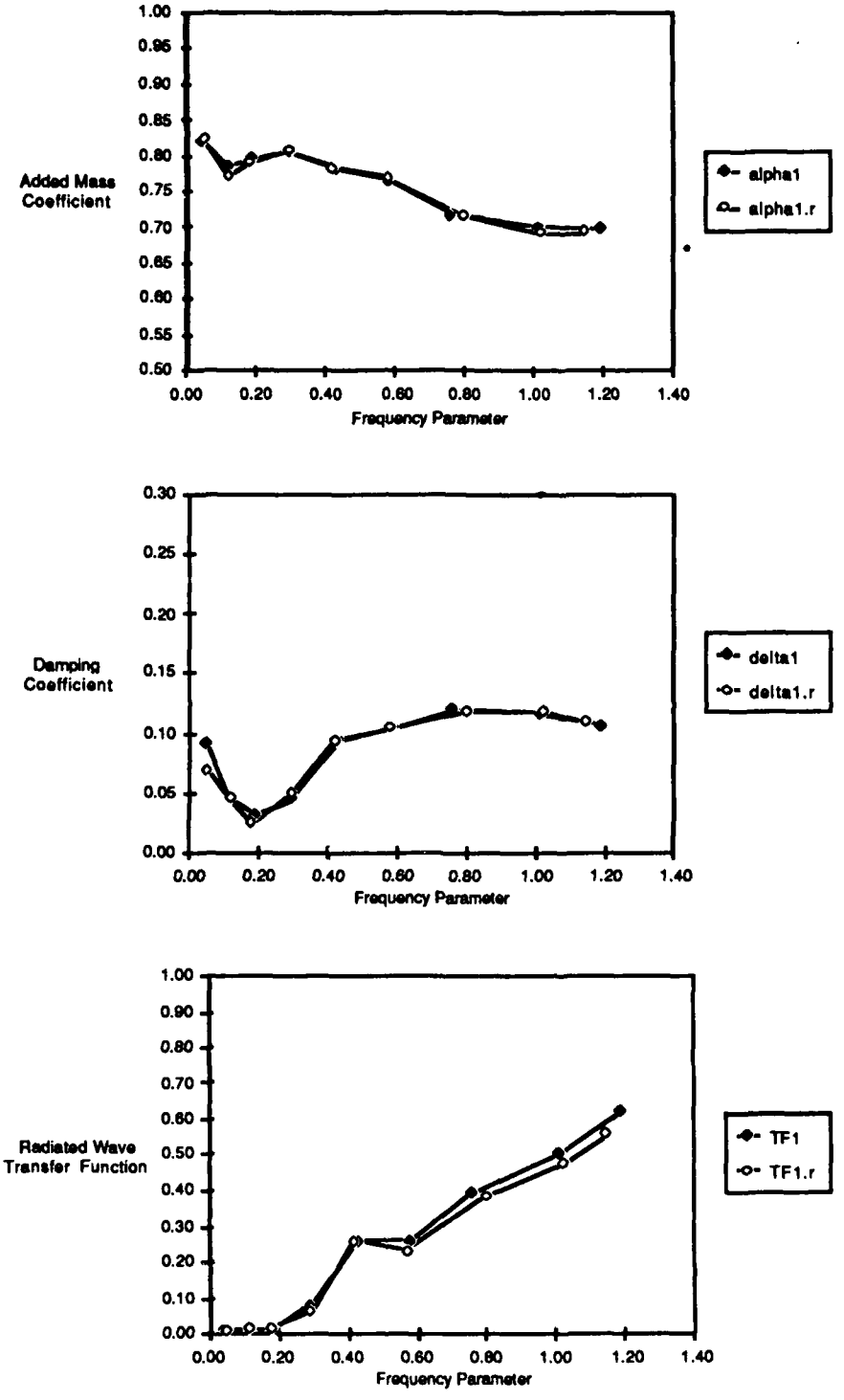

Fig. 21. Example of repeatability of hydrodynamic coefficients for the Z1 gage, and wave TF1, for model A at design draft and the 0.5 inch (1.27 cm) amplitude (.r denotes repeated data series).

SUMMARY AND CONCLUSIONS

The primary objective of this report is to present the results of vertical plane oscillation experiments conducted on a series of two-dimensional SWATH demi-hull section shapes. These cross-sections represent a range of hull/strut configurations encompassing forms that have been under consideration in the design of Navy SWATH ships. The results of tests conducted on eight models at two drafts and oscillation amplitudes provide useful trends in the added mass and damping characteristics. The effects of oscillation amplitude, draft, lower hull shape, strut position (offset), and strut thickness have been presented and discussed.

In general, the hydrodynamic characteristics, as a function of oscillation amplitude were mostly linear with damping exhibiting a slight increase with increased amplitude. While an increase in draft typically caused a reduction in the nondimensional added mass and damping coefficients, the trends varied somewhat, depending on the type of hull form. Of the four (non-golf club) lower hull shapes tested, the addition of a bilge keel to a T-AGOS-like hull form produced the largest damping. The effect of offsetting the strut was to significantly increase added mass at low frequency but to slightly reduce it at high frequencies. The damping was increased considerably throughout the frequency range for the golf club hull forms. The effect on the hydrodynamic characteristics of halving the strut thickness (*thin strut*) was to increase both the added mass and damping throughout the frequency range.

A comparison is presented between the damping calculated from the measured radiated wave data and the total measured damping. The comparison is quite good with the wave damping providing a *qualitative* verification of the damping results, independent of the measured forces. The radiated wave data may also be useful at some point for studying and or modeling the asymmetry of a golf club type hull form.

Also presented are results of zero speed experiments on four models consisting of 3-D extensions added to the 2-D models. The coefficients are presented in the 2-D non-dimensionalization scheme for

comparative purposes. A forthcoming report will present the details of the 3-D experiments including some forward speed heave oscillation data for a T-AGOS-like single hull and both a single and a twin hull golf club model.

The results presented herein should provide a resource for correlation of SWATH added mass and damping characteristics with theory, as well as, in the development, analysis and verification of SWATH ship motion prediction simulations.

ACKNOWLEDGEMENTS

The authors wish to acknowledge those who contributed significantly to the completion of this project:

- R. Thomas Waters and Kathryn McCreight for their assistance and consultation from test planning through data analysis.
- James Hering for setting up the linked graphics capabilities, which saved many hours of creating plot files.
- Martin Dipper, Jim Hickok, and Dan Hayden for providing outstanding support in the area of computer data acquisition during the experiment.
- Electronic technicians William Dixon and Derek Cook for instrumentation support, and John Magee for his assistance during the carriage experiments.
- J. Ray Broussard for his assistance in preparing the final graphics for the Appendices.
- Lisa Eynon for assistance in typing and report preparation.

REFERENCES

1. Newman, J. N., *Marine Hydrodynamics* , Cambridge, Mass., MIT Press (1977).

2. "Measurement Uncertainty," ANSI/ASME PTC 19.1, Performance Test Codes Supplement, New York (1983).

3. "Fluid Flow Measurement Uncertainty," ISO TC30 SC9, New York (Jan 1985).

4. O'Day, J. F. and Jones, H. D., "Absolute and Relative Motion Measurements on a Model of a High-Speed Containership," in: *Proceedings of the Twentieth General Meeting of the American Towing Tank Conference*, 2-4 Aug 1983, Hoboken, N.J., pp. 1001-1036, Vol. II, New York (1983).

APPENDIX A

EXPERIMENTAL DATA FOR MODEL A

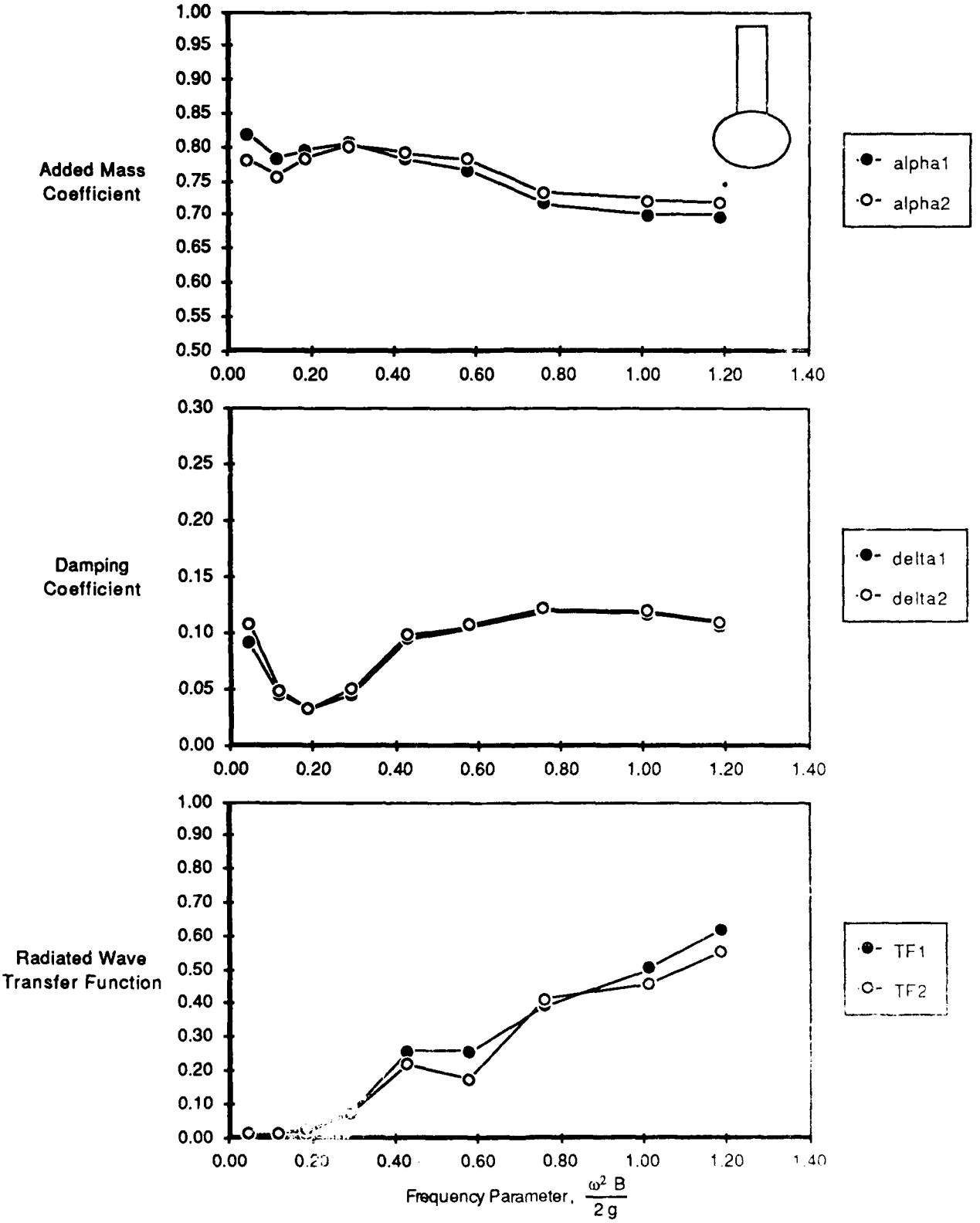

Fig. A1. Data for model A, true ellipse at design draft, for 0.5 inch (1.27 cm) oscillation amplitude.

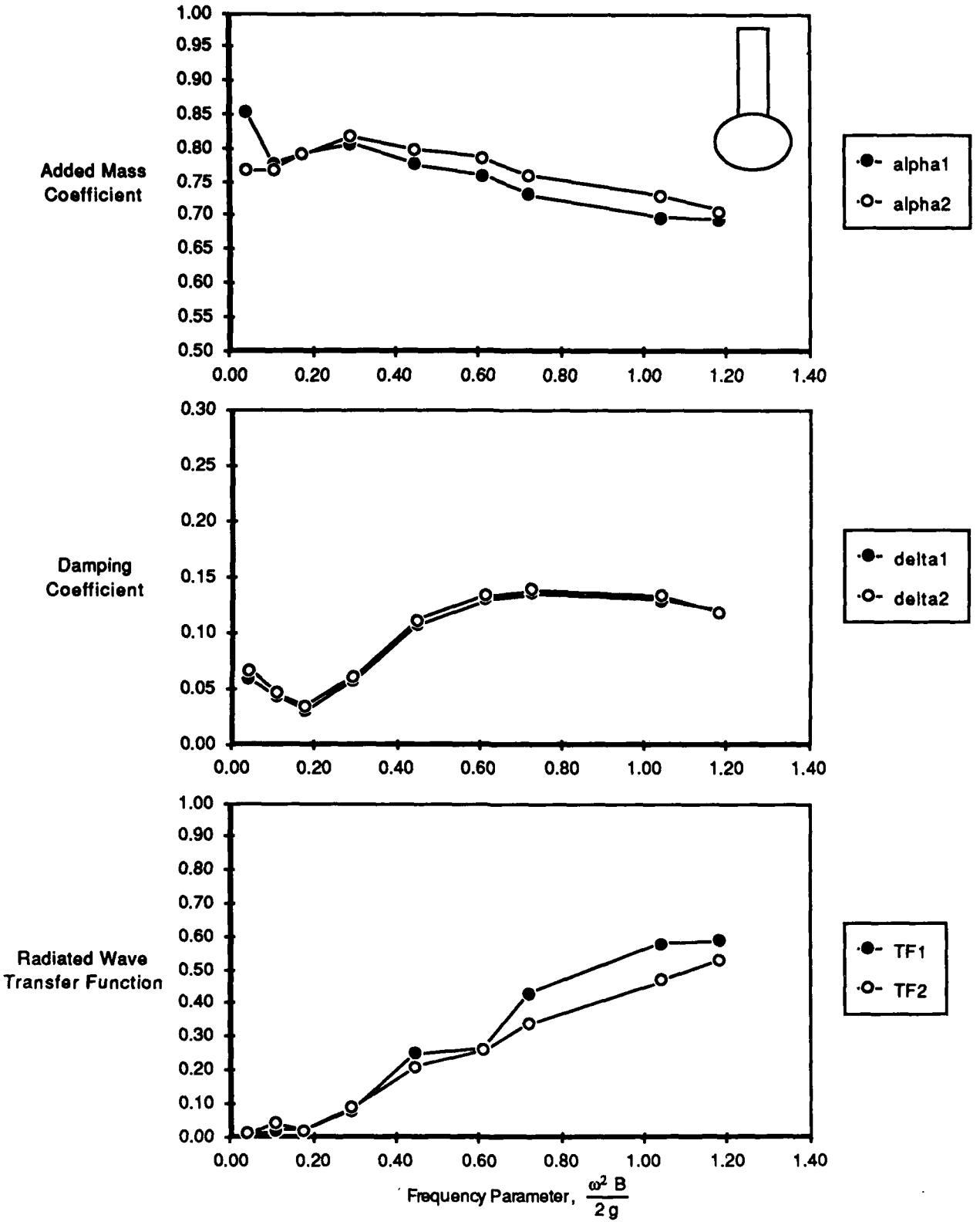

Fig. A2. Data for model A, true ellipse at design draft, for 1 inch (2.54 cm) oscillation amplitude.

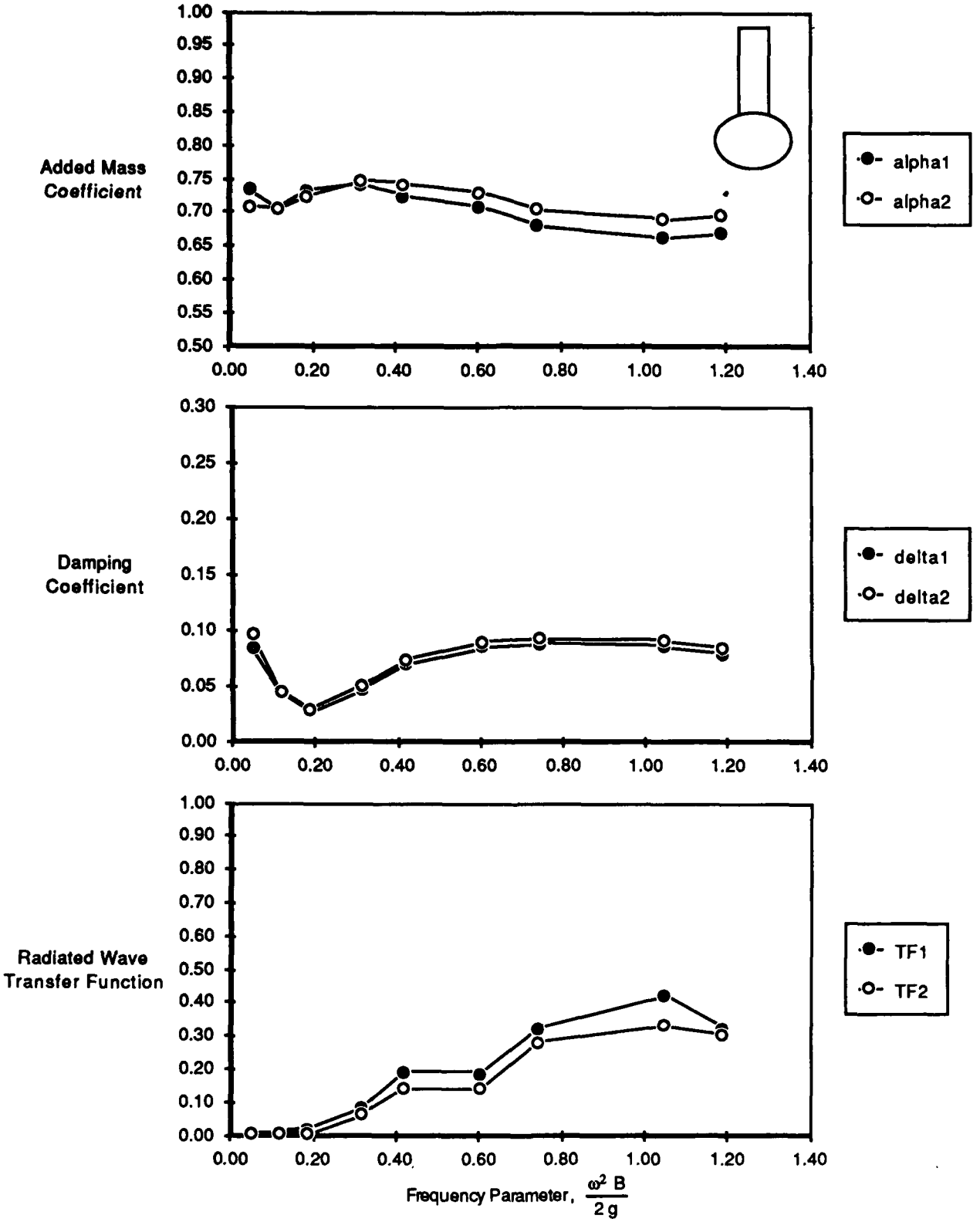

Fig. A3. Data for model A, true ellipse at deep draft, for 0.5 inch (1.27 cm) oscillation amplitude.

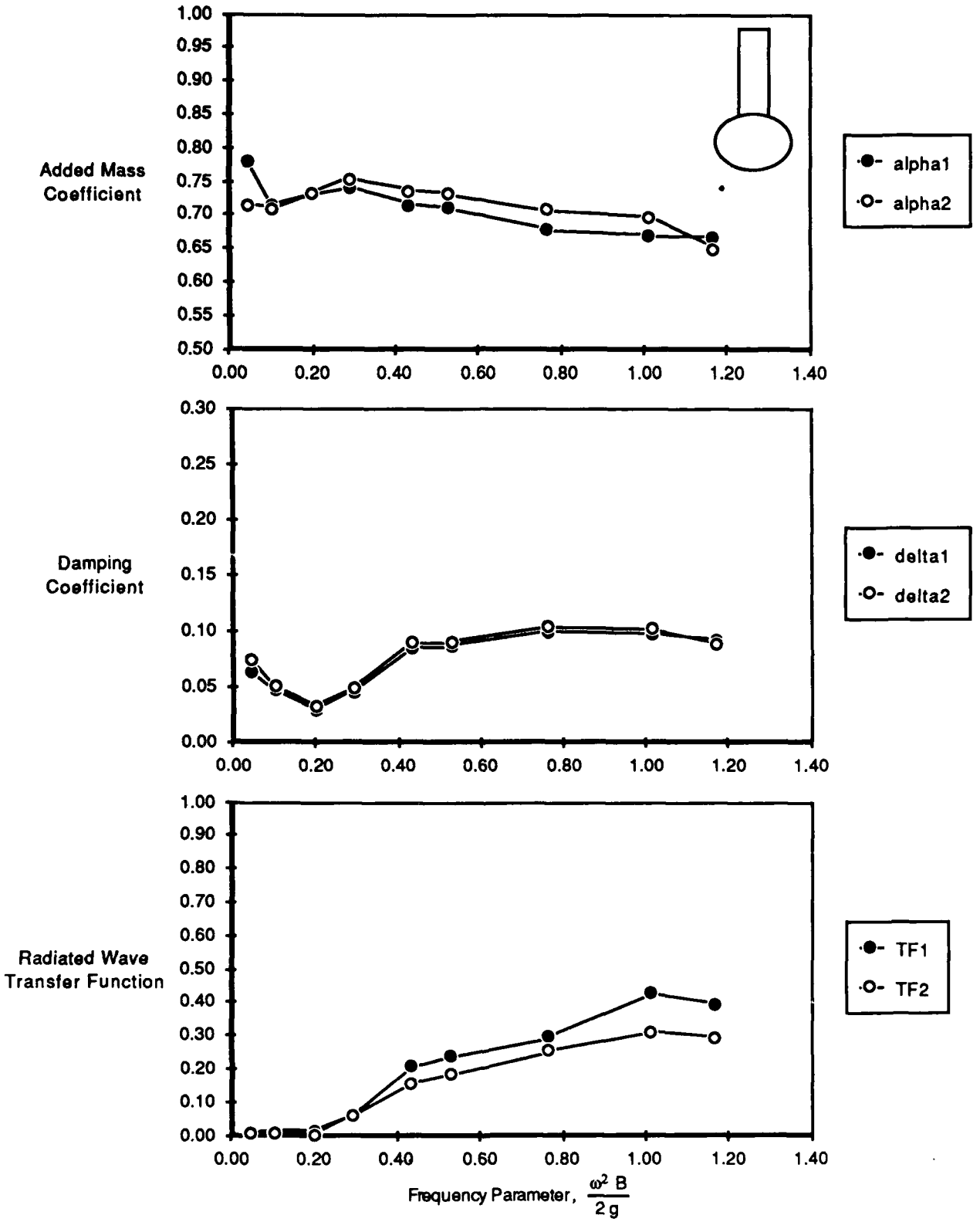

Fig. A4. Data for model A, true ellipse at deep draft, for 1 inch (2.54 cm) oscillation amplitude.

Table A1. Data for Model A, true ellipse at design draft, for 0.5 inch (1.27 cm) oscillation amplitude.

Model Configuration :	A. True Ellipse	
Model Displacement, (lbs.)	125.90	M = 3.92
Gage Wt. Z1, (lbs.)	123.56	M'1 = 3.84
Gage Wt. Z2, (lbs.)	113.41	M'2 = 3.53
Model Draft, (inches)	9.90	
C33, (lbs./ft)	95.22	

Run #	Frequency rad / sec model scale	kB/2	alpha1	delta1	alpha2	delta2
107	1.20	0.02	0.98	0.22	0.81	0.26
108	2.01	0.05	0.82	0.09	0.78	0.11
109	3.16	0.12	0.78	0.05	0.76	0.05
110	4.01	0.19	0.80	0.03	0.78	0.03
111	5.01	0.29	0.81	0.04	0.80	0.05
112	6.07	0.43	0.78	0.09	0.79	0.10
113	7.05	0.58	0.77	0.11	0.78	0.11
114	8.07	0.76	0.72	0.12	0.73	0.12
115	9.31	1.01	0.70	0.12	0.72	0.12
116	10.09	1.19	0.70	0.11	0.72	0.11
117	13.99	2.28	0.73	0.09	0.73	0.09

Table A2. Data for model A, true ellipse at design draft, for 1 inch (2.54 cm) oscillation amplitude.

Model Configuration :	A. True Ellipse	
Model Displacement, (lbs.)	125.90	M = 3.92
Gage Wt. Z1, (lbs.)	123.56	M'1 = 3.84
Gage Wt. Z2, (lbs.)	113.41	M'2 = 3.53
Model Draft, (inches)	9.90	
C33, (lbs./ft)	95.22	

Run #	Frequency rad / sec model scale	kB/2	alpha1	delta1	alpha2	delta2
137	1.09	0.01	0.99	0.10	0.63	0.16
138	1.91	0.04	0.85	0.06	0.77	0.07
139	3.04	0.11	0.78	0.04	0.77	0.05
140	3.90	0.18	0.79	0.03	0.79	0.03
141	5.02	0.29	0.81	0.06	0.82	0.06
142	6.19	0.45	0.78	0.11	0.80	0.11
143	7.25	0.61	0.76	0.13	0.79	0.13
144	7.88	0.72	0.73	0.14	0.76	0.14
145	9.44	1.04	0.70	0.13	0.73	0.13
146	10.06	1.18	0.69	0.12	0.71	0.12
147	14.18	2.34	0.72	0.09		

Table A3. Data for model A, true ellipse at deep draft, for 0.5 inch (1.27 cm) oscillation amplitude.

Model Configuration :	A. True Ellipse	
Model Displacement, (lbs.)	133.84	M = 4.16
Gage Wt. Z1, (lbs.)	131.34	M'1 = 4.08
Gage Wt. Z2, (lbs.)	121.19	M'2 = 3.77
Model Draft, (inches)	10.90	
C33, (lbs./ft)	95.22	

Run #	Frequency rad / sec model scale	kB/2	alpha1	delta1	alpha2	delta2
167	1.15	0.02	0.85	0.25	0.69	0.28
168	2.04	0.05	0.73	0.08	0.71	0.10
169	3.17	0.12	0.71	0.04	0.70	0.05
170	4.01	0.19	0.73	0.03	0.72	0.03
171	5.19	0.31	0.74	0.05	0.75	0.05
172	5.99	0.42	0.72	0.07	0.74	0.07
173	7.19	0.60	0.71	0.09	0.73	0.09
174	7.98	0.74	0.68	0.09	0.70	0.09
175	9.48	1.05	0.66	0.09	0.69	0.09
176	10.09	1.19	0.67	0.08	0.70	0.08
177	14.05	2.30	0.70	0.07		

Table A4. Data for Model A, true ellipse at deep draft, for 1 inch (2.54 cm) oscillation amplitude.

Model Configuration :	A. True Ellipse	
Model Displacement, (lbs.)	133.84	M = 4.16
Gage Wt. Z1, (lbs.)	131.34	M'1 = 4.08
Gage Wt. Z2, (lbs.)	121.19	M'2 = 3.77
Model Draft, (inches)	10.90	
C33, (lbs./ft)	95.22	

Run #	Frequency rad / sec model scale	kB/2	alpha1	delta1	alpha2	delta2
179	1.20	0.02	0.94	0.12	0.69	0.15
180	2.01	0.05	0.78	0.06	0.72	0.07
181	3.00	0.11	0.72	0.05	0.71	0.05
182	4.14	0.20	0.73	0.03	0.73	0.03
183	5.00	0.29	0.74	0.05	0.75	0.05
184	6.10	0.43	0.72	0.08	0.74	0.09
185	6.75	0.53	0.71	0.09	0.73	0.09
186	8.10	0.76	0.68	0.10	0.71	0.10
187	9.32	1.01	0.67	0.10	0.70	0.10
188	10.01	1.17	0.67	0.09	0.65	0.09
189	14.17	2.34	0.70	0.09		

APPENDIX B

EXPERIMENTAL DATA FOR MODEL B

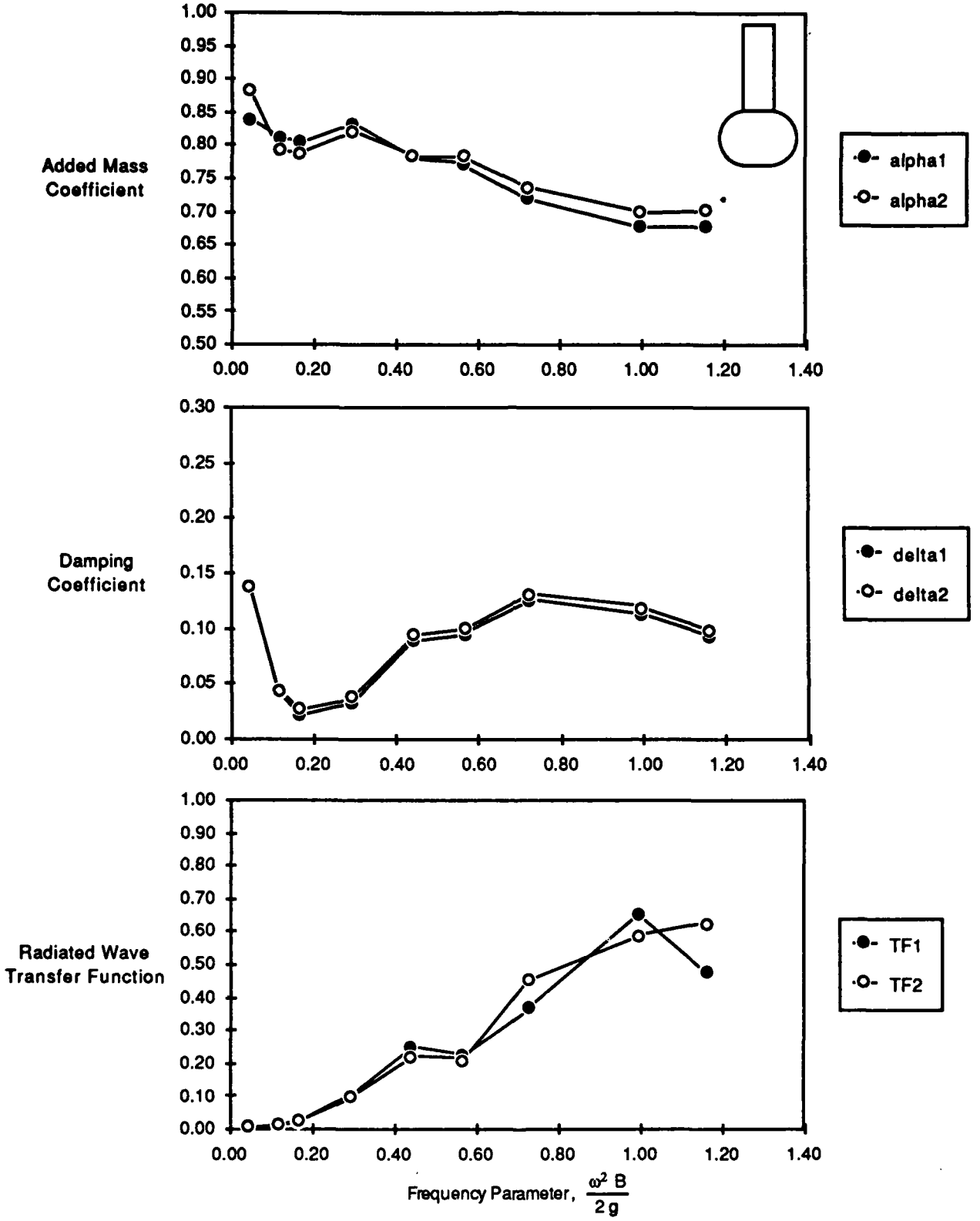

Fig. B1. Data for model B, T-AGOS 19 semi-circle at design draft, for 0.25 inch (0.635 cm) oscillation amplitude.

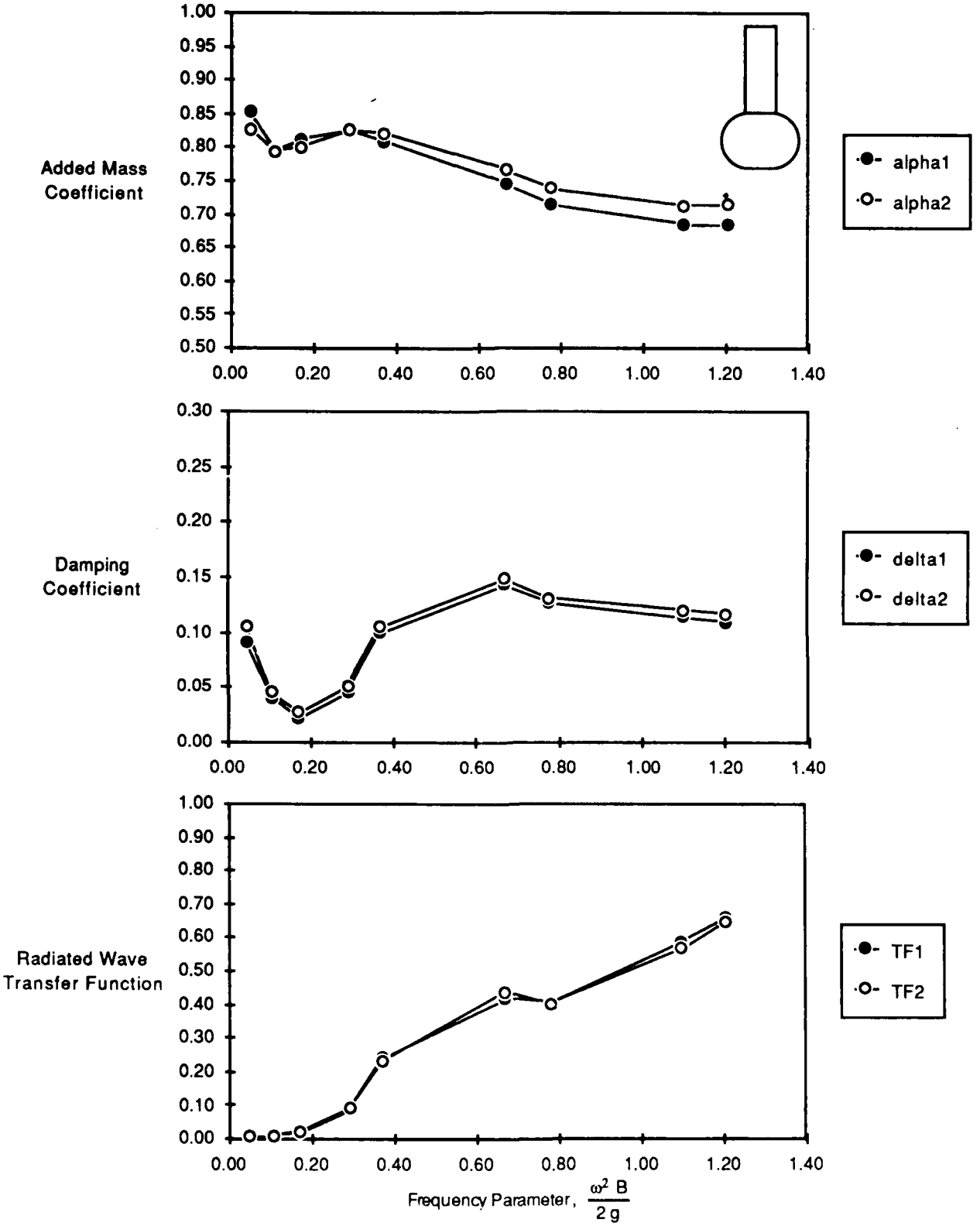

Fig. B2. Data for model B, T-AGOS 19 semi-circle at design draft, for 0.5 inch (1.27 cm) oscillation amplitude.

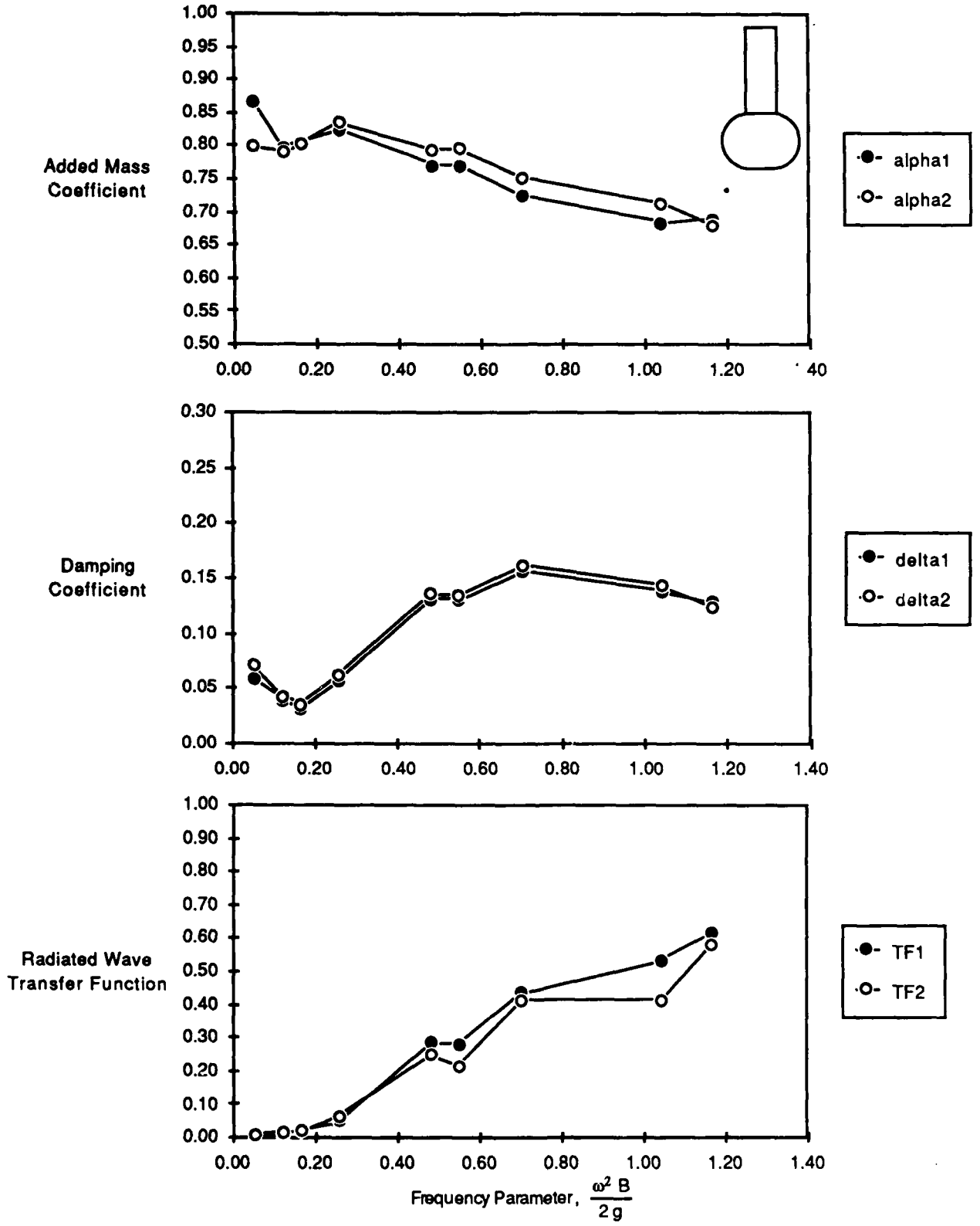

Fig. B3. Data for model B, T-AGOS 19 semi-circle at design draft, for 1 inch (2.54 cm) oscillation amplitude.

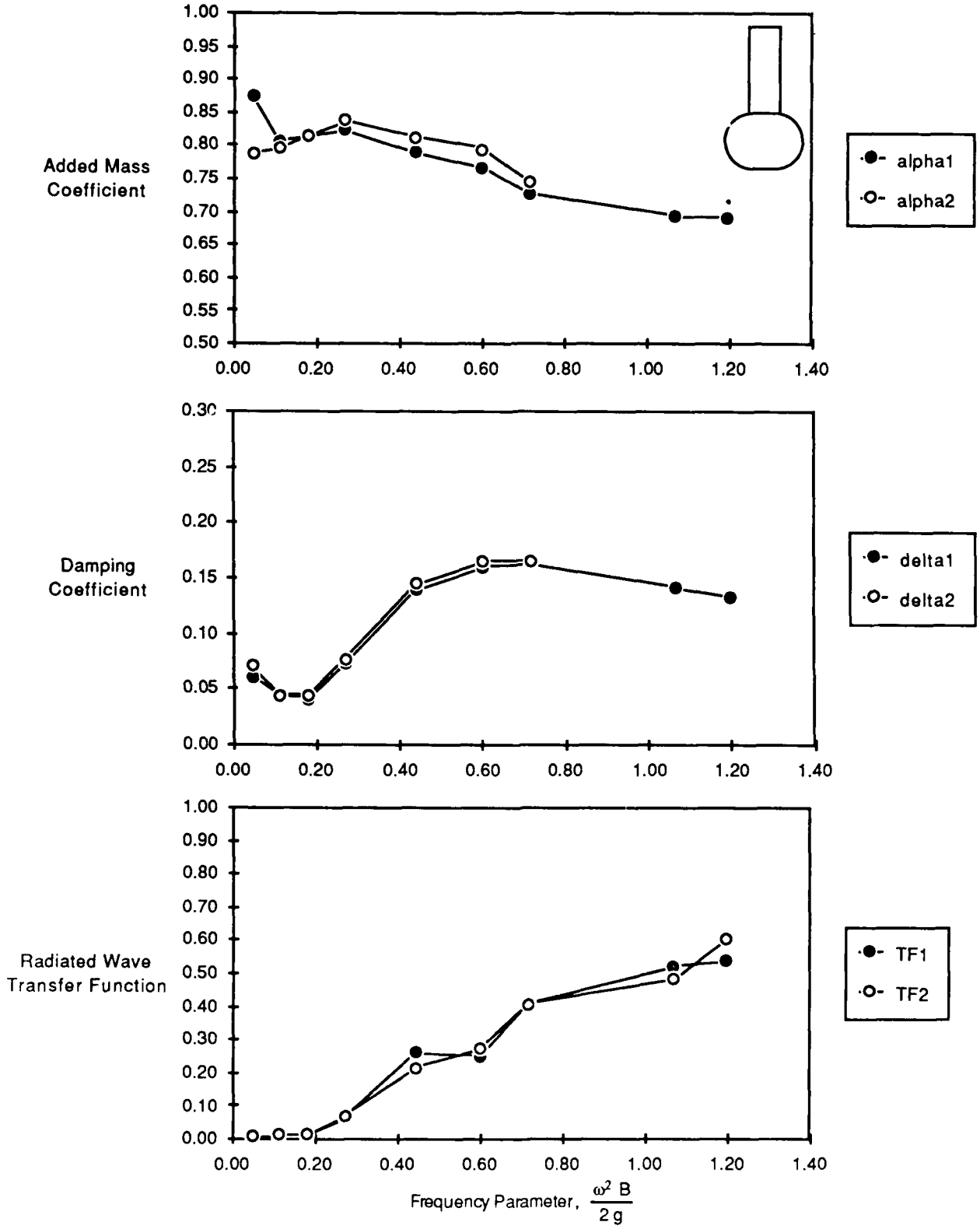

Fig. B4. Data for model B, T-AGOS 19 semi-circle at design draft, for 1.5 inch (3.81 cm) oscillation amplitude.

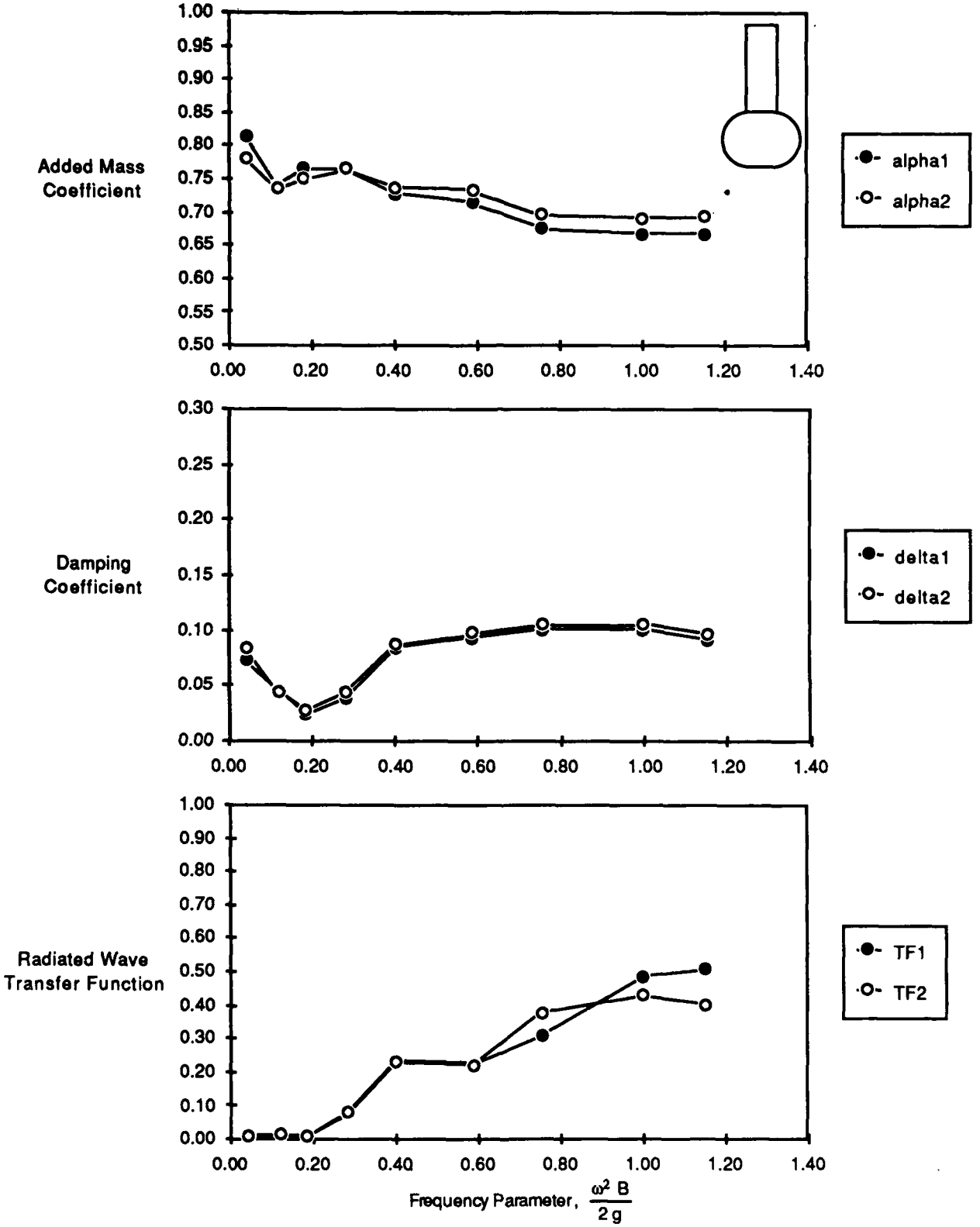

Fig. B5. Data for model B, T-AGOS 19 semi-circle at deep draft, for 0.5 inch (1.27 cm) oscillation amplitude.

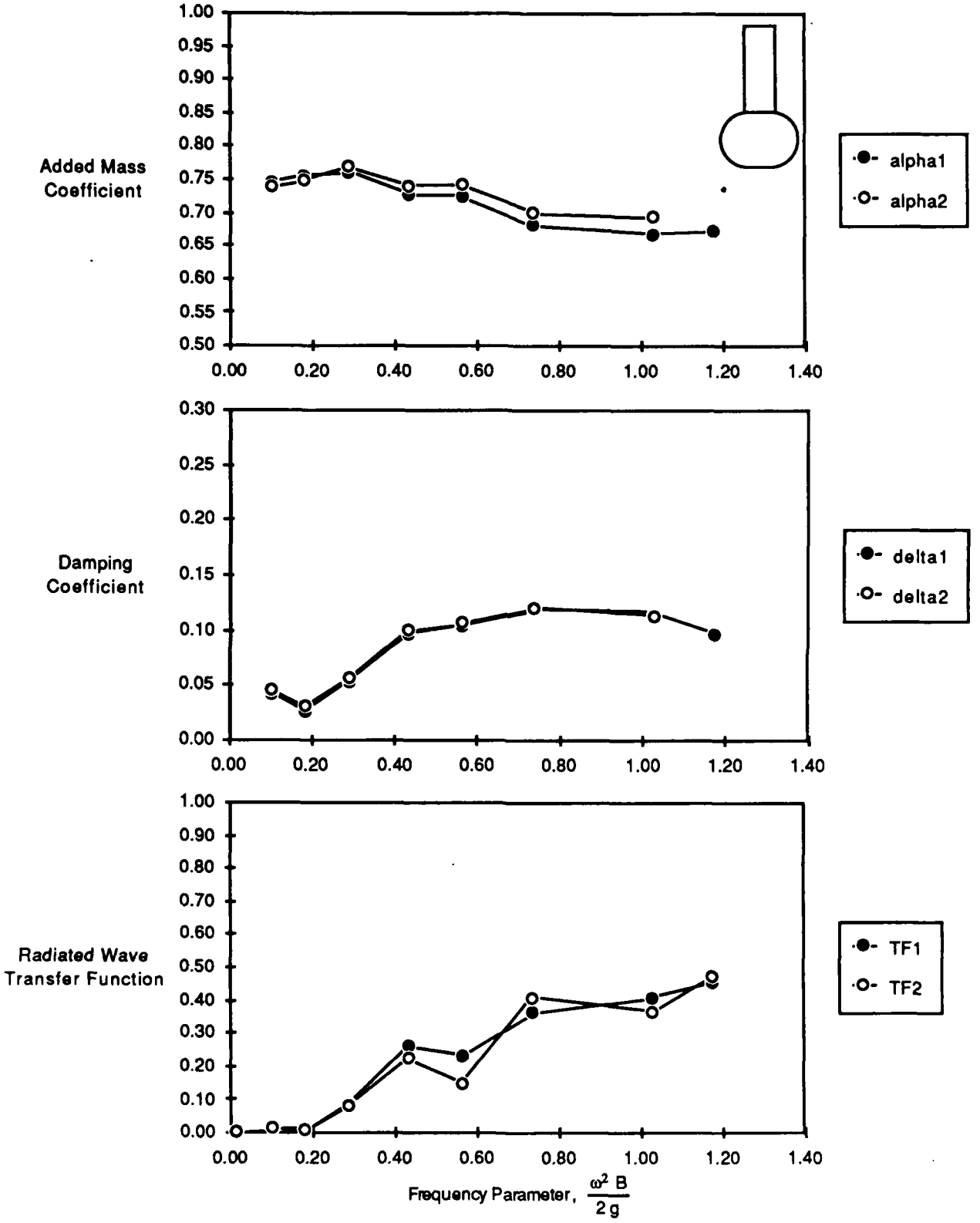

Fig. B6. Data for model B, T-AGOS 19 semi-circle at deep draft, for 1 inch (2.54 cm) oscillation amplitude.

Table B1. Data for model B, T-AGOS 19 semi-circle at design draft, for 0.25 inch (0.635 cm) oscillation amplitude.

Model Configuration :	B. TAGOS 19 Semi-Circle	
Model Displacement, (lbs.)	132.80	M = 4.13
Gage Wt. Z1, (lbs.)	132.95	M'1 = 4.13
Gage Wt. Z2, (lbs.)	122.80	M'2 = 3.82
Model Draft, (inches)	9.90	
C33, (lbs./ft)	96.51	

Run #	Frequency rad / sec model scale	kB/2	alpha1	delta1	alpha2	delta2
57	1.06	0.01	1.07	0.45	1.16	0.47
58	1.93	0.04	0.84	0.14	0.88	0.14
59	3.12	0.11	0.81	0.04	0.79	0.05
60	3.78	0.17	0.81	0.02	0.79	0.03
61	5.00	0.29	0.83	0.03	0.82	0.04
62	6.14	0.44	0.78	0.09	0.78	0.09
63	6.96	0.56	0.77	0.10	0.78	0.10
64	7.87	0.72	0.72	0.13	0.74	0.13
65	9.23	0.99	0.68	0.11	0.70	0.12
66	9.96	1.16	0.68	0.09	0.70	0.10
67	13.92	2.26	0.72	0.09	0.75	0.09

Table B2. Data for model B, T-AGOS 19 semi-circle at design draft, for 0.5 inch (1.27 cm) oscillation amplitude.

Model Configuration :	B. TAGOS 19 Semi Circle	
Model Displacement, (lbs.)	132.80	M = 4.13
Gage Wt. Z1, (lbs.)	132.95	M'1 = 4.13
Gage Wt. Z2, (lbs.)	122.80	M'2 = 3.82
Model Draft, (inches)	9.90	
C33, (lbs./ft)	96.51	

Run #	Frequency rad / sec model scale	kB/2	alpha1	delta1	alpha2	delta2
14	1.02	0.01	1.18	0.30	0.95	0.33
15	1.98	0.05	0.85	0.09	0.83	0.11
16	3.01	0.11	0.80	0.04	0.79	0.05
17	3.82	0.17	0.81	0.02	0.80	0.03
18	4.98	0.29	0.83	0.05	0.83	0.05
19	5.63	0.37	0.81	0.10	0.82	0.11
20	7.57	0.67	0.74	0.14	0.77	0.15
21	8.16	0.78	0.71	0.13	0.74	0.13
22	9.70	1.10	0.69	0.11	0.71	0.12
23	10.15	1.20	0.69	0.11	0.71	0.12

Table B3. Data for model B, TAGOS-19 semi-circle at design draft, for 1 inch (2.54 cm) oscillation amplitude.

Model Configuration :	B. TAGOS 19 Semi-Circle		
Model Displacement, (lbs.)	132.80	M = 4.13	
Gage Wt. Z1, (lbs.)	132.95	M'1 = 4.13	
Gage Wt. Z2, (lbs.)	122.80	M'2 = 3.82	
Model Draft, (inches)	9.90		
C33, (lbs./ft)	96.51		

Run #	Frequency rad / sec model scale	kB/2	alpha1	delta1	alpha2	delta2
57	1.06	0.01	1.07	0.45	1.16	0.47
58	1.93	0.04	0.84	0.14	0.88	0.14
59	3.12	0.11	0.81	0.04	0.79	0.05
60	3.78	0.17	0.81	0.02	0.79	0.03
61	5.00	0.29	0.83	0.03	0.82	0.04
62	6.14	0.44	0.78	0.09	0.78	0.09
63	6.96	0.56	0.77	0.10	0.78	0.10
64	7.37	0.72	0.72	0.13	0.74	0.13
65	9.23	0.99	0.68	0.11	0.70	0.12
66	9.96	1.16	0.68	0.09	0.70	0.10
67	13.92	2.26	0.72	0.09	0.75	0.09

Table B4. Data for model B, T-AGOS 19 semi-circle at design draft, for 1.5 inch (3.81 cm) oscillation amplitude.

Model Configuration :	B. TAGOS 19 Semi-Circle		
Model Displacement, (lbs.)	132.80	M = 4.13	
Gage Wt. Z1, (lbs.)	132.95	M'1 = 4.13	
Gage Wt. Z2, (lbs.)	122.80	M'2 = 3.82	
Model Draft, (inches)	9.90		
C33, (lbs./ft)	96.51		

Run #	Frequency rad / sec model scale	kB/2	alpha1	delta1	alpha2	delta2
45	0.89	0.01	1.32	0.13	0.75	0.18
46	1.99	0.05	0.87	0.06	0.79	0.07
47	3.07	0.11	0.81	0.04	0.80	0.05
48	3.92	0.18	0.81	0.04	0.81	0.04
49	4.80	0.27	0.82	0.07	0.84	0.08
50	6.14	0.44	0.79	0.14	0.81	0.15
51	7.17	0.60	0.77	0.16	0.80	0.17
52	7.83	0.71	0.73	0.16	0.74	0.17
53	9.56	1.07	0.69	0.14	-0.67	0.00
54	10.12	1.19	0.69	0.13	-0.70	0.00
55	13.89	2.25	0.74	0.11	-0.80	0.00

Table B5. Data for model B, T-AGOS 19 semi-circle at deep draft, for 0.5 inch (1.27cm) oscillation amplitude.

Model Configuration :	B. TAGOS 19 Semi-Circle	
Model Displacement, (lbs.)	140.84	M = 4.38
Gage Wt. Z1, (lbs.)	140.73	M'1 = 4.38
Gage Wt. Z2, (lbs.)	130.58	M'2 = 4.06
Model Draft, (inches)	10.90	
C33, (lbs./ft)	96.51	

Run #	Frequency rad / sec model scale	kB/2	alpha1	delta1	alpha2	delta2
69	1.06	0.01	1.14	0.24	0.92	0.25
70	1.91	0.04	0.81	0.07	0.78	0.08
71	3.19	0.12	0.74	0.05	0.74	0.05
72	3.95	0.18	0.77	0.02	0.75	0.03
73	4.92	0.28	0.76	0.04	0.77	0.04
74	5.85	0.40	0.73	0.08	0.74	0.09
75	7.10	0.59	0.71	0.09	0.73	0.10
76	8.05	0.76	0.68	0.10	0.70	0.11
77	9.26	1.00	0.67	0.10	0.69	0.11
78	9.93	1.15	0.67	0.09	0.69	0.10
79	13.98	2.28	0.71	0.09		

Table B6. Data for model B, T-AGOS 19 semi circle at deep draft, for 1 inch (2.54 cm) oscillation amplitude.

Model Configuration :	B. TAGOS 19 Semi-Circle	
Model Displacement, (lbs.)	140.84	M = 4.38
Gage Wt. Z1, (lbs.)	140.73	M'1 = 4.38
Gage Wt. Z2, (lbs.)	130.58	M'2 = 4.06
Model Draft, (inches)	10.90	
C33, (lbs./ft)	96.51	

Run #	Frequency rad / sec model scale	kB/2	alpha1	delta1	alpha2	delta2
81	1.02	0.01	1.23	0.14	0.91	0.19
83	2.96	0.10	0.75	0.04	0.74	0.05
84	3.94	0.18	0.75	0.03	0.75	0.03
85	4.97	0.29	0.76	0.05	0.77	0.06
86	6.08	0.43	0.73	0.10	0.74	0.10
87	6.95	0.56	0.72	0.10	0.74	0.11
88	7.95	0.74	0.68	0.12	0.70	0.12
89	9.38	1.03	0.67	0.12	0.69	0.11
90	10.03	1.17	0.67	0.10		
91	13.90	2.25	0.70	0.09		

APPENDIX C

EXPERIMENTAL DATA FOR MODEL C

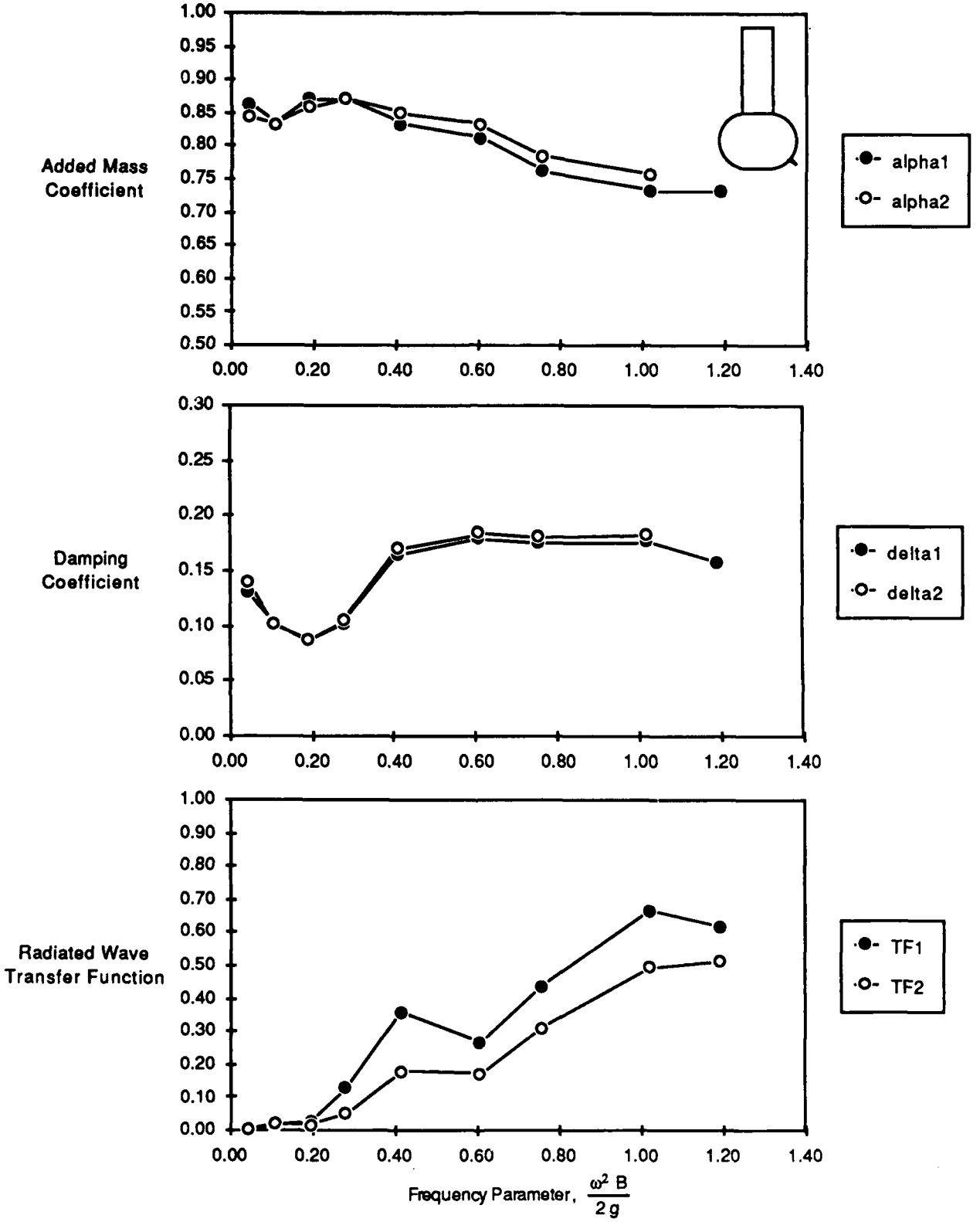

Fig. C1. Data for model C, semi-circle with bilge keel at design draft, for 0.5 inch (1.27 cm) oscillation amplitude.

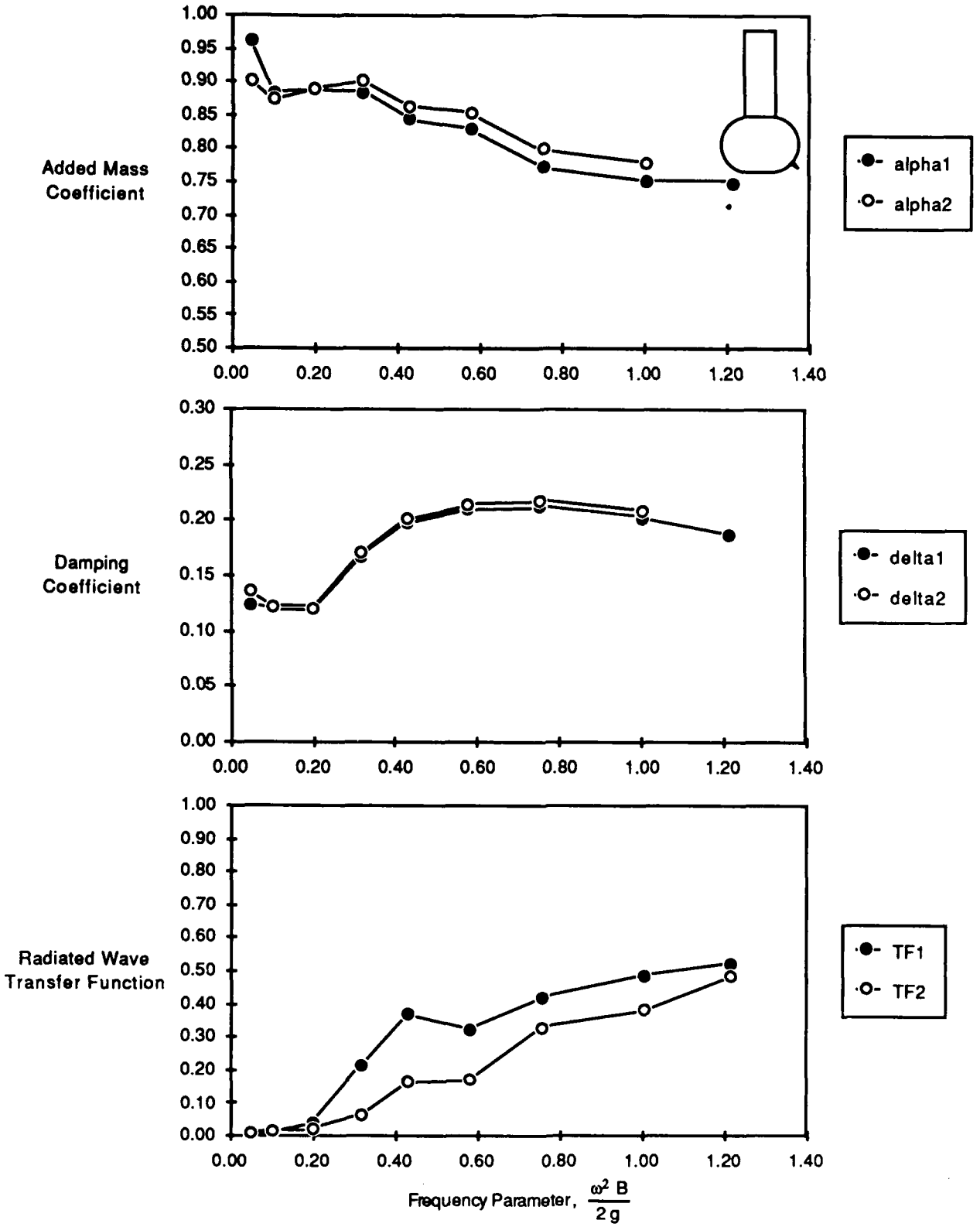

Fig. C2. Data for model C, semi-circle with bilge keel at design draft, for 1 inch (2.54 cm) oscillation amplitude.

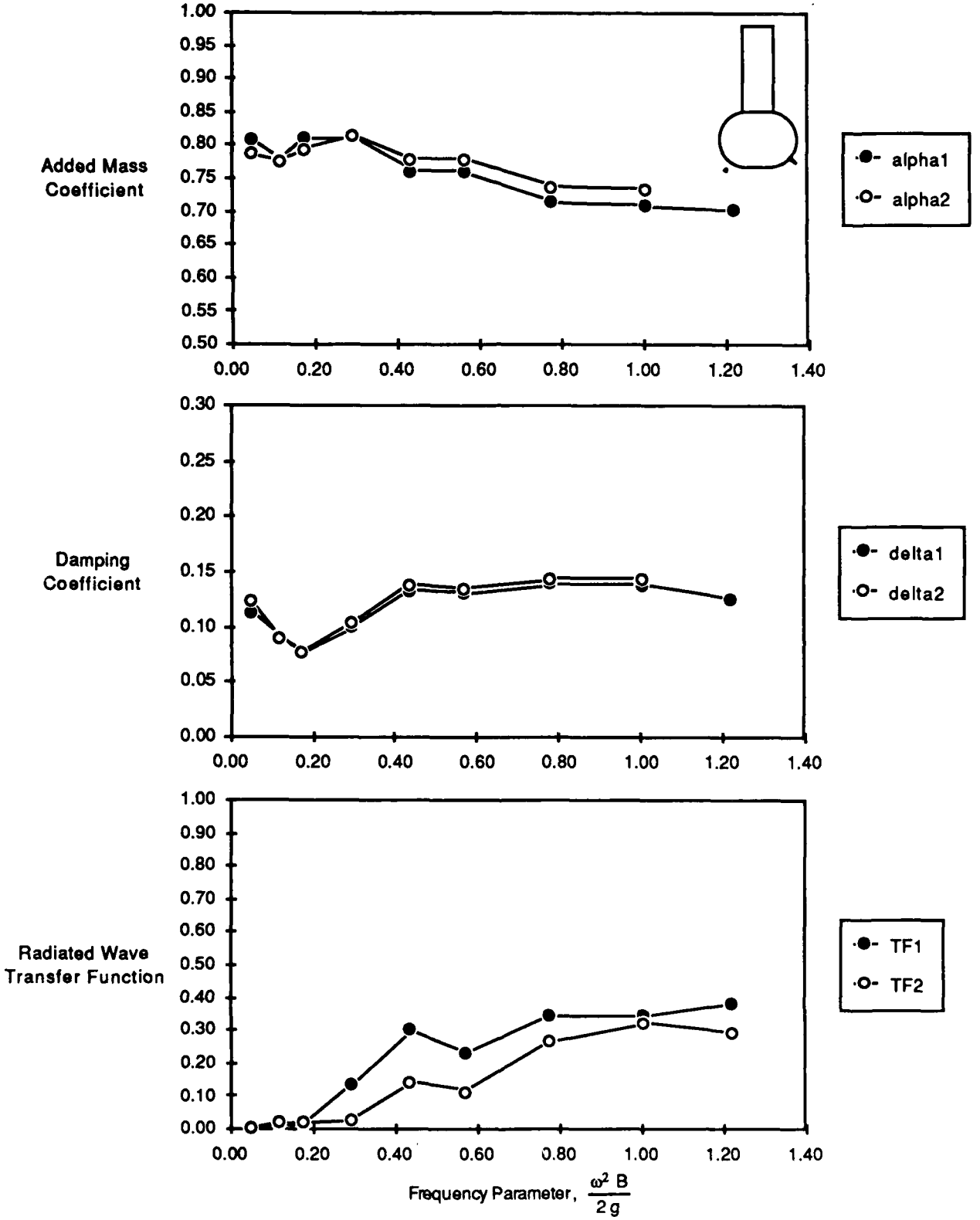

Fig. C3. Data for model C, semi-circle with bilge keel at deep draft, for 0.5 inch (1.27 cm) oscillation amplitude.

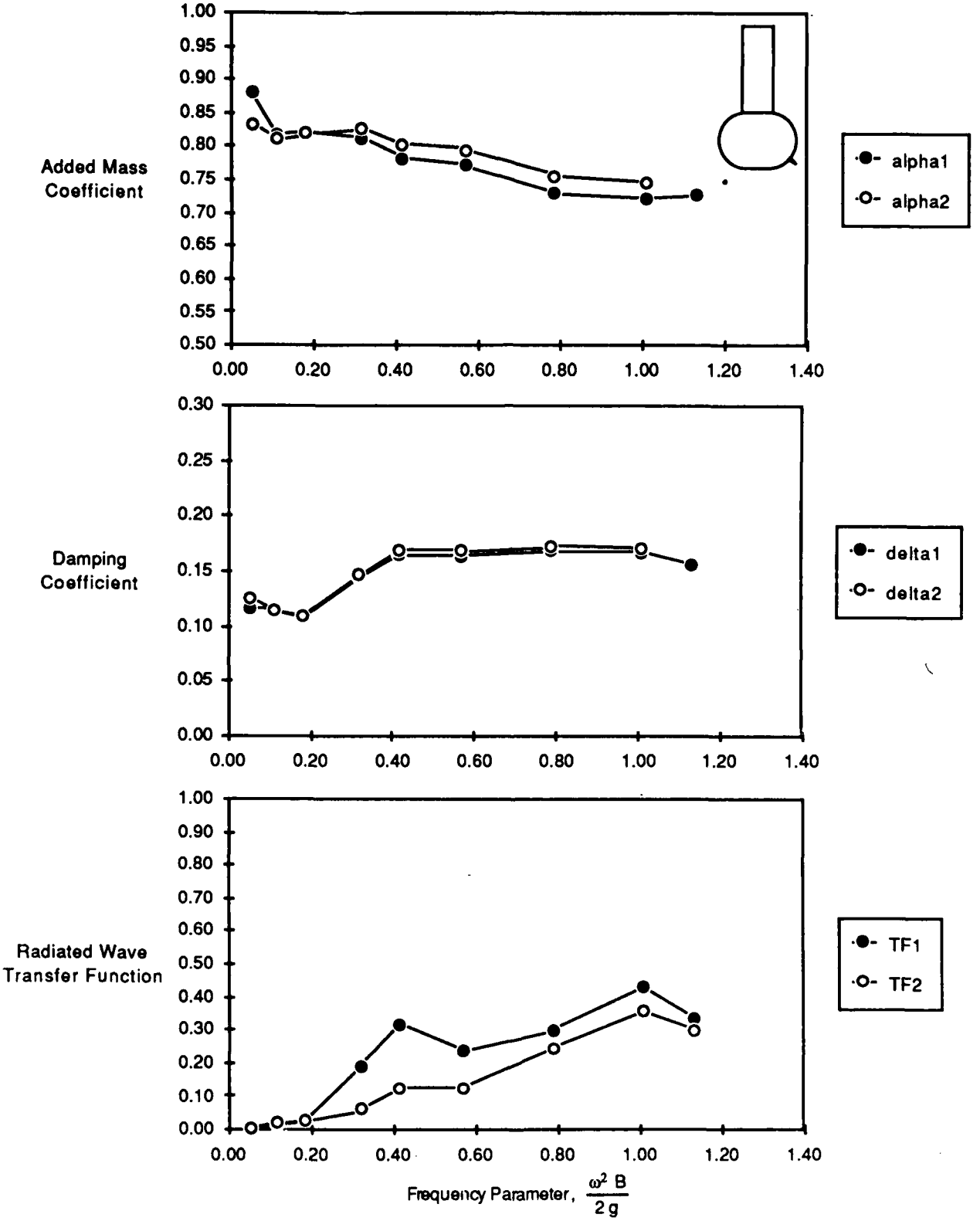

Fig. C4. Data for model C, semi-circle with bilge keel at deep draft, for 1 inch (2.54 cm) oscillation amplitude.

Table C1. Data for model C, semi-circle with bilge keel, at design draft, for 0.5 inch (1.27 cm) oscillation amplitude.

Model Configuration :	C. Semi-Circle w/ Bilge Keel					
Model Displacement, (lbs.)	133.13	M = 4.14				
Gage Wt. Z1, (lbs.)	133.28	M'1 = 4.14				
Gage Wt. Z2, (lbs.)	123.13	M'2 = 3.83				
Model Draft, (inches)	9.90					
C33, (lbs./ft)	96.51					
Run #	Frequency rad / sec model scale	kB/2	alpha1	delta1	alpha2	delta2
203	1.21	0.02	0.99	0.25	0.87	0.29
204	1.95	0.04	0.86	0.13	0.84	0.14
205	3.01	0.11	0.84	0.10	0.83	0.10
206	4.05	0.19	0.87	0.09	0.86	0.09
207	4.87	0.28	0.87	0.10	0.87	0.11
208	5.94	0.41	0.83	0.17	0.85	0.17
209	7.20	0.61	0.81	0.18	0.83	0.18
210	8.04	0.75	0.76	0.18	0.79	0.18
211	9.35	1.02	0.73	0.18	0.76	0.18
212	10.09	1.19	0.73	0.16	0.76	0.16
213	13.65	2.17	0.76	0.13		

Table C2. Data for model C, semi-circle with bilge keel at design draft, for 1 inch (2.54 cm) oscillation amplitude.

Model Configuration :	C. Semi-Circle w/ Bilge Keel					
Model Displacement, (lbs.)	133.13	M = 4.14				
Gage Wt. Z1, (lbs.)	133.28	M'1 = 4.14				
Gage Wt. Z2, (lbs.)	123.13	M'2 = 3.83				
Model Draft, (inches)	9.90					
C33, (lbs./ft)	96.51					
Run #	Frequency rad / sec model scale	kB/2	alpha1	delta1	alpha2	delta2
191	1.00	0.01	1.37	0.25	1.02	0.30
192	1.99	0.05	0.96	0.12	0.90	0.14
193	2.93	0.10	0.88	0.12	0.87	0.12
194	4.11	0.20	0.89	0.12	0.89	0.12
195	5.21	0.32	0.88	0.17	0.90	0.17
196	6.06	0.43	0.84	0.20	0.86	0.20
197	7.04	0.58	0.83	0.21	0.85	0.21
198	8.04	0.75	0.77	0.21	0.80	0.22
199	9.27	1.00	0.75	0.20	0.78	0.21
200	10.20	1.21	0.75	0.19		
201	13.84	2.23	0.78	0.16		

Table C3. Data for model C, semi-circle with bilge keel at deep draft, for 0.5 inch (1.27 cm) oscillation amplitude.

Model Configuration :	C. Semi-Circle w/ Bilge Keel	
Model Displacement, (lbs.)	141.17	M = 4.39
Gage Wt. Z1, (lbs.)	141.06	M'1 = 4.39
Gage Wt. Z2, (lbs.)	130.91	M'2 = 4.07
Model Draft, (inches)	10.90	
C33, (lbs./ft)	96.51	

Run #	Frequency rad / sec model scale	kB/2	alpha1	delta1	alpha2	delta2
215	1.09	0.01	1.05	0.25	0.88	0.29
216	2.04	0.05	0.81	0.11	0.79	0.12
217	3.18	0.12	0.78	0.09	0.78	0.09
218	3.85	0.17	0.81	0.08	0.79	0.08
219	5.01	0.29	0.81	0.10	0.82	0.10
220	6.10	0.43	0.76	0.13	0.78	0.14
221	6.98	0.57	0.76	0.13	0.78	0.13
222	8.16	0.78	0.71	0.14	0.74	0.14
223	9.28	1.00	0.71	0.14	0.73	0.14
224	10.22	1.22	0.70	0.12	0.73	0.13
225	14.02	2.29	0.73	0.13		

Table C4. Data for model C, semi-circle with bilge keel at deep draft, for 1 inch (2.54 cm) oscillation amplitude.

Model Configuration :	C. Semi-Circle w/ Bilge Keel	
Model Displacement, (lbs.)	141.17	M = 4.39
Gage Wt. Z1, (lbs.)	141.06	M'1 = 4.39
Gage Wt. Z2, (lbs.)	130.91	M'2 = 4.07
Model Draft, (inches)	10.90	
C33, (lbs./ft)	96.51	

Run #	Frequency rad / sec model scale	kB/2	alpha1	delta1	alpha2	delta2
227	1.10	0.01	1.19	0.19	0.91	0.24
228	2.09	0.05	0.88	0.12	0.83	0.13
229	3.11	0.11	0.82	0.11	0.81	0.11
230	3.94	0.18	0.82	0.11	0.82	0.11
231	5.23	0.32	0.81	0.14	0.83	0.15
232	5.96	0.41	0.78	0.16	0.80	0.17
233	6.98	0.57	0.77	0.16	0.79	0.17
234	8.21	0.79	0.73	0.17	0.76	0.17
235	9.30	1.01	0.72	0.17	0.75	0.17
236	9.85	1.13	0.73	0.16		
237	14.10	2.32	0.77	0.16		

APPENDIX D

EXPERIMENTAL DATA FOR MODEL D

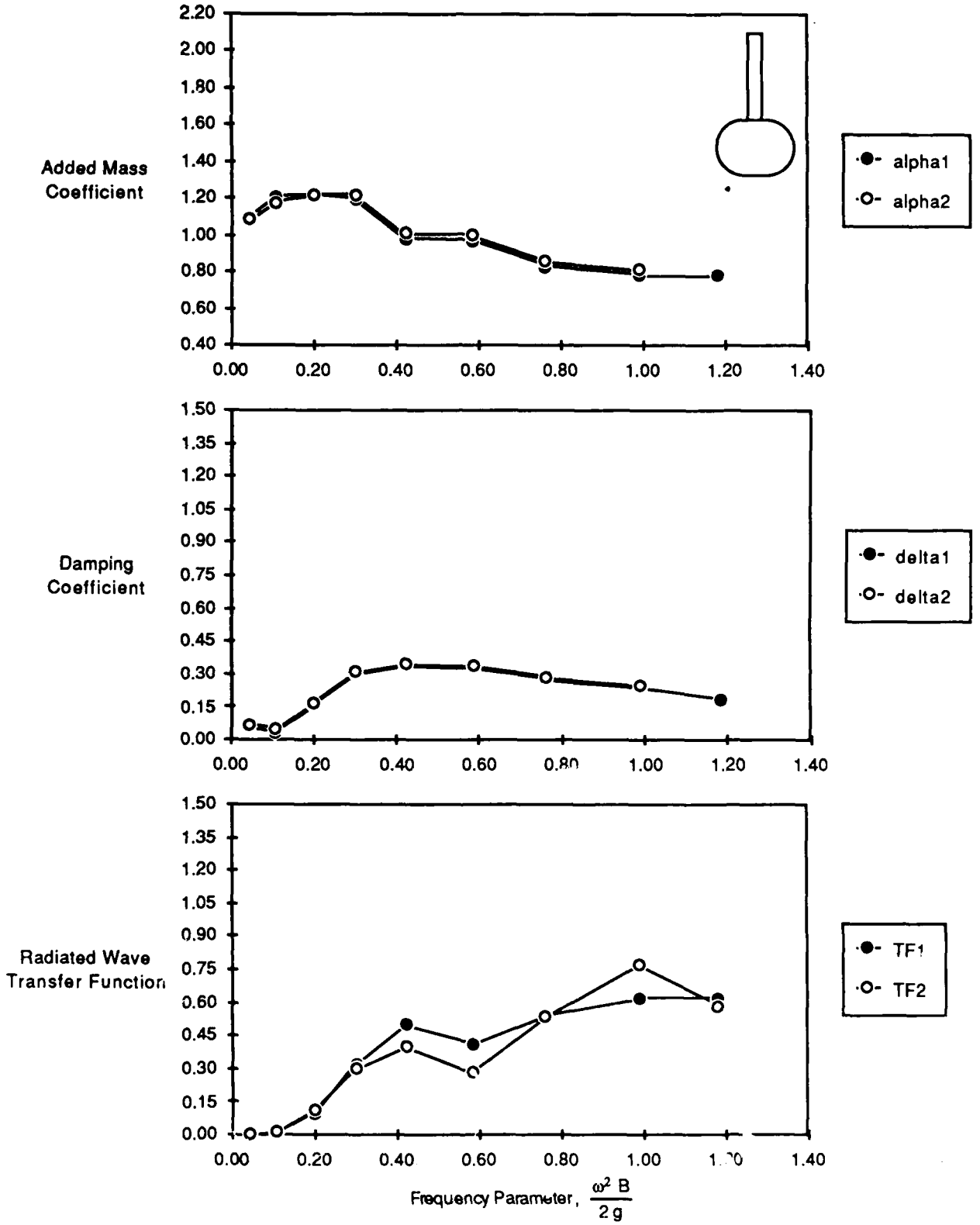

Fig. D1. Data for model D, semi-circle with thin strut at design draft, for 0.5 inch (1.27 cm) oscillation amplitude.

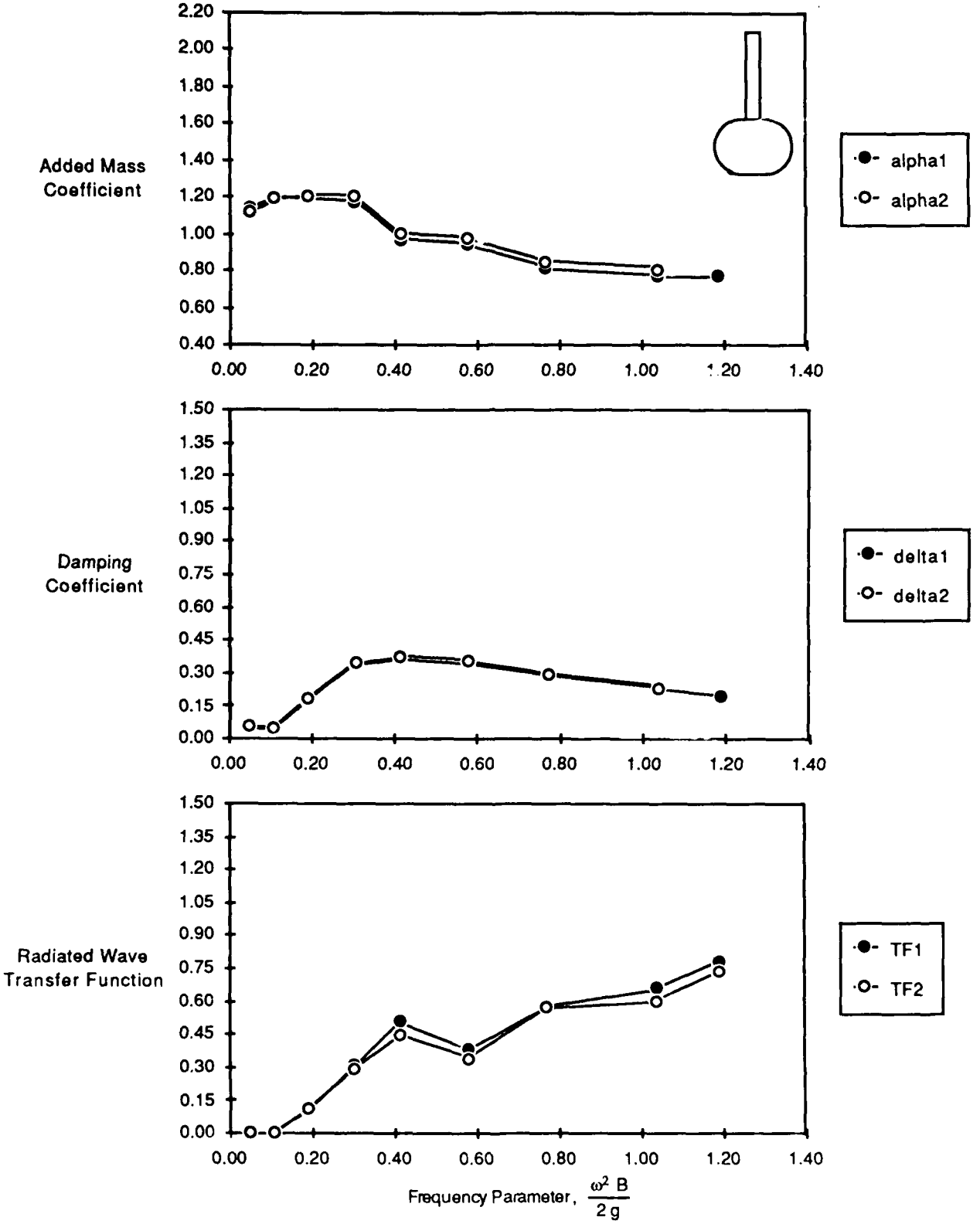

Fig. D2. Data for model D, semi-circle with thin strut at design ddraft, for 1 inch (2.54 cm) oscillation amplitude.

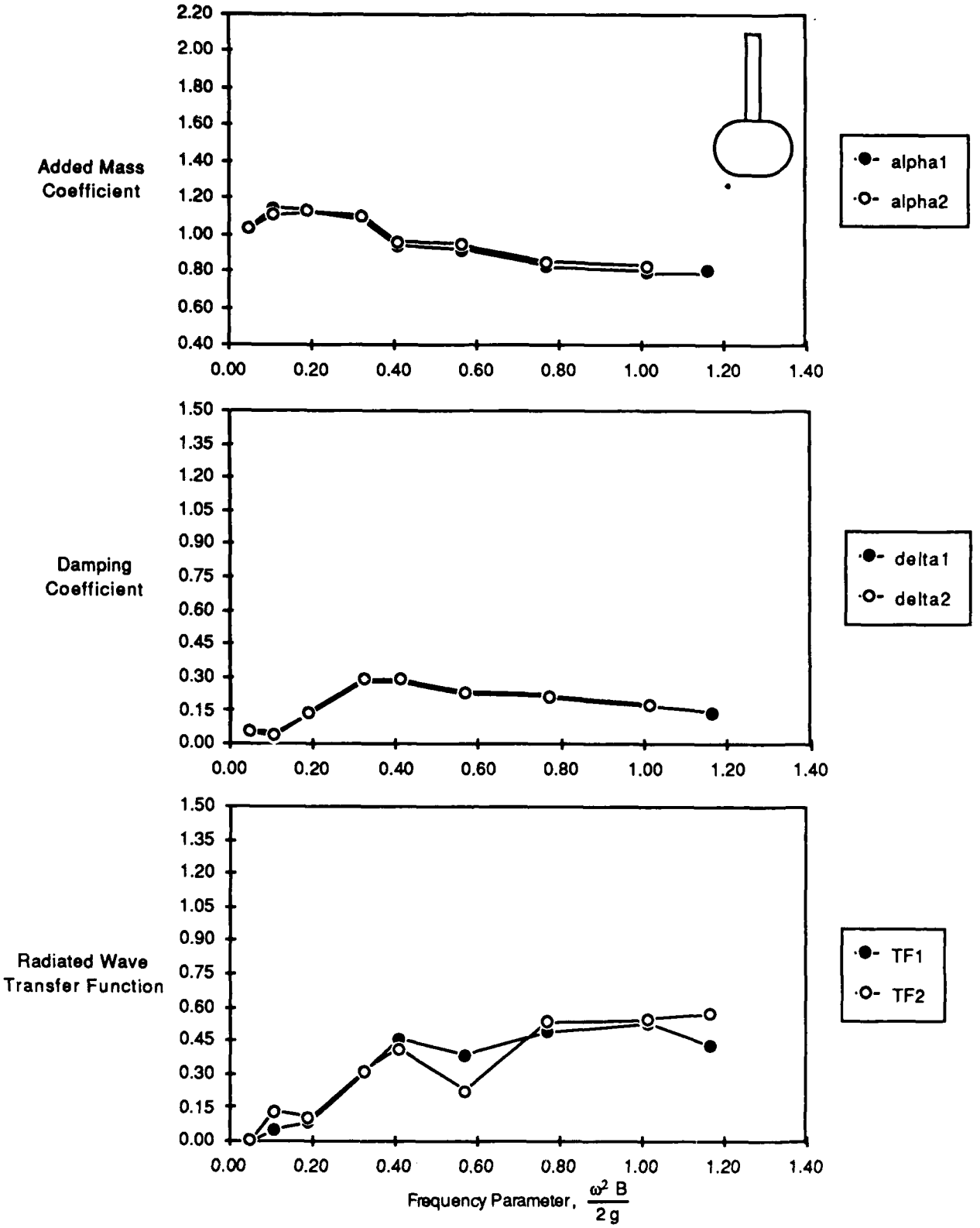

Fig. D3. Data for model D, semi-circle with thin strut at deep draft, for 0.5 inch (1.27 cm) oscillation amplitude.

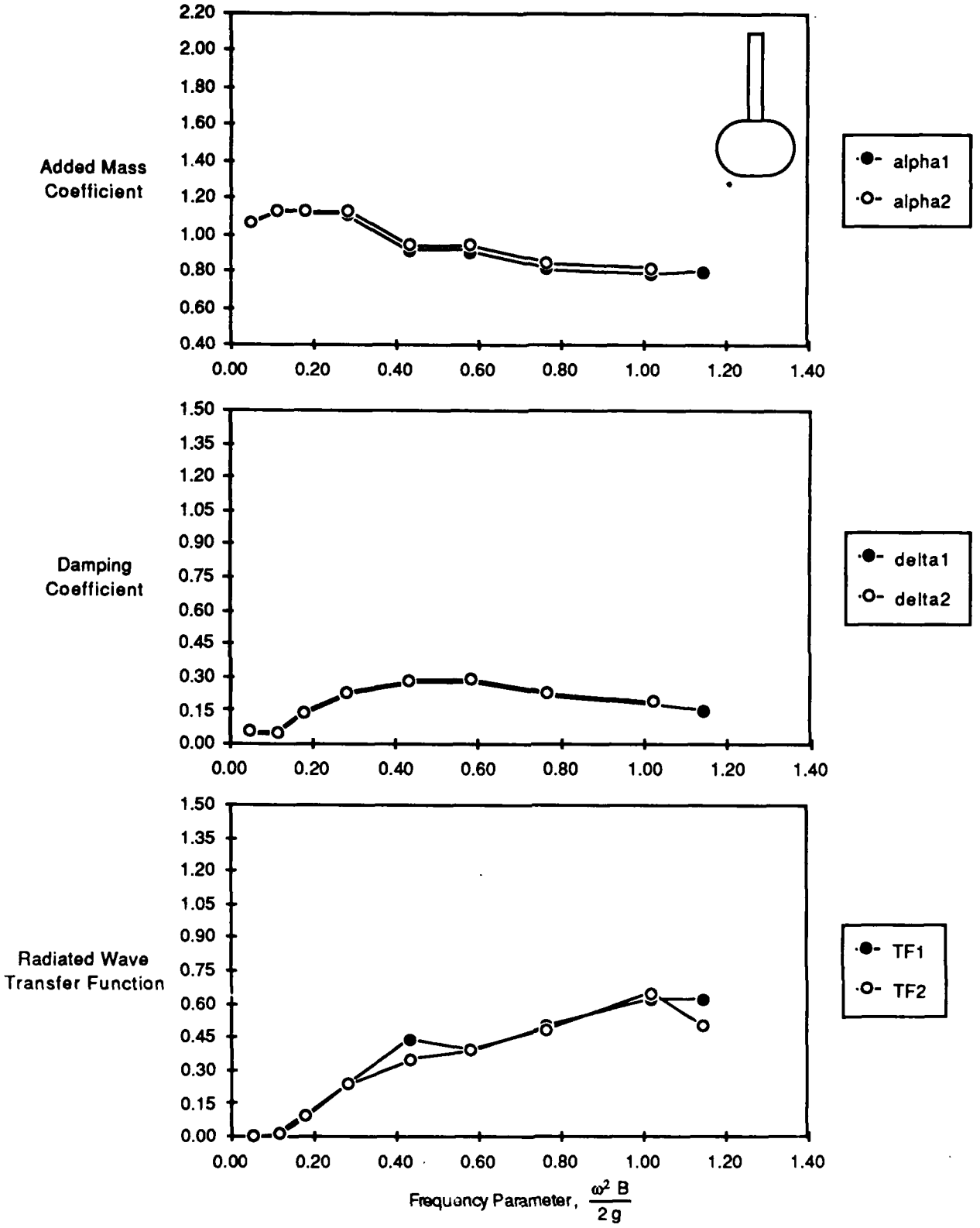

Fig. D4. Data for model D, semi-circle with thin strut at deep draft, for 1 inch (2.54 cm) oscillation amplitude.

Table D1. Data for model D, semi-circle with thin strut at design draft, for 0.5 inch (1.27 cm) oscillation amplitude.

Model Configuration :	D. Semi-Circle w/ Thin Strut	
Model Displacement, (lbs.)	119.10	M = 3.70
Gage Wt. Z1, (lbs.)	104.37	M'1 = 3.25
Gage Wt. Z2, (lbs.)	94.22	M'2 = 2.93
Model Draft, (inches)	9.90	
C33, (lbs./ft)	48.10	

Run #	Frequency rad / sec model scale	kB/2	alpha1	delta1	alpha2	delta2
302	1.13	0.01	1.01	0.15	0.99	0.18
303	1.95	0.04	1.10	0.06	1.09	0.07
304	3.02	0.11	1.21	0.04	1.18	0.05
305	4.13	0.20	1.22	0.16	1.22	0.17
306	5.08	0.30	1.19	0.30	1.21	0.31
307	6.02	0.42	0.98	0.34	1.01	0.35
308	7.07	0.58	0.97	0.33	1.00	0.34
309	8.08	0.76	0.83	0.27	0.86	0.28
310	9.21	0.99	0.78	0.24	0.82	0.25
311	10.06	1.18	0.79	0.19	0.83	0.20
312	14.06	2.31	0.86	0.09	0.89	0.10

Table D2. Data for model D, semi-circle with thin strut at design draft, for 1 inch (2.54"cm) oscillation amplitude.

Model Configuration :	D. Semi-Circle w/ Thin Strut	
Model Displacement, (lbs.)	119.10	M = 3.70
Gage Wt. Z1, (lbs.)	104.37	M'1 = 3.25
Gage Wt. Z2, (lbs.)	94.22	M'2 = 2.93
Model Draft, (inches)	9.90	
C33, (lbs./ft)	48.10	

Run #	Frequency rad / sec model scale	kB/2	alpha1	delta1	alpha2	delta2
290	0.97	0.01	1.29	0.11	1.11	0.16
291	2.03	0.05	1.14	0.05	1.12	0.06
292	3.04	0.11	1.21	0.05	1.20	0.05
293	4.01	0.19	1.20	0.17	1.21	0.18
294	5.10	0.30	1.18	0.34	1.21	0.35
295	5.94	0.41	0.97	0.37	1.00	0.38
296	7.03	0.58	0.95	0.34	0.98	0.35
297	8.11	0.77	0.82	0.29	0.85	0.30
298	9.43	1.04	0.77	0.23	0.81	0.23
299	10.09	1.19	0.78	0.20	0.79	0.20
300	13.87	2.24	0.86	0.11		

Table D3. Data for model D, semi-circle with thin strut at deep draft, for 0.5 inch (1.27 cm) oscillation amplitude.

Model Configuration :	D. Semi-Circle w/ Thin Strut	
Model Displacement, (lbs.)	123.11	M = 3.83
Gage Wt. Z1, (lbs.)	108.27	M'1 = 3.37
Gage Wt. Z2, (lbs.)	98.12	M'2 = 3.05
Model Draft, (inches)	10.90	
C33, (lbs./ft)	48.10	

Run #	Frequency rad / sec model scale	kB/2	alpha1	delta1	alpha2	delta2
314	1.07	0.01	0.91	0.16	0.93	0.20
315	2.05	0.05	1.04	0.06	1.03	0.06
316	3.01	0.11	1.14	0.03	1.11	0.05
317	4.03	0.19	1.13	0.13	1.13	0.14
318	5.26	0.32	1.08	0.28	1.10	0.29
319	5.92	0.41	0.94	0.28	0.96	0.29
320	6.97	0.57	0.92	0.23	0.95	0.23
321	8.12	0.77	0.82	0.21	0.85	0.22
322	9.32	1.01	0.79	0.17	0.83	0.18
323	9.99	1.16	0.80	0.14	0.84	0.15
324	13.97	2.28	0.87	0.09	0.89	0.10

Table D4. Data for model D, semi-circle with thin strut at deep draft, for 1 inch (2.54 cm) oscillation amplitude.

Model Configuration :	D. Semi-Circle w/ Thin Strut	
Model Displacement, (lbs.)	123.11	M = 3.83
Gage Wt. Z1, (lbs.)	108.27	M'1 = 3.37
Gage Wt. Z2, (lbs.)	98.12	M'2 = 3.05
Model Draft, (inches)	10.90	
C33, (lbs./ft)	48.10	

Run #	Frequency rad / sec model scale	kB/2	alpha1	delta1	alpha2	delta2
326	1.01	0.01	1.19	0.11	1.04	0.15
327	2.06	0.05	1.08	0.05	1.07	0.06
328	3.12	0.11	1.14	0.04	1.13	0.05
329	3.93	0.18	1.12	0.14	1.13	0.15
330	4.91	0.28	1.11	0.22	1.13	0.23
331	6.08	0.43	0.92	0.28	0.95	0.29
332	7.06	0.58	0.91	0.28	0.94	0.29
333	8.10	0.77	0.82	0.22	0.85	0.23
334	9.35	1.02	0.79	0.18	0.82	0.19
335	9.91	1.14	0.80	0.15	0.83	0.16
336	13.94	2.26	0.87	0.10		

APPENDIX E

EXPERIMENTAL DATA FOR MODEL E

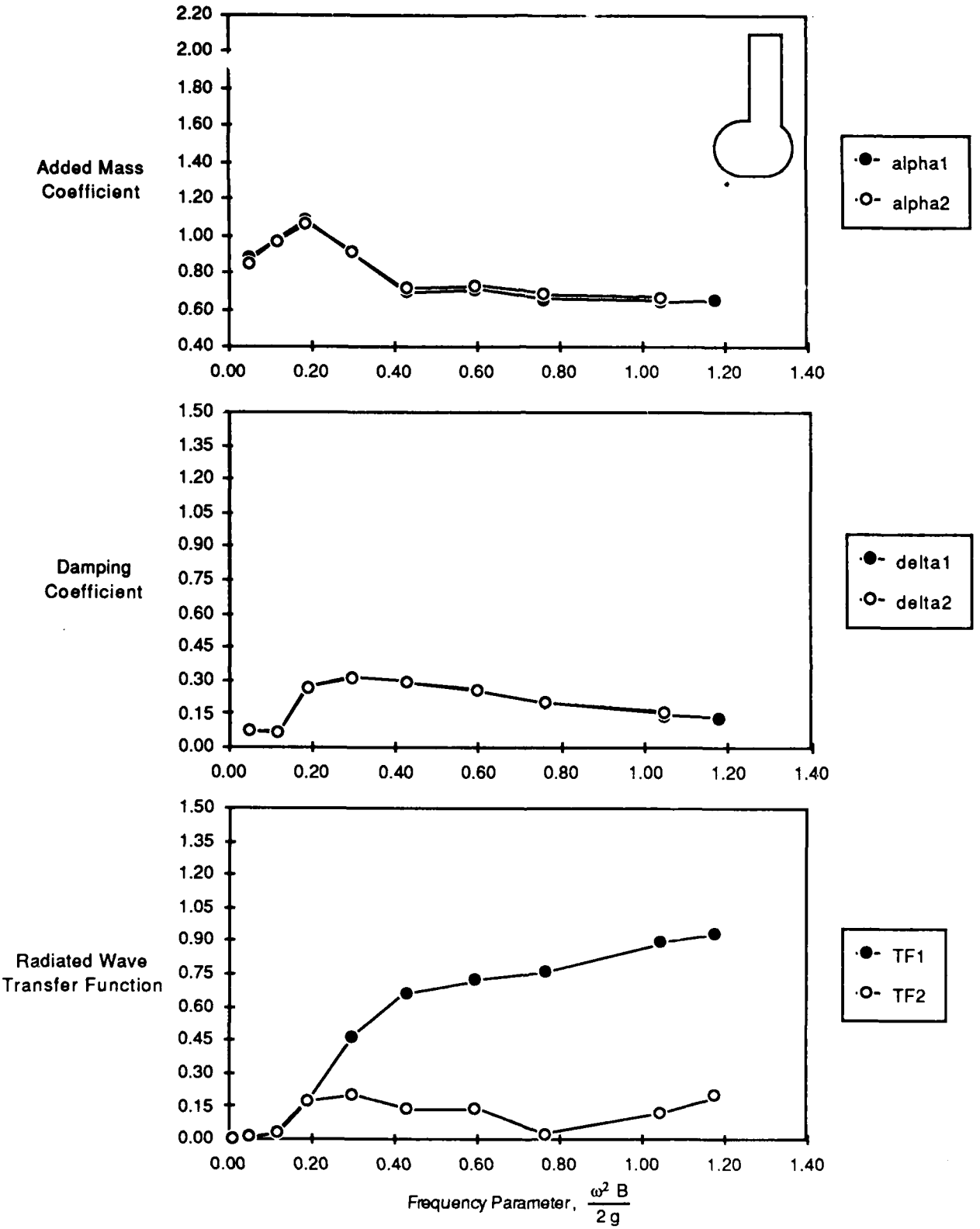

Fig. E1. Data for model E, half golf club at design draft, for 0.5 inch (1.27 cm) oscillation amplitude.

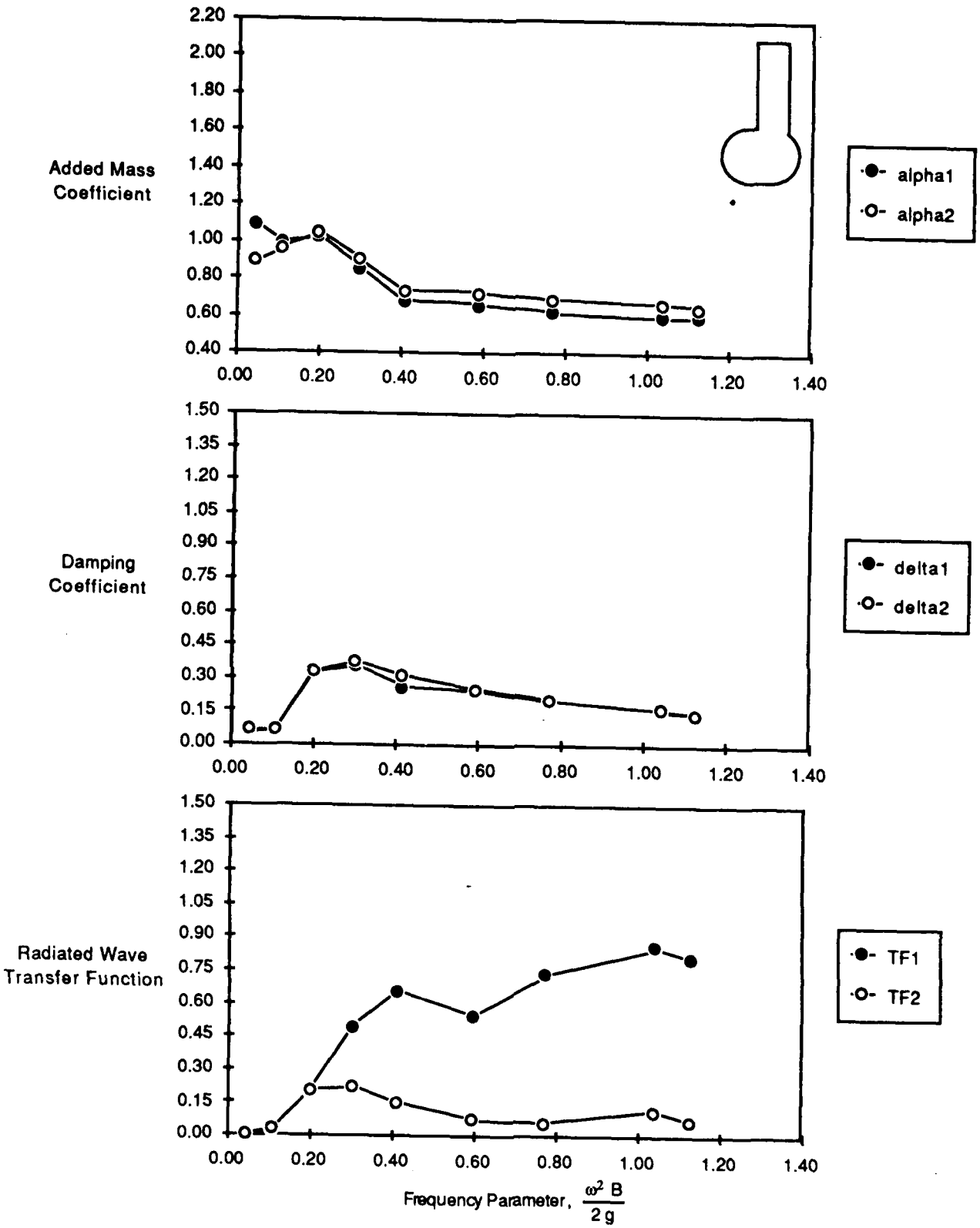

Fig. E2. Data for model E, half golf club at design draft, for 1 inch (2.54 cm) oscillation amplitude.

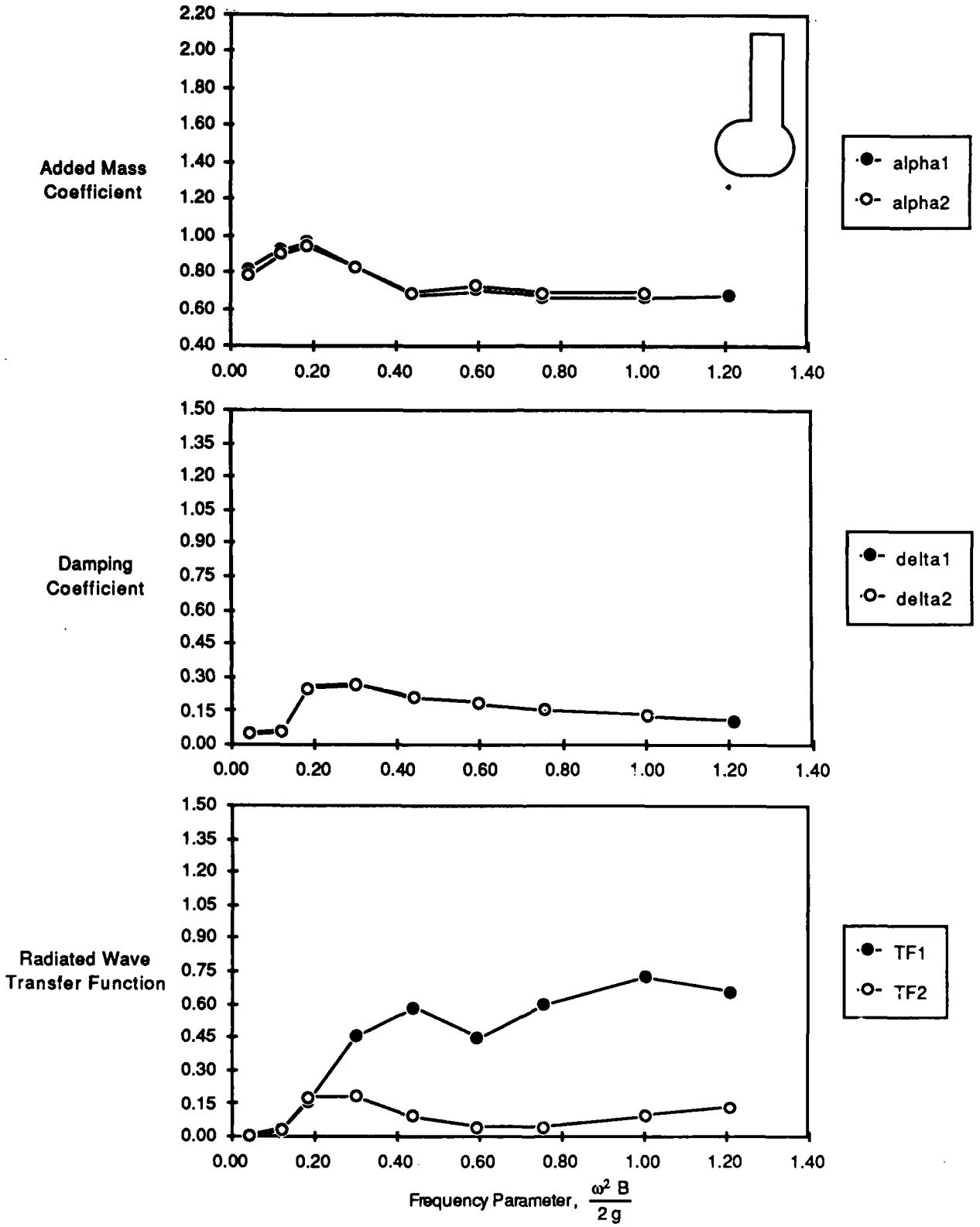

Fig. E3. Data for model E, half golf club at deep draft, for 0.5 inch (1.27 cm) oscillation amplitude.

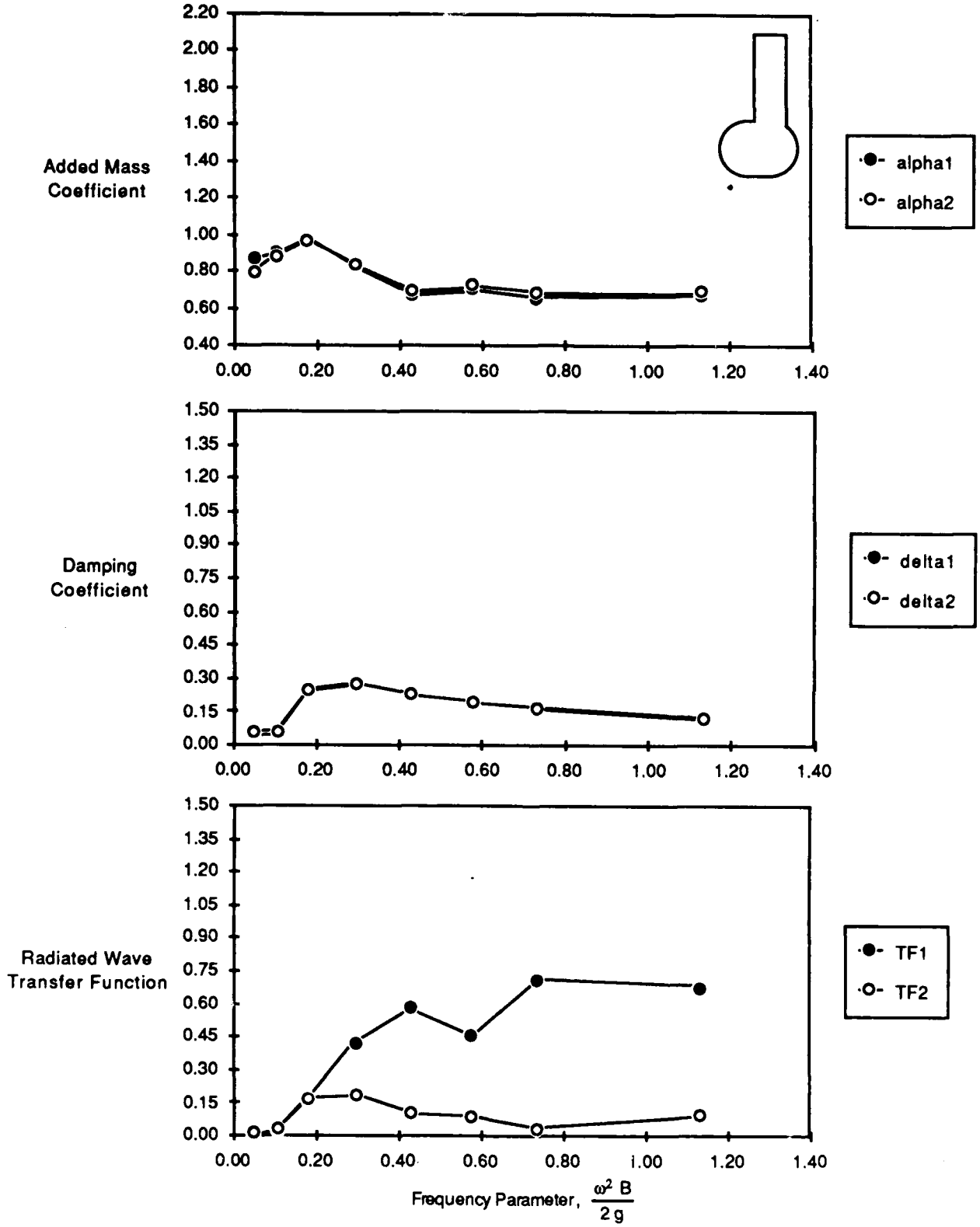

Fig. E4. Data for model E, half golf club at deep draft, for 1 inch (2.54 cm) oscillation amplitude.

Table E1. Data for model E, half golf club at design draft for 0.5 inch (1.27 cm) oscillation amplitude.

Model Configuration :	E. Half Golf Club	
Model Displacement, (lbs.)	133.40	M = 4.15
Gage Wt. Z1, (lbs.)	133.24	M'1 = 4.14
Gage Wt. Z2, (lbs.)	123.09	M'2 = 3.83
Model Draft, (inches)	9.90	
C33, (lbs./ft)	94.78	

Run #	Frequency rad / sec model scale	kB/2	alpha1	delta1	alpha2	delta2
359	0.94	0.01	0.79	0.27	0.55	0.31
360	2.03	0.05	0.88	0.07	0.85	0.08
361	3.16	0.12	0.98	0.06	0.97	0.06
362	4.00	0.19	1.09	0.27	1.07	0.27
363	5.03	0.29	0.91	0.32	0.91	0.32
364	6.05	0.43	0.70	0.29	0.72	0.29
365	7.14	0.59	0.71	0.25	0.74	0.26
366	8.08	0.76	0.66	0.20	0.68	0.20
367	9.46	1.04	0.64	0.14	0.67	0.16
368	10.04	1.18	0.65	0.13	0.68	0.14
369	14.03	2.30	0.72	0.09	0.68	0.10

Table E2. Data for model E, half golf club at design draft, for 1 inch (2.54 cm) oscillation amplitude.

Model Configuration :	E. Half Golf Club	
Model Displacement, (lbs.)	133.40	M = 4.15
Gage Wt. Z1, (lbs.)	133.24	M'1 = 4.14
Gage Wt. Z2, (lbs.)	123.09	M'2 = 3.83
Model Draft, (inches)	9.90	
C33, (lbs./ft)	94.78	

Run #	Frequency rad / sec model scale	kB/2	alpha1	delta1	alpha2	delta2
347	1.10	0.01	1.67	0.10	0.86	0.13
348	1.93	0.04	1.09	0.06	0.89	0.06
349	3.04	0.11	0.99	0.07	0.96	0.07
350	4.10	0.20	1.03	0.33	1.05	0.33
351	5.06	0.30	0.86	0.36	0.90	0.38
352	5.93	0.41	0.68	0.26	0.73	0.32
353	7.12	0.59	0.66	0.24	0.73	0.25
354	8.13	0.77	0.62	0.20	0.69	0.20
355	9.44	1.04	0.60	0.16	0.67	0.17
356	9.82	1.12	0.60	0.14	0.65	0.14

Table E3. Data for model E, half golf club at deep draft, for 0.5 inch (1.27 cm) oscillation amplitude.

Model Configuration :	E. Half Golf Club	
Model Displacement, (lbs.)	141.30	M = 4.39
Gage Wt. Z1, (lbs.)	141.02	M'1 = 4.39
Gage Wt. Z2, (lbs.)	130.87	M'2 = 4.07
Model Draft, (inches)	10.90	
C33, (lbs./ft)	94.78	

Run #	Frequency rad / sec model scale	kB/2	alpha1	delta1	alpha2	delta2
372	1.12	0.01	0.66	0.15	0.46	0.18
373	1.95	0.04	0.82	0.05	0.78	0.05
374	3.23	0.12	0.92	0.06	0.90	0.06
375	3.99	0.19	0.97	0.26	0.94	0.25
376	5.07	0.30	0.83	0.27	0.83	0.27
377	6.13	0.44	0.68	0.21	0.69	0.21
378	7.14	0.59	0.71	0.18	0.73	0.19
379	8.05	0.76	0.67	0.15	0.69	0.16
380	9.28	1.00	0.66	0.13	0.69	0.13
381	10.18	1.21	0.68	0.11	0.70	0.11

Table E4. Data for model E, half golf club at deep draft, for 1 inch (2.54 cm) oscillation amplitude.

Model Configuration :	E. Half Golf Club	
Model Displacement, (lbs.)	141.30	M = 4.39
Gage Wt. Z1, (lbs.)	141.02	M'1 = 4.39
Gage Wt. Z2, (lbs.)	130.87	M'2 = 4.07
Model Draft, (inches)	10.90	
C33, (lbs./ft)	94.78	

Run #	Frequency rad / sec model scale	kB/2	alpha1	delta1	alpha2	delta2
383	0.98	0.01	0.95	0.19	0.51	0.25
384	2.00	0.05	0.87	0.05	0.80	0.06
385	2.99	0.10	0.90	0.06	0.89	0.06
386	3.90	0.18	0.98	0.25	0.97	0.25
387	5.02	0.29	0.83	0.28	0.84	0.28
388	6.05	0.43	0.68	0.23	0.70	0.23
389	7.02	0.57	0.71	0.19	0.73	0.19
390	7.93	0.73	0.66	0.17	0.69	0.17
391	9.85	1.13	0.68	0.12	0.69	0.12

APPENDIX F

EXPERIMENTAL DATA FOR MODEL F

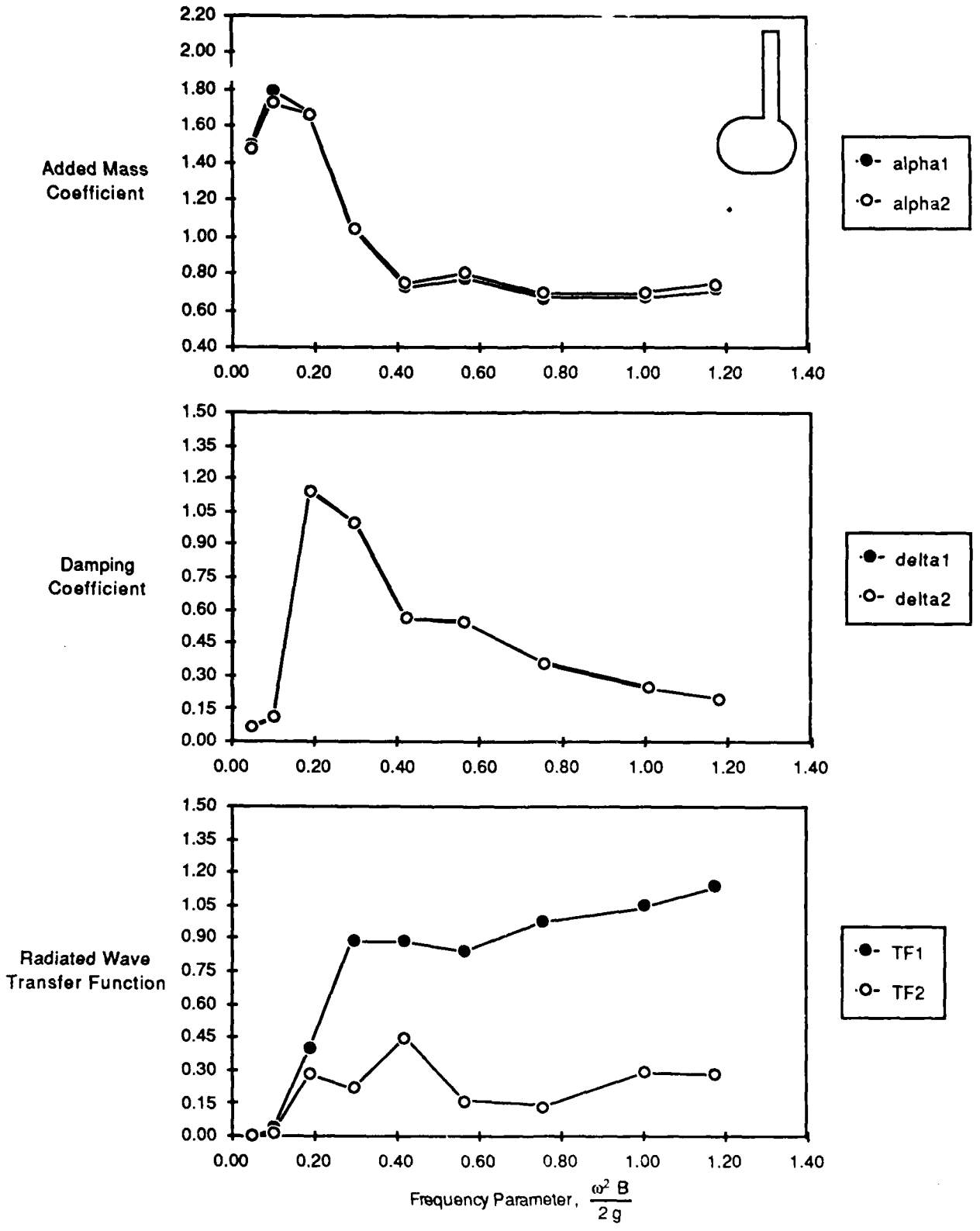

Fig. F1. Data for model F, half golf club with thin strut at design draft, for 0.5 inch (1.27 cm) oscillation amplitude.

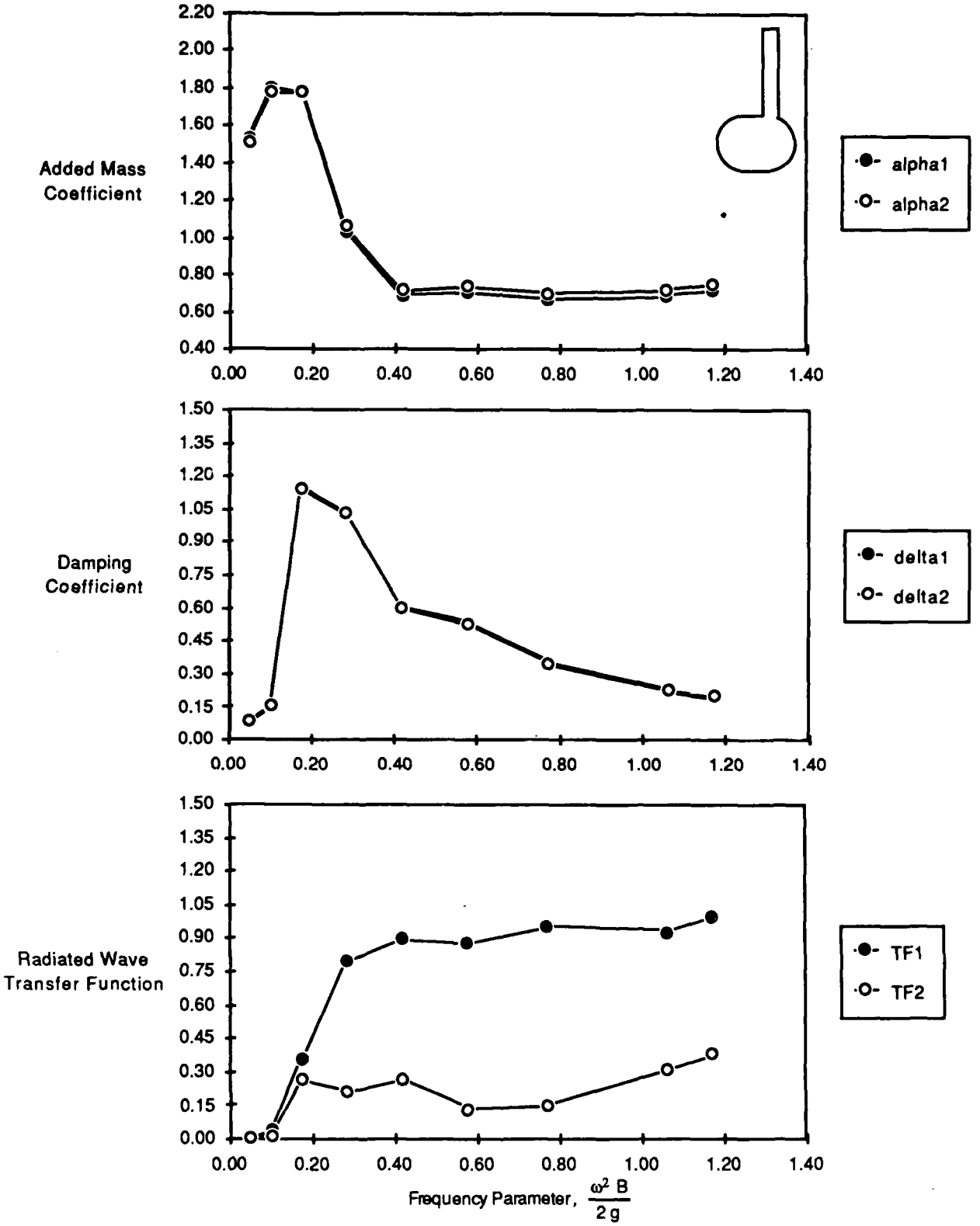

Fig. F2. Data for model F, half golf club with thin strut at design draft, for 1 inch (2.54 cm) oscillation amplitude.

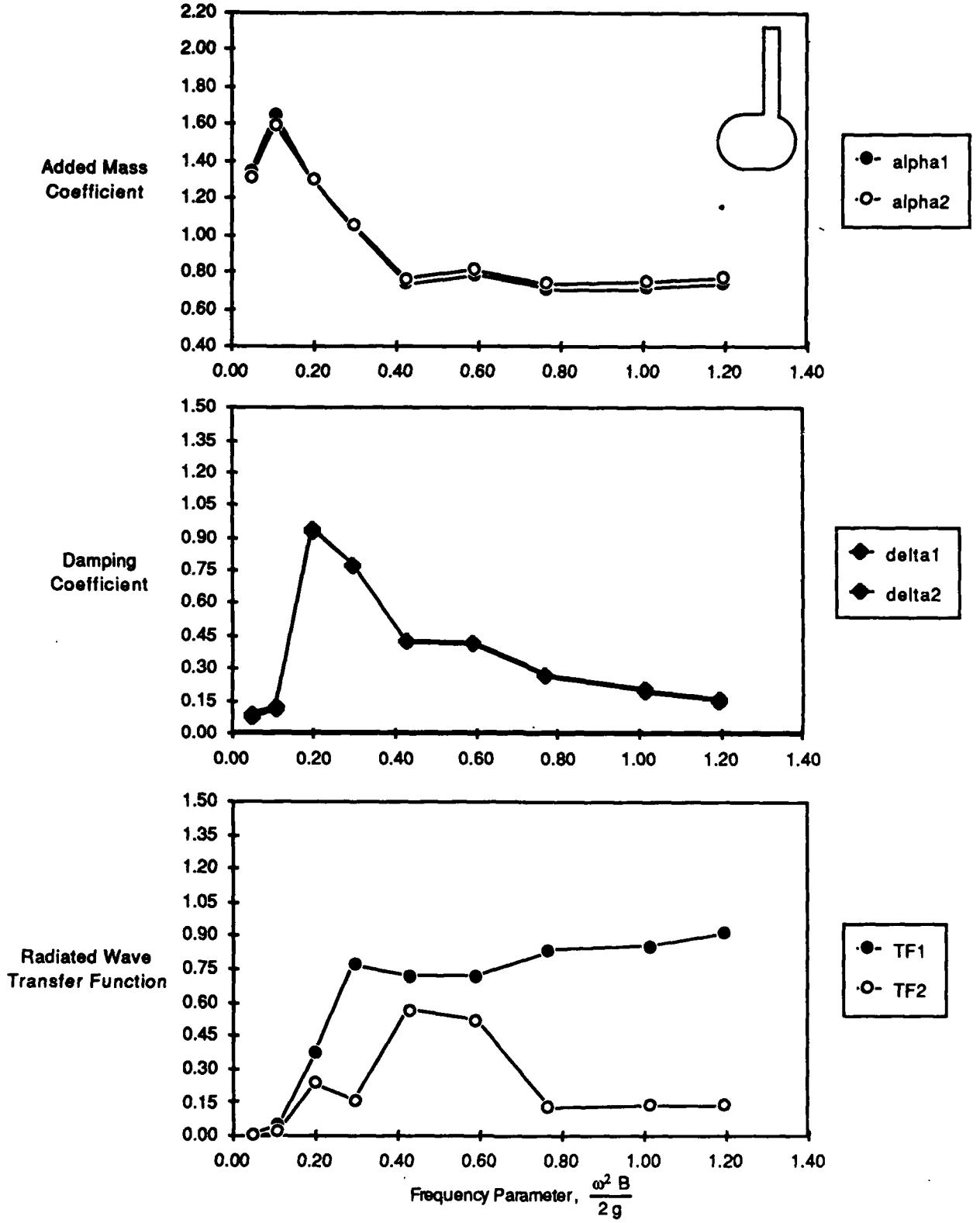

Fig. F3. Data for model F, half golf club with thin strut at deep draft, for 0.5 inch (1.27 cm) oscillation amplitude.

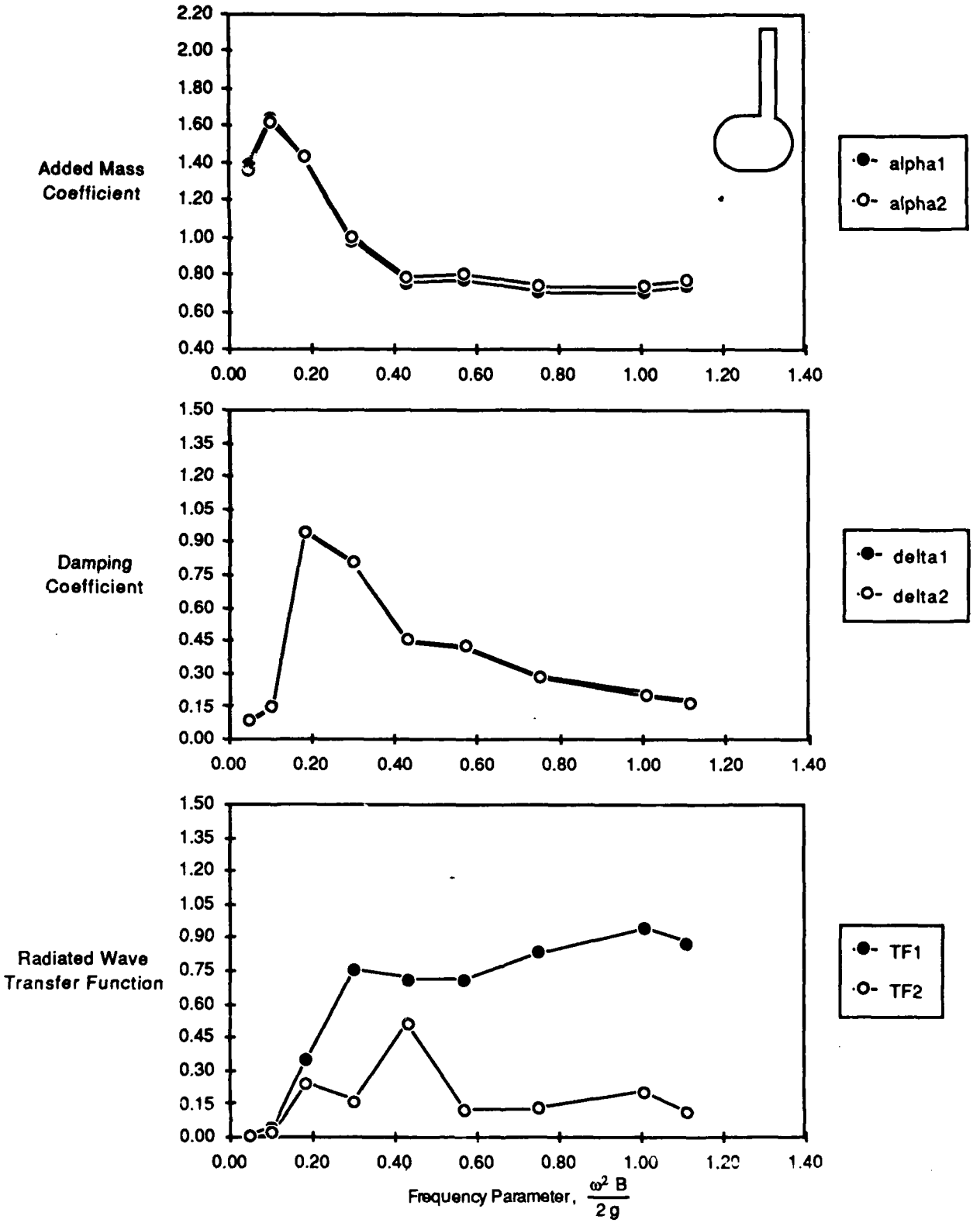

Fig. F4. Data for model F, half golf club with thin strut at deep draft, for 1 inch (2.54 cm) oscillation amplitude.

Table F1. Data for model F, half golf club with thin strut at design draft, for 0.5 inch (1.27 cm) oscillation amplitude.

Model Configuration :	F. Half Golf Club w/ Thin Strut		
Model Displacement, (lbs.)	119.50	M = 3.72	
Gage Wt. Z1, (lbs.)	103.68	M'1 = 3.22	
Gage Wt. Z2, (lbs.)	93.53	M'2 = 2.91	
Model Draft, (inches)	9.90		
C33, (lbs./ft)	48.42		

Run #	Frequency rad / sec model scale	kB/2	alpha1	delta1	alpha2	delta2
416	2.03	0.05	1.50	0.06	1.48	0.07
417	2.93	0.10	1.79	0.10	1.73	0.11
418	4.02	0.19	1.67	1.15	1.66	1.14
419	5.03	0.30	1.04	1.00	1.05	1.00
420	6.00	0.42	0.73	0.56	0.75	0.56
421	6.95	0.56	0.78	0.54	0.81	0.55
422	8.05	0.76	0.67	0.35	0.70	0.36
423	9.28	1.00	0.67	0.24	0.70	0.25
424	10.04	1.18	0.72	0.19	0.75	0.20
425	13.97	2.28	0.92	0.10		

Table F2. Data for model F, half golf club with thin strut at design draft, for 1 inch (2.54 cm) oscillation amplitude.

Model Configuration :	F. Half Golf Club w/ Thin Strut		
Model Displacement, (lbs.)	119.50	M = 3.72	
Gage Wt. Z1, (lbs.)	103.68	M'1 = 3.22	
Gage Wt. Z2, (lbs.)	93.53	M'2 = 2.91	
Model Draft, (inches)	9.90		
C33, (lbs./ft)	48.42		

Run #	Frequency rad / sec model scale	kB/2	alpha1	delta1	alpha2	delta2
427	2.00	0.05	1.54	0.08	1.51	0.08
428	2.93	0.10	1.81	0.15	1.78	0.16
429	3.87	0.17	1.77	1.14	1.78	1.14
430	4.91	0.28	1.04	1.03	1.06	1.03
431	5.98	0.42	0.69	0.60	0.72	0.60
432	7.03	0.58	0.71	0.52	0.74	0.53
433	8.13	0.77	0.67	0.34	0.70	0.35
434	9.53	1.06	0.69	0.22	0.72	0.23
435	10.01	1.17	0.72	0.19	0.75	0.20
437	13.86	2.24	0.99	0.11		

Table F3. Data for model F, half golf club with thin strut at deep draft, for 0.5 inch (1.27 cm) oscillation amplitude.

Model Configuration :	F. Half Golf Club w/ Thin Strut	
Model Displacement, (lbs.)	123.54	M = 3.84
Gage Wt. Z1, (lbs.)	107.57	M'1 = 3.35
Gage Wt. Z2, (lbs.)	97.42	M'2 = 3.03
Model Draft, (inches)	10.90	
C33, (lbs./ft)	48.42	

Run #	Frequency rad / sec model scale	kB/2	alpha1	delta1	alpha2	delta2
439	1.99	0.05	1.35	0.08	1.31	0.09
440	3.02	0.11	1.65	0.12	1.60	0.13
441	4.12	0.20	1.31	0.94	1.30	0.93
442	5.03	0.30	1.05	0.78	1.06	0.78
443	6.04	0.43	0.74	0.42	0.77	0.43
444	7.11	0.59	0.79	0.41	0.82	0.42
445	8.10	0.77	0.71	0.27	0.74	0.27
446	9.31	1.01	0.72	0.20	0.75	0.20
447	10.12	1.19	0.74	0.15	0.78	0.16
448	14.00	2.29	0.88	0.09		

Table F4. Data for model F, half golf club with thin strut at deep draft, for 1 inch (2.54 cm) oscillation amplitude.

Model Configuration :	F. Half Golf Club w/ Thin Strut	
Model Displacement, (lbs.)	123.54	M = 3.84
Gage Wt. Z1, (lbs.)	107.57	M'1 = 3.35
Gage Wt. Z2, (lbs.)	97.42	M'2 = 3.03
Model Draft, (inches)	10.90	
C33, (lbs./ft)	48.42	

Run #	Frequency rad / sec model scale	kB/2	alpha1	delta1	alpha2	delta2
450	1.99	0.05	1.39	0.08	1.36	0.08
451	2.97	0.10	1.64	0.14	1.62	0.15
452	3.97	0.18	1.42	0.95	1.43	0.94
453	5.06	0.30	0.98	0.80	1.01	0.80
454	6.08	0.43	0.76	0.45	0.79	0.45
455	7.00	0.57	0.77	0.42	0.80	0.43
456	8.02	0.75	0.71	0.28	0.74	0.29
457	9.29	1.01	0.71	0.20	0.75	0.21
458	9.76	1.11	0.74	0.17	0.77	0.17
459	13.98	2.28	0.89	0.10		

APPENDIX G

EXPERIMENTAL DATA FOR MODEL G

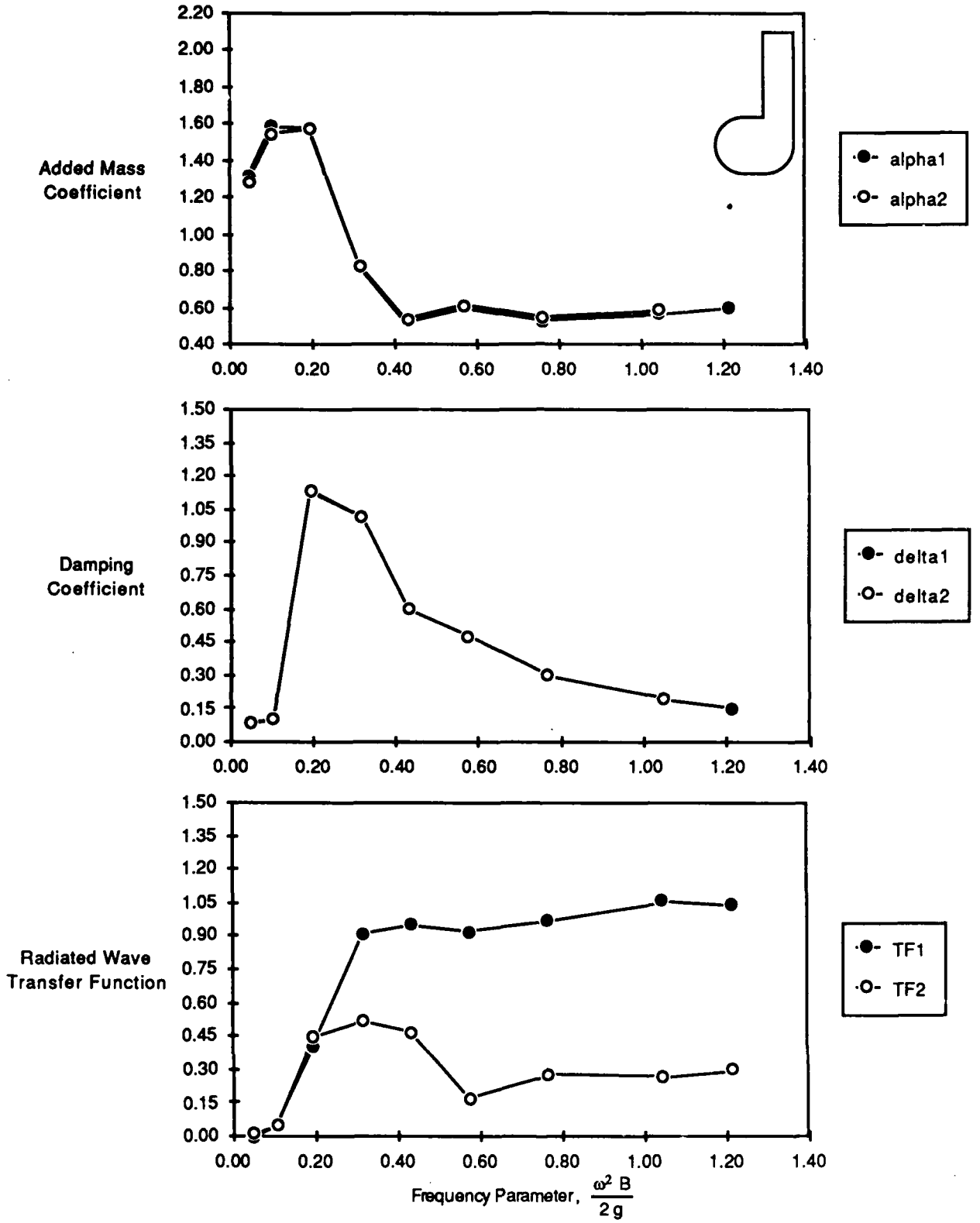

Fig. G1. Data for model G, full golf club at design draft, for 0.5 inch (1.27 cm) oscillation amplitude.

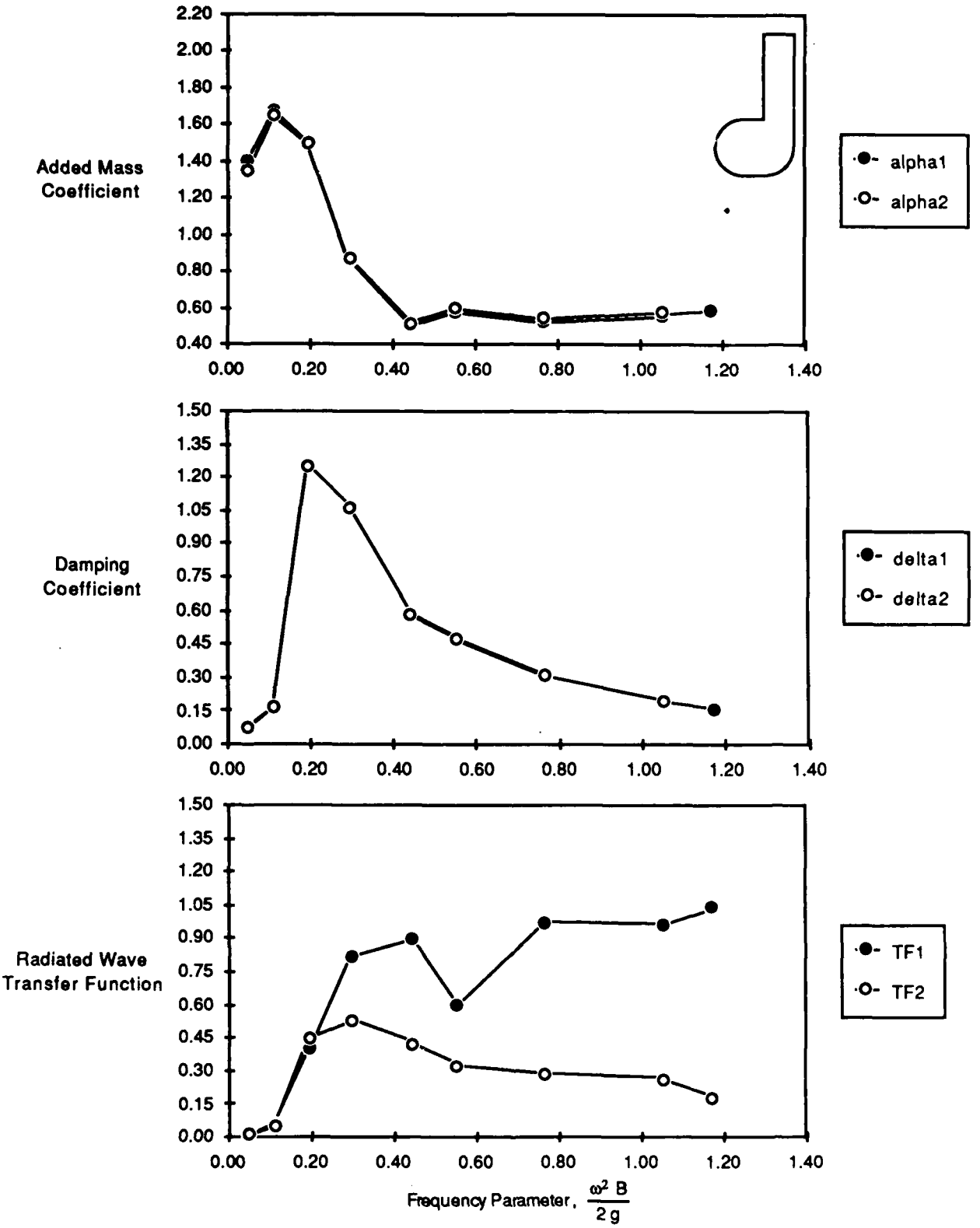

Fig. G2. Data for model G, full golf club at design draft, for 1 inch (2.54 cm) oscillation amplitude.

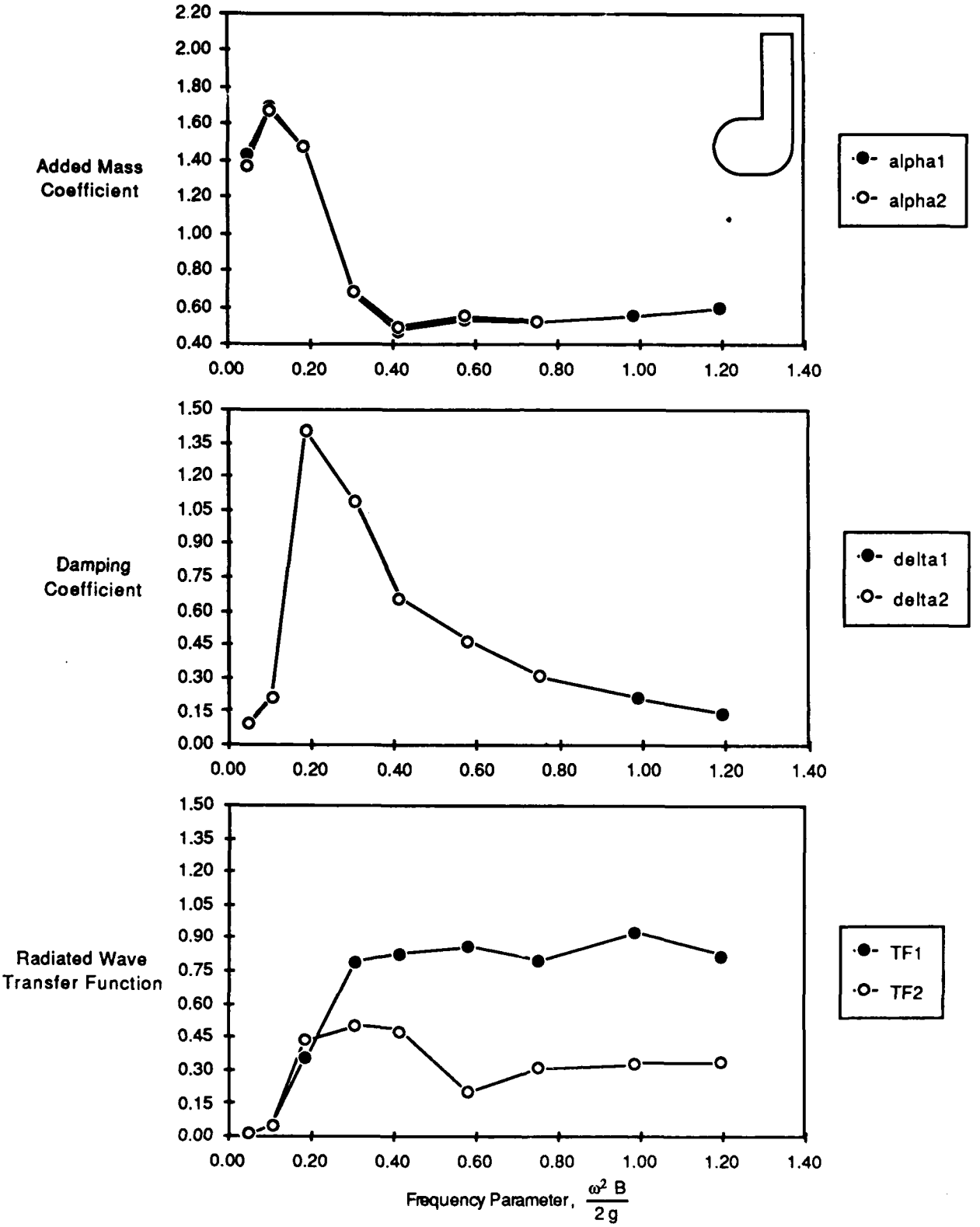

Fig. G3. Data for model G, full golf club at design draft, for 1.5 inch (3.81 cm) oscillation amplitude.

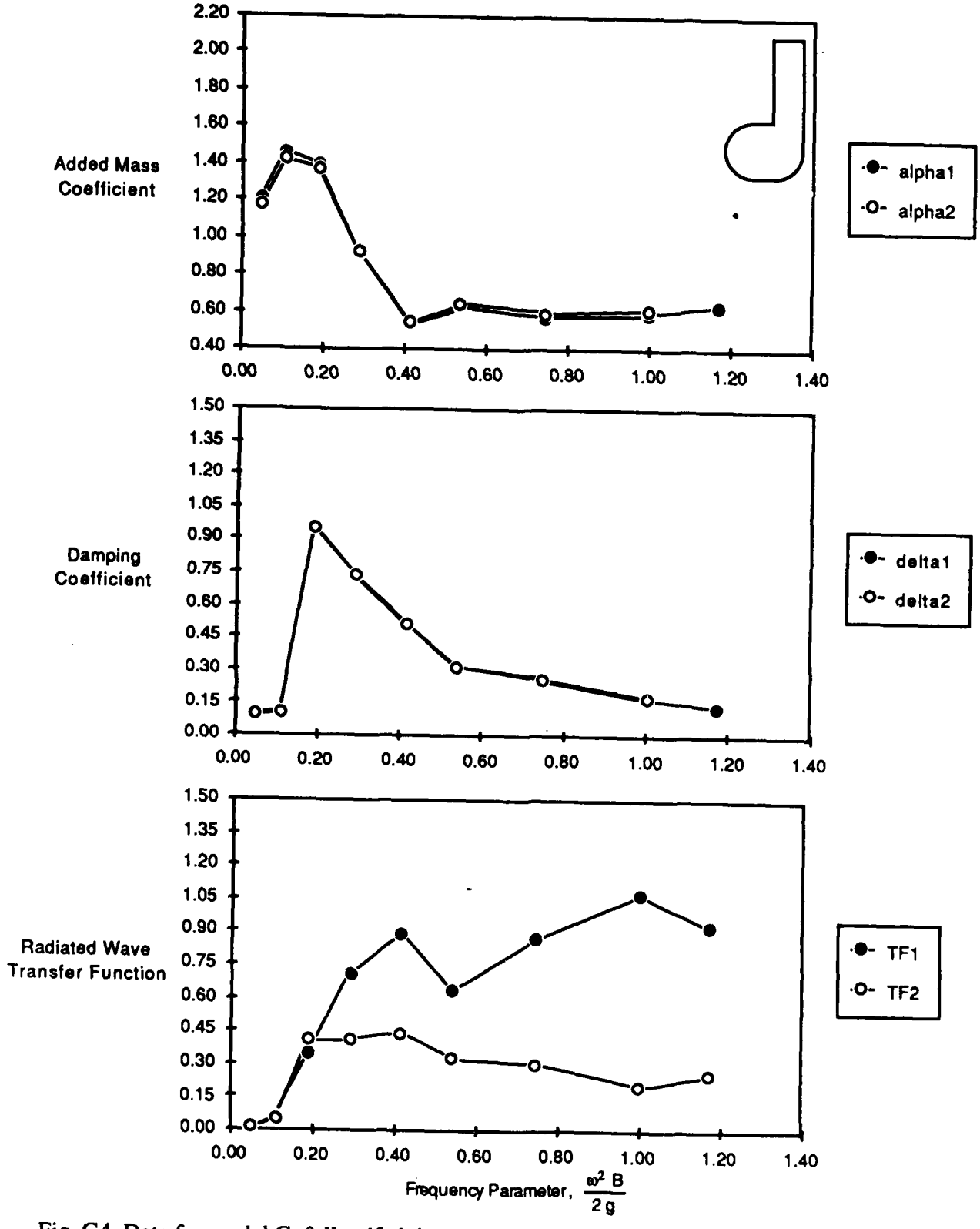

Fig. G4. Data for model G, full golf club at deep draft, for 0.5 inch (1.27 cm) oscillation amplitude.

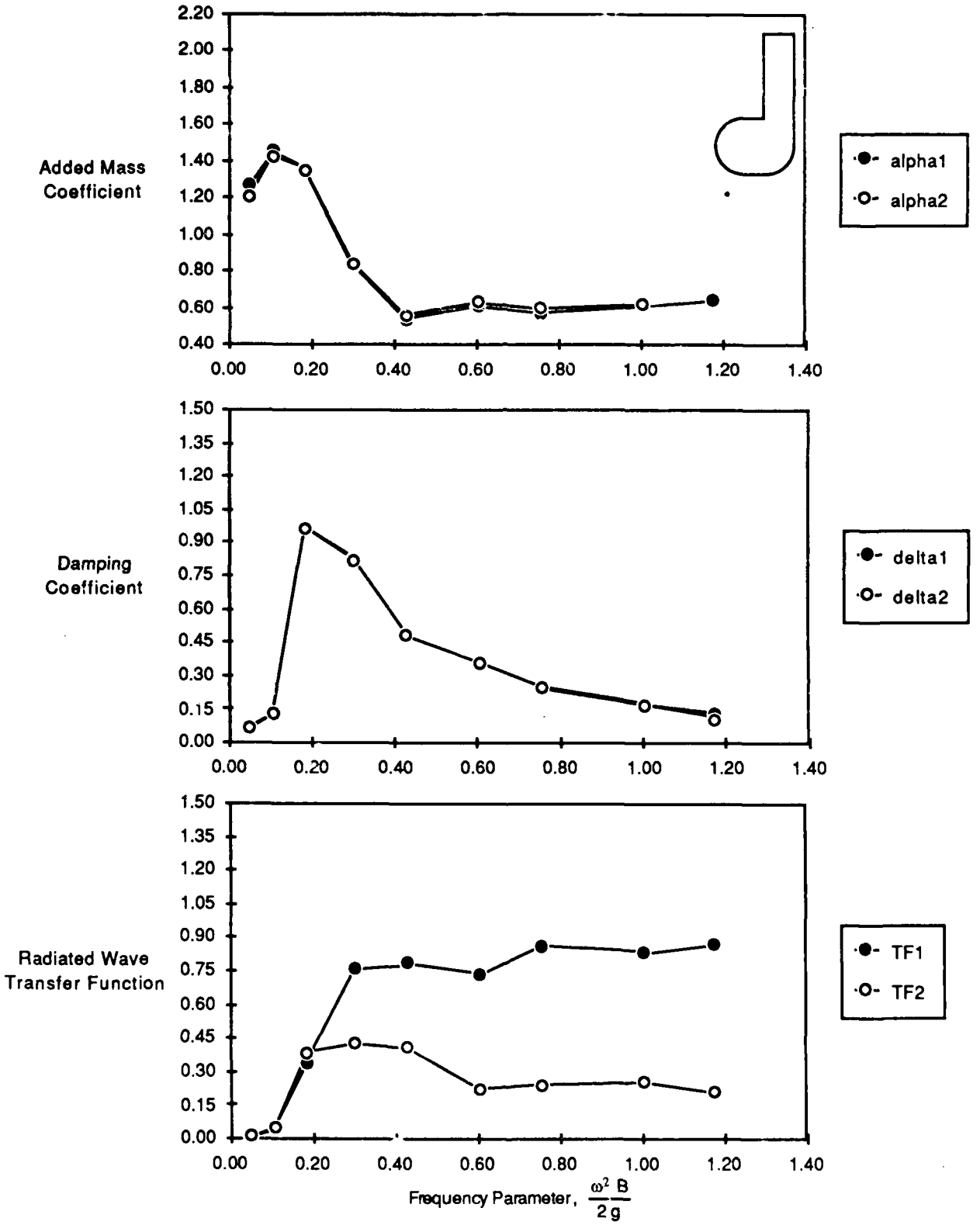

Fig. G5. Data for model G, full golf club at deep draft, for 1 inch (2.54 cm) oscillation amplitude.

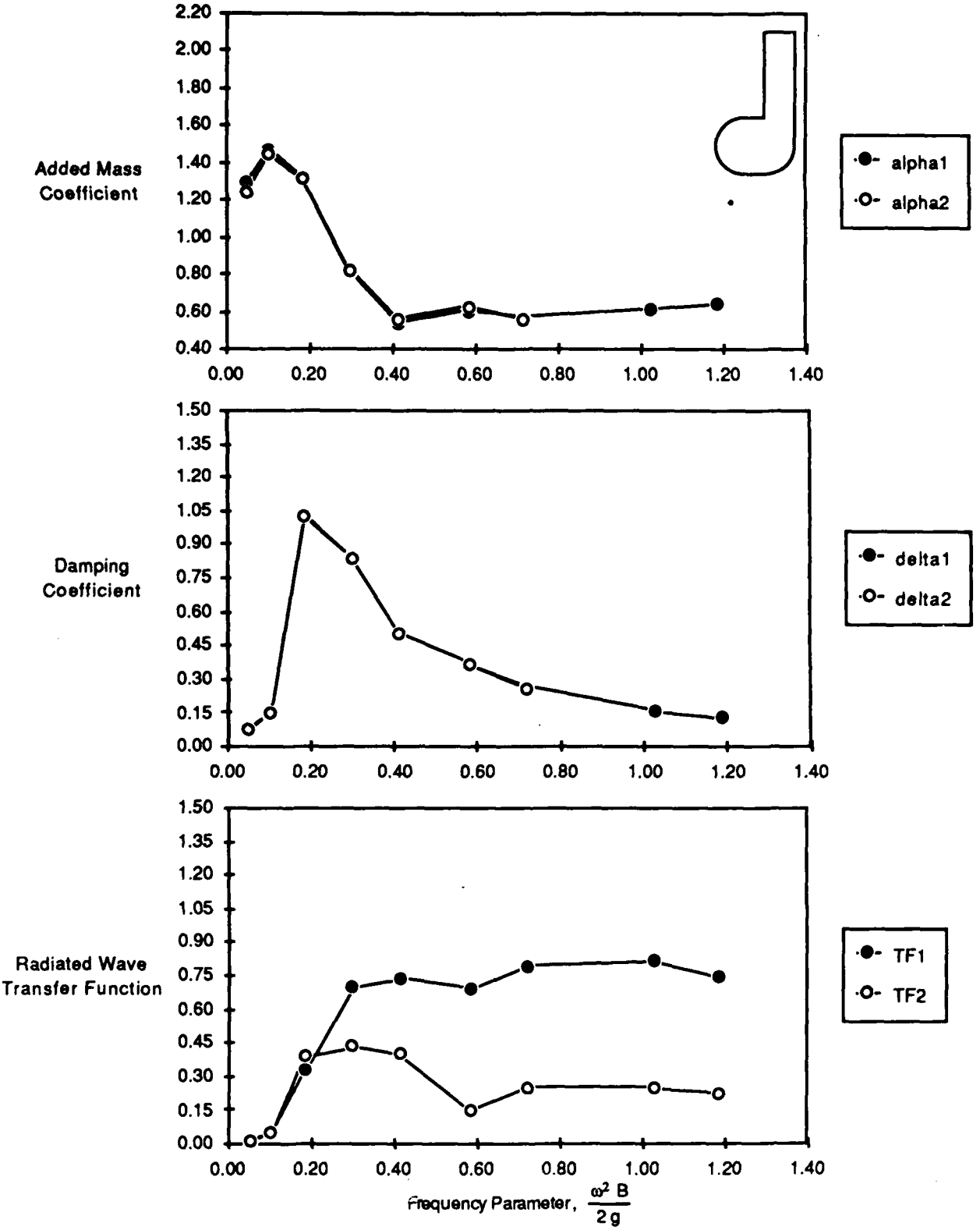

Fig. G6. Data for model G, full golf club at deep draft, for 1.5 inch (3.81 cm) oscillation amplitude.

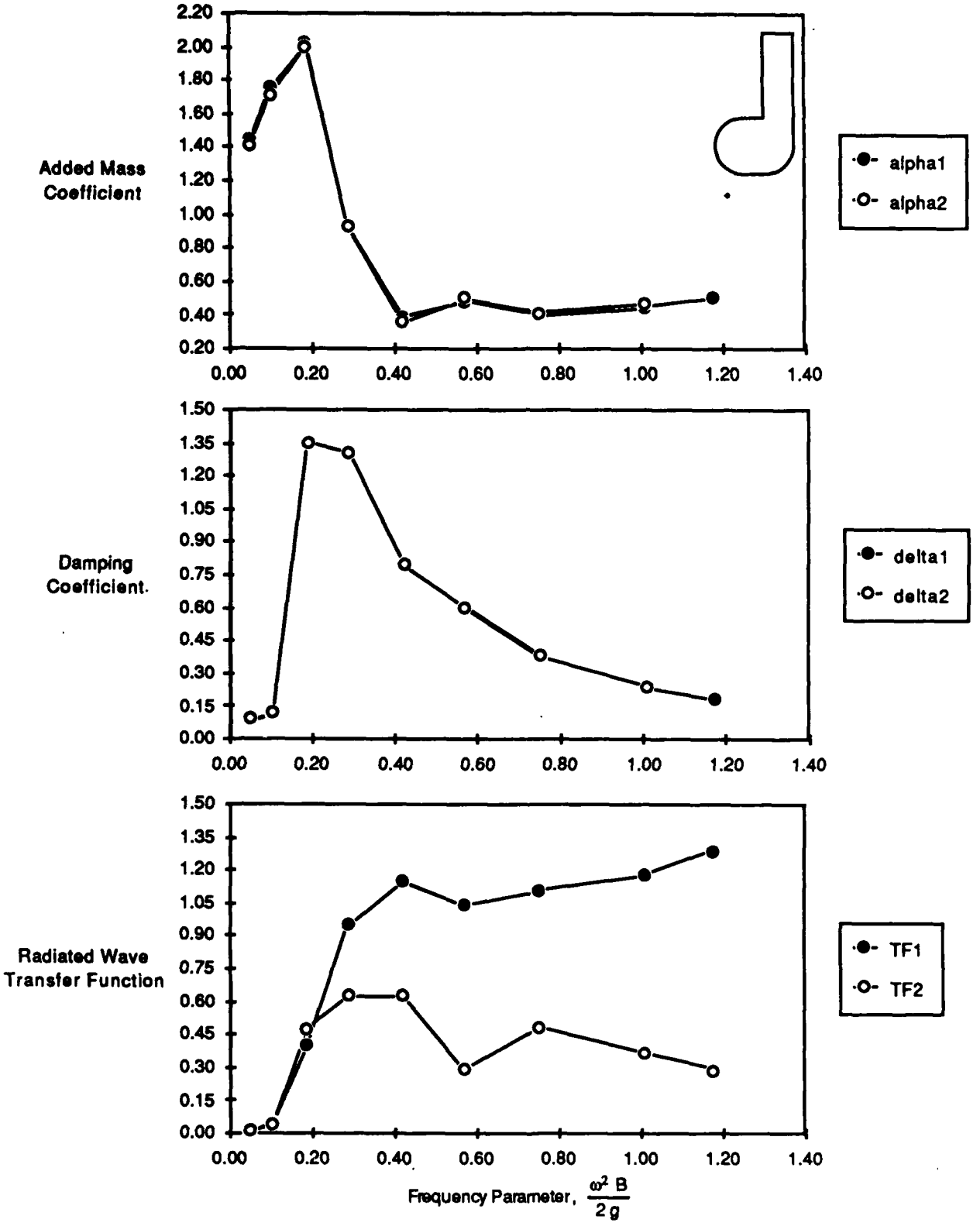

Fig. G7. Data for model G, full golf club at shallow draft, for 0.5 inch (1.27 cm) oscillation amplitude.

Table G1. Data for model G, full golf club at design draft, for 0.5 inch (1.27 cm) oscillation amplitude.

Model Configuration :	G. Full Golf Club	
Model Displacement, (lbs.)	137.50	M = 4.28
Gage Wt. Z1, (lbs.)	143.97	M'1 = 4.48
Gage Wt. Z2, (lbs.)	133.82	M'2 = 4.16
Model Draft, (inches)	9.90	
C33, (lbs./ft)	95.79	

Run #	Frequency rad / sec model scale	kB/2	alpha1	delta1	alpha2	delta2
475	1.17	0.02	1.27	0.20	1.10	0.23
476	2.02	0.05	1.32	0.08	1.29	0.09
477	2.98	0.10	1.59	0.10	1.55	0.11
478	4.07	0.19	1.59	1.14	1.57	1.13
479	5.20	0.32	0.83	1.02	0.83	1.02
480	6.08	0.43	0.52	0.60	0.54	0.60
481	7.00	0.57	0.60	0.48	0.62	0.48
482	8.09	0.76	0.53	0.30	0.55	0.30
483	9.46	1.04	0.57	0.19	0.59	0.20
484	10.20	1.21	0.60	0.15	0.62	0.16
485	13.97	2.28	0.76	0.09		

Table G2. Data for model G, full golf club at design draft, for 1 inch (2.54 cm) oscillation amplitude.

Model Configuration :	G. Full Golf Club	
Model Displacement, (lbs.)	137.50	M = 4.28
Gage Wt. Z1, (lbs.)	143.97	M'1 = 4.48
Gage Wt. Z2, (lbs.)	133.82	M'2 = 4.16
Model Draft, (inches)	9.90	
C33, (lbs./ft)	95.79	

Run #	Frequency rad / sec model scale	kB/2	alpha1	delta1	alpha2	delta2
463	1.06	0.01	1.55	0.15	1.24	0.19
464	2.04	0.05	1.41	0.07	1.35	0.08
465	3.08	0.11	1.67	0.17	1.65	0.17
466	4.08	0.19	1.50	1.26	1.50	1.25
467	5.04	0.30	0.86	1.06	0.87	1.06
468	6.16	0.44	0.50	0.58	0.52	0.58
469	6.88	0.55	0.58	0.47	0.60	0.48
470	8.10	0.76	0.52	0.30	0.55	0.31
471	9.49	1.05	0.56	0.19	0.58	0.20
472	10.02	1.17	0.59	0.16	0.54	0.14
473	13.96	2.27	0.76	0.10		

Table G3. Data for model G, full golf club at design draft, for 1.5 inch (3.81 cm) oscillation amplitude.

Model Configuration :	G. Full Golf Club	
Model Displacement, (lbs.)	137.50	M = 4.28
Gage Wt. Z1, (lbs.)	143.97	M'1 = 4.48
Gage Wt. Z2, (lbs.)	133.82	M'2 = 4.16
Model Draft, (inches)	9.90	
C33, (lbs./ft)	95.79	

Run #	Frequency rad / sec model scale	kB/2	alpha1	delta1	alpha2	delta2
487	1.22	0.02	1.49	0.11	1.26	0.14
488	1.98	0.05	1.43	0.09	1.37	0.10
489	2.98	0.10	1.69	0.21	1.67	0.21
490	4.00	0.19	1.48	1.41	1.48	1.41
491	5.12	0.31	0.68	1.09	0.69	1.09
492	5.95	0.41	0.48	0.66	0.50	0.66
493	7.03	0.58	0.53	0.47	0.56	0.47
494	8.01	0.75	0.52	0.31	0.53	0.31
495	9.19	0.99	0.56	0.21		
496	10.11	1.19	0.60	0.15		
497	14.14	2.33	0.79	0.11		

Table G4. Data for model G, full golf club at deep draft, for 0.5 inch (1.27 cm) oscillation amplitude.

Model Configuration :	G. Full Golf Club	
Model Displacement, (lbs.)	145.48	M = 4.52
Gage Wt. Z1, (lbs.)	151.75	M'1 = 4.72
Gage Wt. Z2, (lbs.)	141.42	M'2 = 4.40
Model Draft, (inches)	10.90	
C33, (lbs./ft)	95.79	

Run #	Frequency rad / sec model scale	kB/2	alpha1	delta1	alpha2	delta2
529	2.02	0.05	1.21	0.09	1.17	0.10
530	3.05	0.11	1.46	0.10	1.42	0.11
531	4.01	0.19	1.39	0.97	1.37	0.95
532	4.98	0.29	0.92	0.74	0.92	0.74
533	5.96	0.41	0.53	0.51	0.54	0.51
534	6.79	0.54	0.63	0.31	0.65	0.31
535	7.99	0.74	0.57	0.26	0.59	0.26
536	9.26	1.00	0.59	0.17	0.62	0.17
537	10.02	1.17	0.64	0.13	0.66	0.13
538	14.04	2.30	0.77	0.09		

Table G5. Data for model G, full golf club at deep draft, for 1 inch (2.54 cm) oscillation amplitude.

Model Configuration :	G. Full Golf Club	
Model Displacement, (lbs.)	145.48	M = 4.52
Gage Wt. Z1, (lbs.)	151.75	M'1 = 4.72
Gage Wt. Z2, (lbs.)	141.42	M'2 = 4.40
Model Draft, (inches)	10.90	
C33, (lbs./ft)	95.79	

Run #	Frequency rad / sec model scale	kB/2	alpha1	delta1	alpha2	delta2
517	1.03	0.01	1.38	0.13	1.06	0.17
518	2.03	0.05	1.27	0.06	1.21	0.07
519	3.00	0.10	1.45	0.13	1.43	0.13
520	3.97	0.18	1.36	0.97	1.35	0.96
521	5.09	0.30	0.82	0.82	0.84	0.82
522	6.06	0.43	0.54	0.48	0.56	0.48
523	7.19	0.60	0.61	0.36	0.63	0.36
524	8.04	0.75	0.57	0.25	0.60	0.25
525	9.28	1.00	0.61	0.17	0.62	0.17
526	10.03	1.17	0.64	0.13	0.53	0.11
527	14.10	2.32	0.78	0.10		

Table G6. Data for model G, full golf club at deep draft, for 1.5 inch (3.81 cm) oscillation amplitude.

Model Configuration :	G. Full Golf Club	
Model Displacement, (lbs.)	145.48	M = 4.52
Gage Wt. Z1, (lbs.)	151.75	M'1 = 4.72
Gage Wt. Z2, (lbs.)	141.42	M'2 = 4.40
Model Draft, (inches)	10.90	
C33, (lbs./ft)	95.79	

Run #	Frequency rad / sec model scale	kB/2	alpha1	delta1	alpha2	delta2
505	1.04	0.01	1.42	0.10	1.11	0.14
506	2.07	0.05	1.30	0.07	1.24	0.08
507	2.95	0.10	1.47	0.14	1.44	0.15
508	3.98	0.18	1.31	1.03	1.31	1.03
509	5.05	0.30	0.81	0.84	0.82	0.84
510	5.95	0.41	0.54	0.51	0.56	0.50
511	7.07	0.58	0.60	0.36	0.63	0.37
512	7.85	0.72	0.57	0.27	0.56	0.26
513	9.38	1.03	0.61	0.16		
514	10.08	1.18	0.65	0.13		
515	14.06	2.30	0.80	0.11		

Table G7. Data for model G, full golf club at shallow draft, for 0.5 inch (1.27 cm) oscillation amplitude.

Model Configuration :	G. Full Golf Club	
Model Displacement, (lbs.)	136.19	M = 4.24
Gage Wt. Z1, (lbs.)	136.15	M'1 = 4.23
Gage Wt. Z2, (lbs.)	126.00	M'2 = 3.92
Model Draft, (inches)	8.90	
C33, (lbs./ft)	95.79	

Run #	Frequency rad / sec model scale	kB/2	alpha1	delta1	alpha2	delta2
540	2.05	0.05	1.44	0.09	1.41	0.09
541	2.96	0.10	1.76	0.12	1.71	0.12
542	3.99	0.19	2.02	1.36	2.00	1.35
543	4.96	0.29	0.93	1.31	0.93	1.31
544	6.00	0.42	0.39	0.80	0.36	0.80
545	6.98	0.57	0.49	0.60	0.50	0.60
546	8.01	0.75	0.40	0.38	0.42	0.38
547	9.29	1.01	0.45	0.24	0.47	0.24
548	10.03	1.17	0.50	0.18	0.53	0.19
549	13.99	2.28	0.70	0.08		

APPENDIX H

EXPERIMENTAL DATA FOR MODEL H

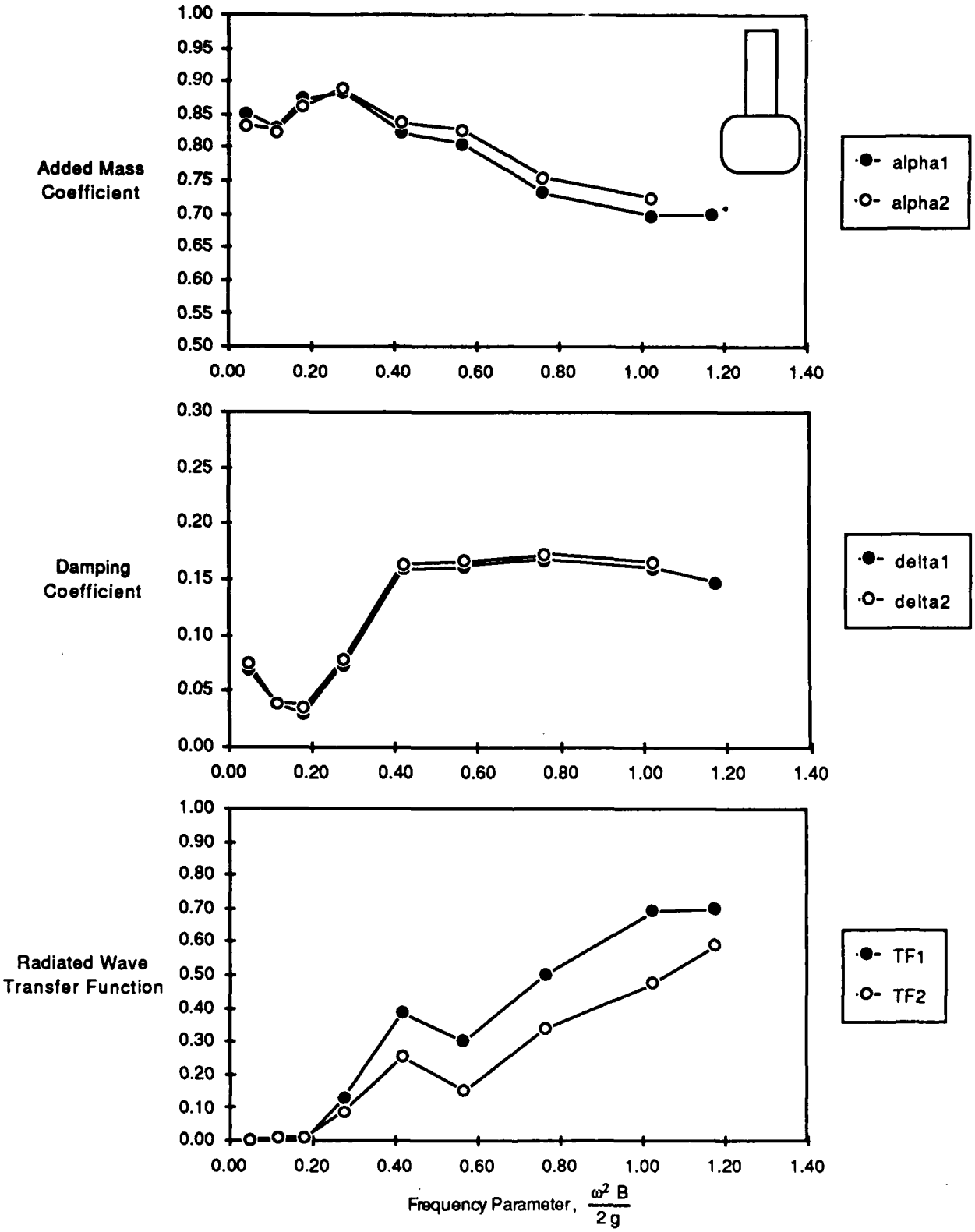

Fig. H1. Data for model H, radiused rectangle at design draft, for 0.5 inch (1.27 cm) oscillation amplitude.

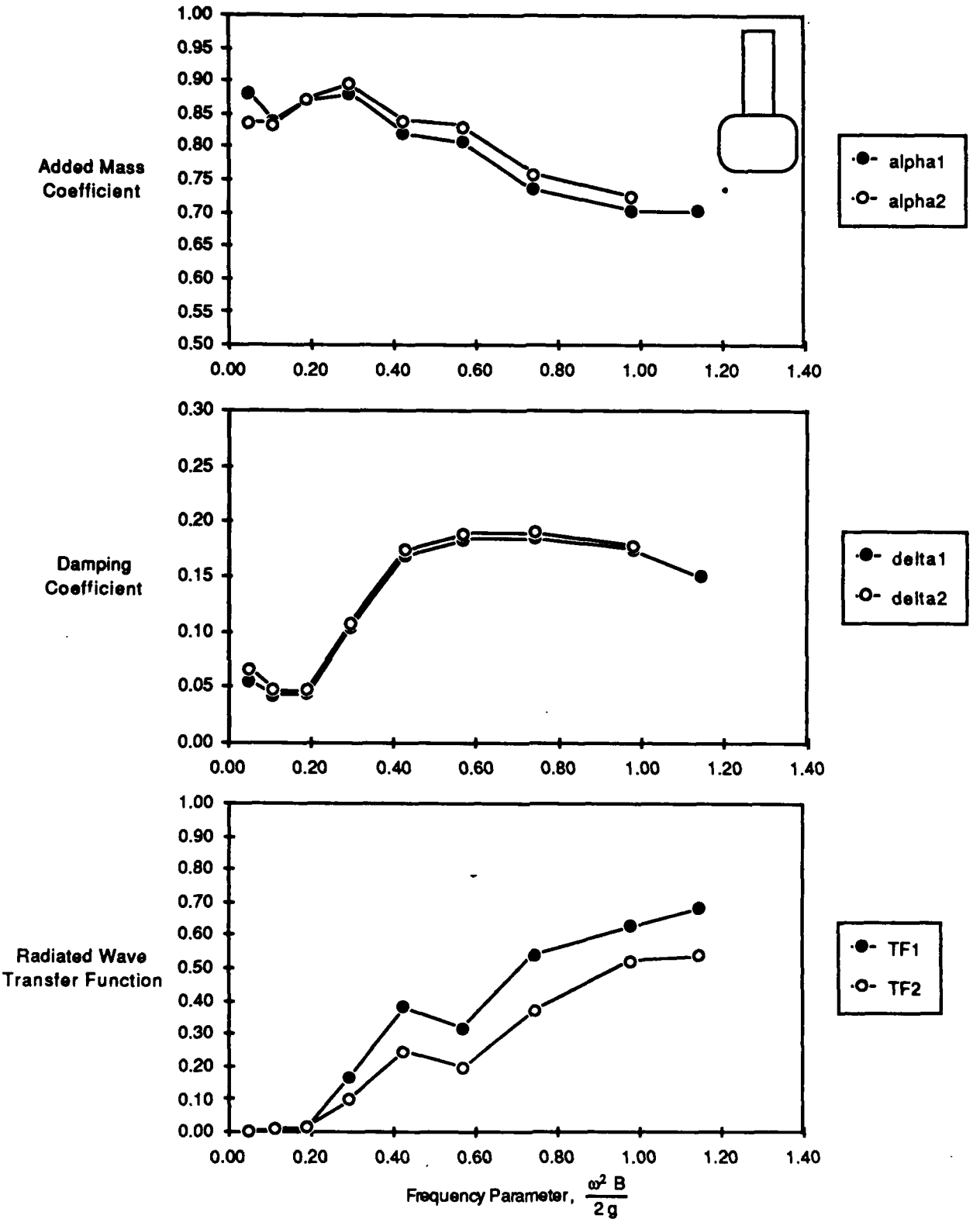

Fig. H2. Data for model H, radiused rectangle at design draft, for 1 inch (2.54 cm) oscillation amplitude.

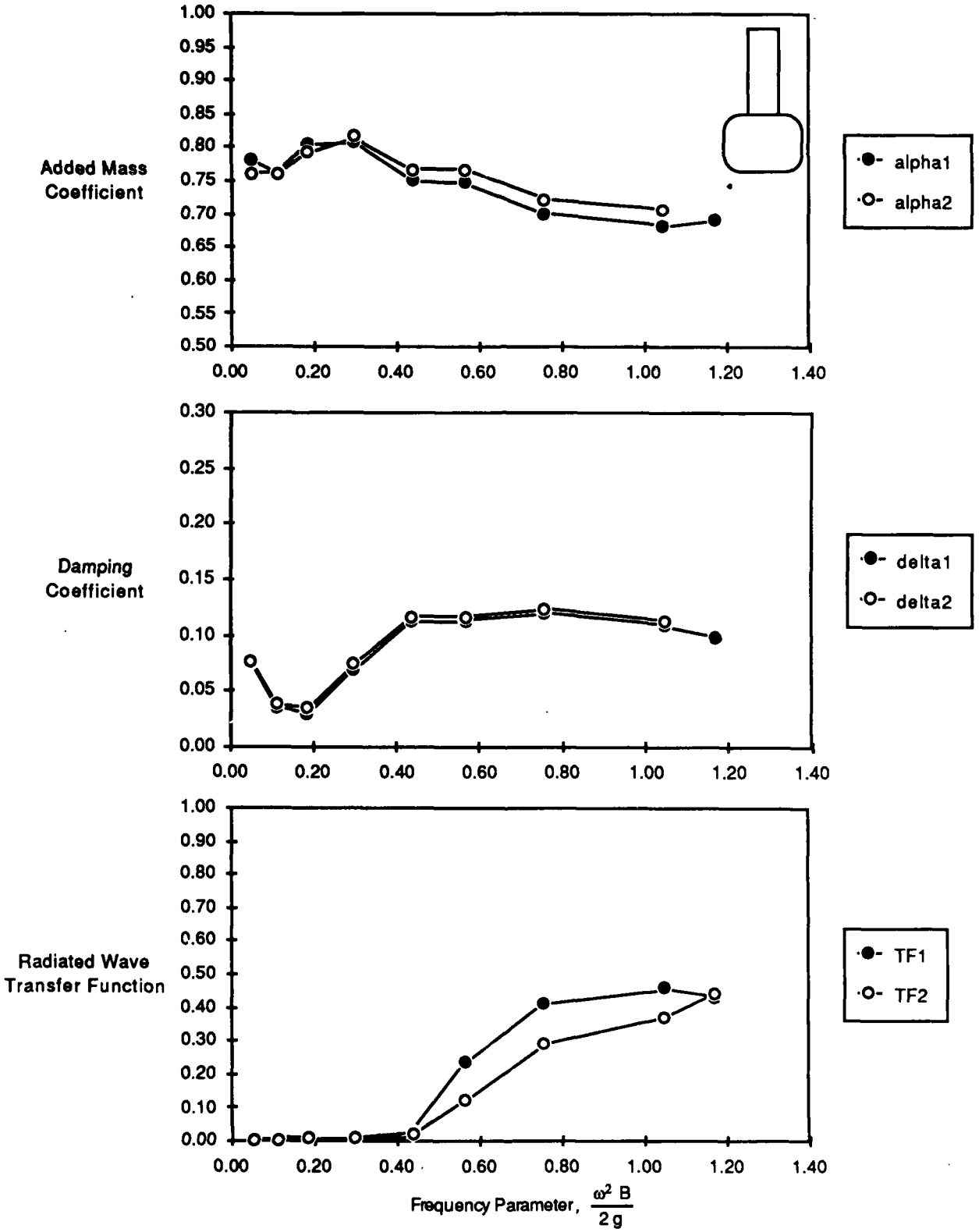

Fig. H3. Data for model H, radiused rectangle at deep draft, for 0.5 inch (1.27 cm) oscillation amplitude.

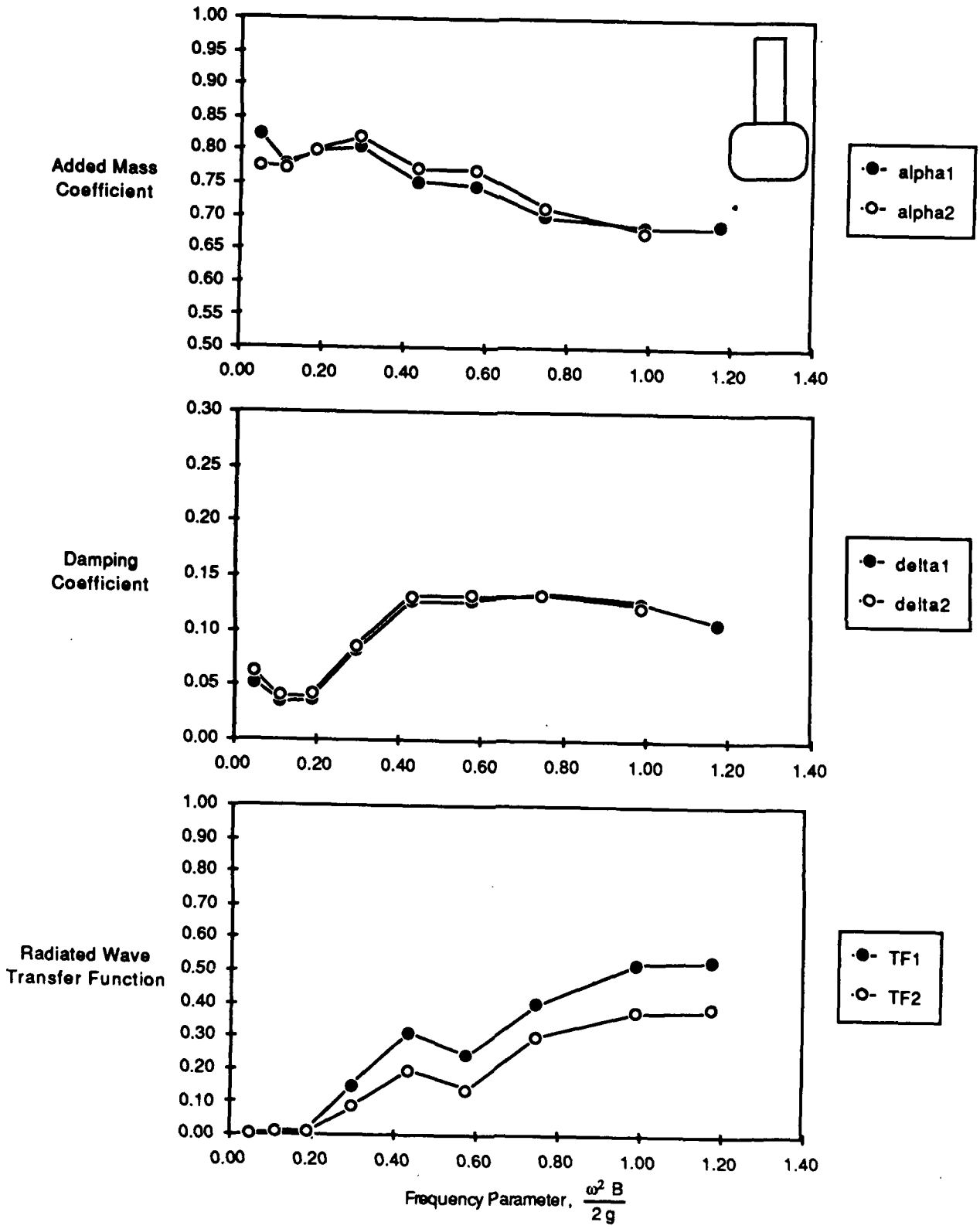

Fig. H4. Data for model H, radiused rectangle at deep draft, for 1 inch (2.54 cm) oscillation amplitude.

Table H1. Data for model H, radiused rectangle at design draft, for 0.5 inch (1.27 cm) oscillation amplitude.

Model Configuration :	H. Radiused Rectangle	
Model Displacement, (lbs.)	144.30	M = 4.49
Gage Wt. Z1, (lbs.)	149.06	M'1 = 4.64
Gage Wt. Z2, (lbs.)	138.91	M'2 = 4.32
Model Draft, (inches)	9.90	
C33, (lbs./ft)	95.98	

Run #	Frequency rad / sec model scale	kB/2	alpha1	delta1	alpha2	delta2
244	1.03	0.01	1.04	0.22	0.87	0.27
245	1.97	0.05	0.85	0.07	0.83	0.08
246	3.14	0.11	0.83	0.04	0.83	0.04
247	3.92	0.18	0.87	0.03	0.86	0.04
248	4.86	0.28	0.88	0.07	0.89	0.08
249	5.99	0.42	0.82	0.16	0.84	0.16
250	6.96	0.56	0.81	0.16	0.83	0.17
251	8.08	0.76	0.73	0.17	0.76	0.17
252	9.37	1.02	0.70	0.16	0.72	0.17
253	10.03	1.17	0.70	0.15	0.73	0.15
254	13.99	2.28	0.72	0.09		

Table H2. Data for model H, radiused rectangle at design draft, for 1 inch (2.54 cm) oscillation amplitude.

Model Configuration :	H. Radiused Rectangle	
Model Displacement, (lbs.)	144.30	M = 4.49
Gage Wt. Z1, (lbs.)	149.06	M'1 = 4.64
Gage Wt. Z2, (lbs.)	138.91	M'2 = 4.32
Model Draft, (inches)	9.90	
C33, (lbs./ft)	95.98	

Run #	Frequency rad / sec model scale	kB/2	alpha1	delta1	alpha2	delta2
255	0.99	0.01	1.22	0.14	0.90	0.18
256	2.04	0.05	0.88	0.06	0.84	0.07
257	3.05	0.11	0.84	0.04	0.83	0.05
258	4.03	0.19	0.87	0.04	0.87	0.05
259	5.01	0.29	0.88	0.10	0.90	0.11
260	6.04	0.43	0.82	0.17	0.84	0.17
261	6.98	0.57	0.81	0.18	0.83	0.19
262	7.98	0.74	0.74	0.18	0.76	0.19
263	9.17	0.98	0.70	0.17	0.72	0.18
264	9.90	1.14	0.70	0.15		
265	13.99	2.28	0.74	0.10		

Table H3. Data for model H, radiused rectangle at deep draft, for 0.5 inch (1.27 cm) oscillation amplitude.

Model Configuration :	H. Radiused Rectangle	
Model Displacement, (lbs.)	152.30	M = 4.74
Gage Wt. Z1, (lbs.)	156.84	M'1 = 4.88
Gage Wt. Z2, (lbs.)	146.69	M'2 = 4.56
Model Draft, (inches)	10.90	
C33, (lbs./ft)	95.98	

Run #	Frequency rad / sec model scale	kB/2	alpha1	delta1	alpha2	delta2
267	1.09	0.01	0.88	0.18	0.74	0.22
268	2.06	0.05	0.78	0.08	0.76	0.08
269	3.08	0.11	0.76	0.04	0.76	0.04
270	3.99	0.19	0.80	0.03	0.79	0.03
271	5.04	0.30	0.81	0.07	0.82	0.07
272	6.11	0.44	0.75	0.11	0.77	0.12
273	6.96	0.56	0.75	0.11	0.77	0.12
274	8.04	0.75	0.70	0.12	0.72	0.12
275	9.47	1.05	0.68	0.11	0.71	0.11
276	10.01	1.17	0.69	0.10	0.72	0.10
277	13.85	2.24	0.72	0.09		

Table H4. Data for model H, radiused rectangle at deep draft, for 1 inch (2.54 cm) oscillation amplitude.

Model Configuration :	H. Radiused Rectangle	
Model Displacement, (lbs.)	152.30	M = 4.74
Gage Wt. Z1, (lbs.)	156.84	M'1 = 4.88
Gage Wt. Z2, (lbs.)	146.69	M'2 = 4.56
Model Draft, (inches)	10.90	
C33, (lbs./ft)	95.98	

Run #	Frequency rad / sec model scale	kB/2	alpha1	delta1	alpha2	delta2
278	1.08	0.01	1.07	0.13	0.80	0.17
279	2.04	0.05	0.82	0.05	0.78	0.06
280	3.08	0.11	0.78	0.04	0.77	0.04
281	4.00	0.19	0.80	0.04	0.80	0.04
282	5.02	0.29	0.80	0.08	0.82	0.09
283	6.09	0.43	0.75	0.13	0.77	0.13
284	7.02	0.57	0.75	0.13	0.77	0.13
285	7.99	0.75	0.70	0.13	0.71	0.13
286	9.21	0.99	0.69	0.13	0.68	0.12
287	10.03	1.17	0.69	0.11		
288	14.01	2.29	0.73	0.10		

APPENDIX I

EXPERIMENTAL DATA FOR MODEL I

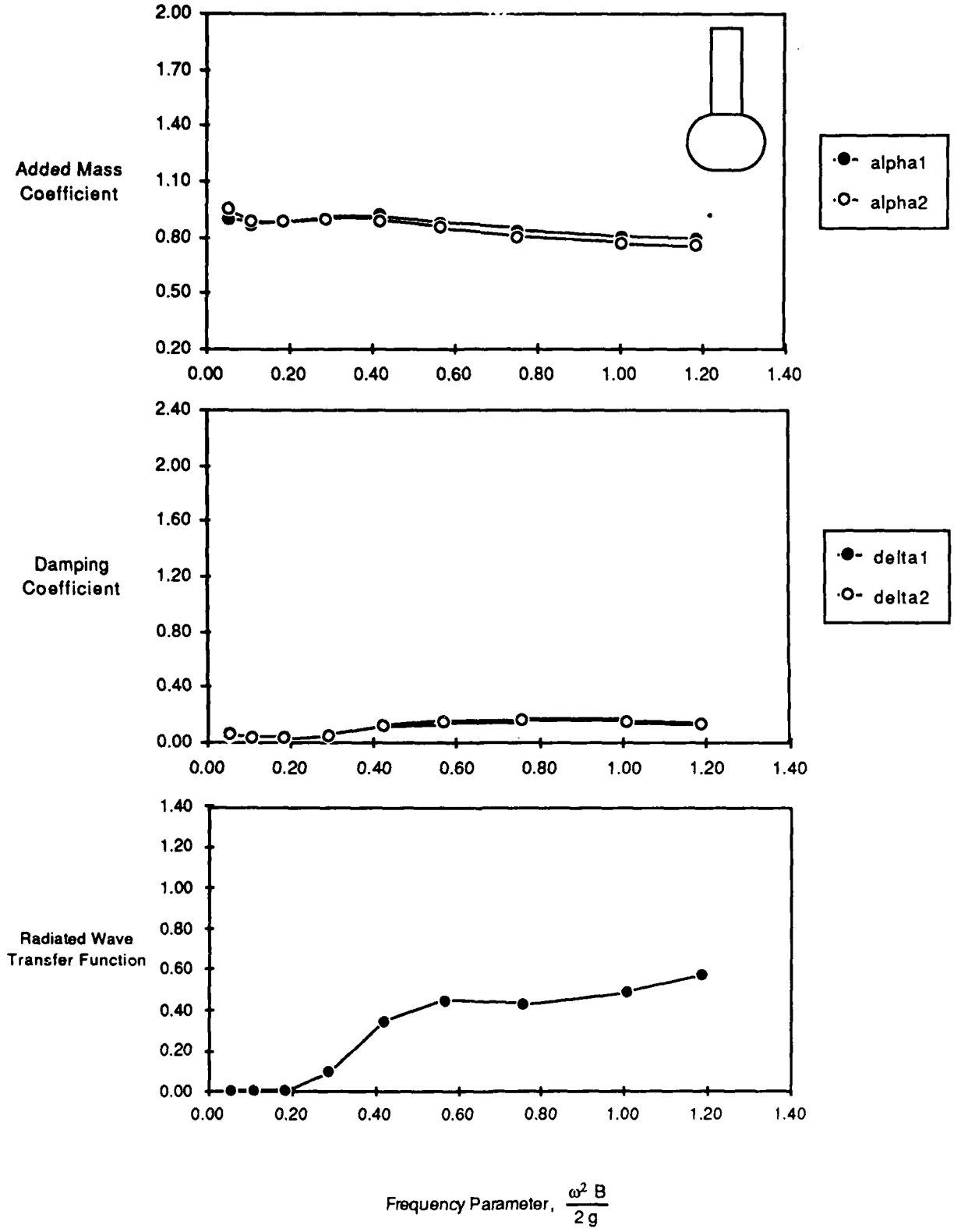

Fig. I1. Data for model I, 3-D single hull semi-circle at design draft, for 1 inch (2.54 cm) oscillation amplitude.

Table I1. Data for model I, 3-D single hull semi-circle at design draft, for 1 inch (2.54 cm) oscillation amplitude.

Model Configuration :	I. 3D Single Hull Semi-Circle	
Model Displacement, (lbs.)	171.23	M = 5.33
Gage Wt. Z1, (lbs.)	171.30	M'1 = 5.33
Gage Wt. Z2, (lbs.)	161.15	M'2 = 5.01
Model Draft, (inches)	9.90	
C33, (lbs./ft)	118.32	

Run #	Frequency rad / sec model scale	kB/2	alpha1	delta1	alpha2	delta2
609	2.11	0.05	0.90	0.05	0.95	0.06
610	3.03	0.11	0.87	0.04	0.89	0.04
611	3.97	0.18	0.88	0.03	0.89	0.03
612	4.97	0.29	0.91	0.06	0.90	0.06
613	6.01	0.42	0.92	0.13	0.89	0.12
614	6.97	0.57	0.88	0.16	0.85	0.15
615	8.04	0.75	0.84	0.17	0.81	0.16
616	9.29	1.01	0.81	0.16	0.77	0.15
617	10.08	1.19	0.79	0.14	0.75	0.13

APPENDIX J

EXPERIMENTAL DATA FOR MODEL J

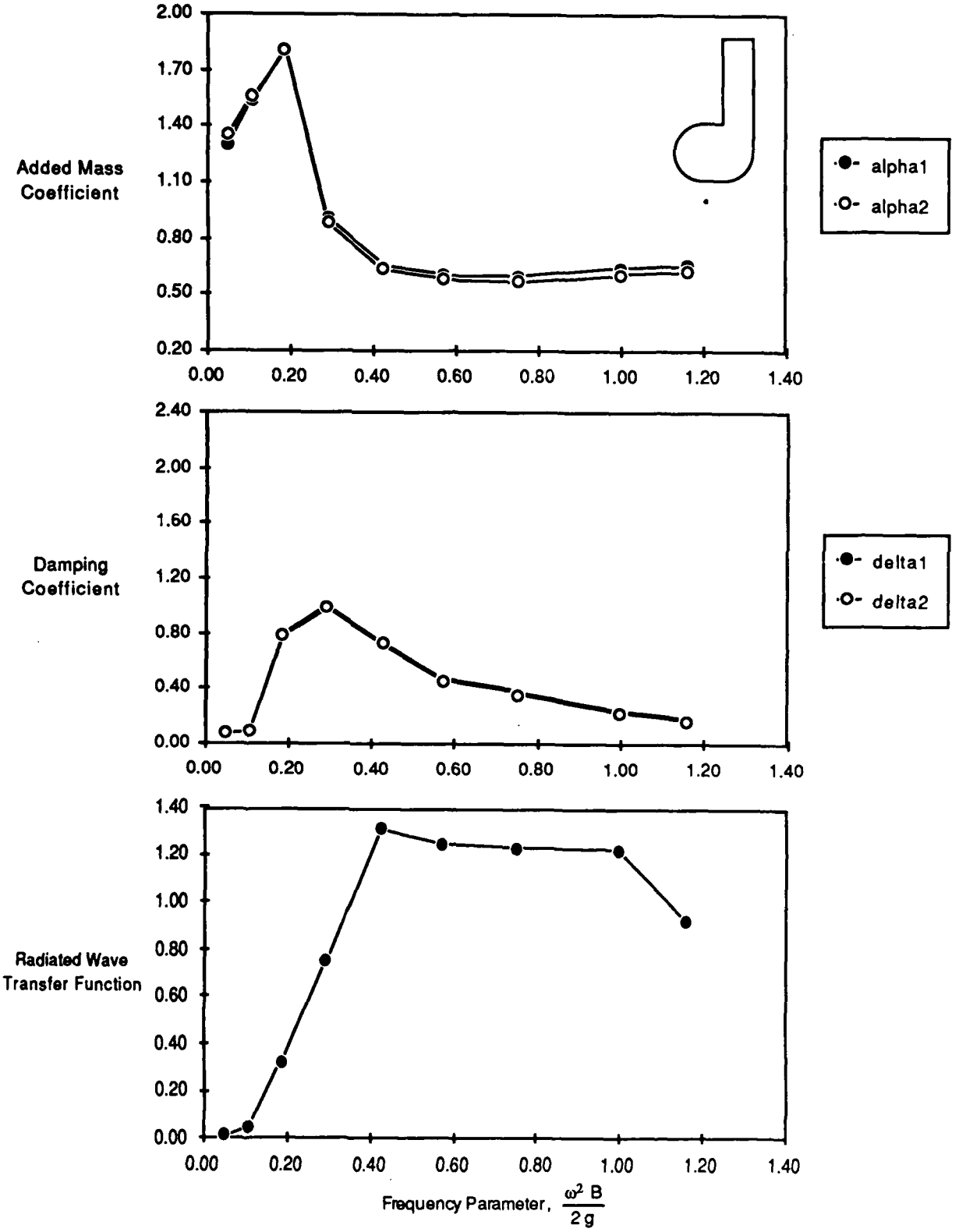

Fig. J1. Data for model J, 3-D single hull golf club at design draft, for 1 inch (2.54 cm) oscillation amplitude.

Table J1. Data for model J, 3-D single hull golf club at design draft, for 1 inch (2.54 cm) oscillation amplitude.

Model Configuration :	J. Single Hull Golf Club	
Model Displacement, (lbs.)	178.27	M = 5.54
Gage Wt. Z1, (lbs.)	178.26	M'1 = 5.54
Gage Wt. Z2, (lbs.)	168.11	M'2 = 5.23
Model Draft, (inches)	9.90	
C33, (lbs./ft)	116.12	

Run #	Frequency rad / sec model scale	kB/2	alpha1	delta1	alpha2	delta2
624	2.06	0.05	1.30	0.07	1.36	0.08
625	3.03	0.11	1.54	0.10	1.56	0.10
626	3.99	0.19	1.82	0.79	1.81	0.79
627	5.00	0.29	0.91	1.01	0.89	0.99
628	6.02	0.42	0.65	0.74	0.63	0.72
629	7.00	0.57	0.61	0.48	0.58	0.46
630	8.03	0.75	0.60	0.38	0.57	0.36
631	9.25	1.00	0.64	0.24	0.61	0.23
632	9.97	1.16	0.66	0.18	0.63	0.17

APPENDIX K

EXPERIMENTAL DATA FOR MODEL K

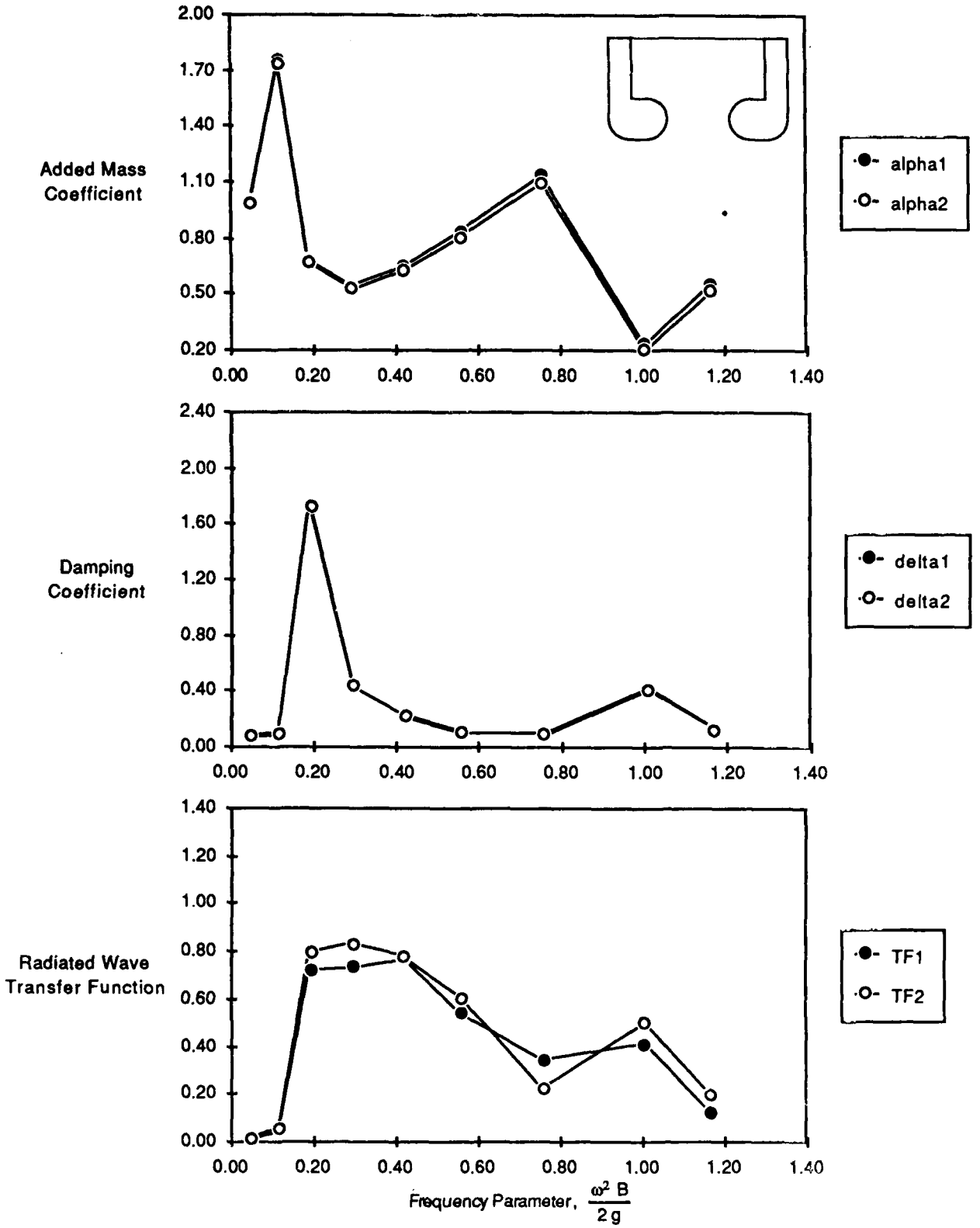

Fig. K1. Data for model K, 3-D twin hull golf club at design draft, for 0.5 inch (1.27 cm) oscillation amplitude.

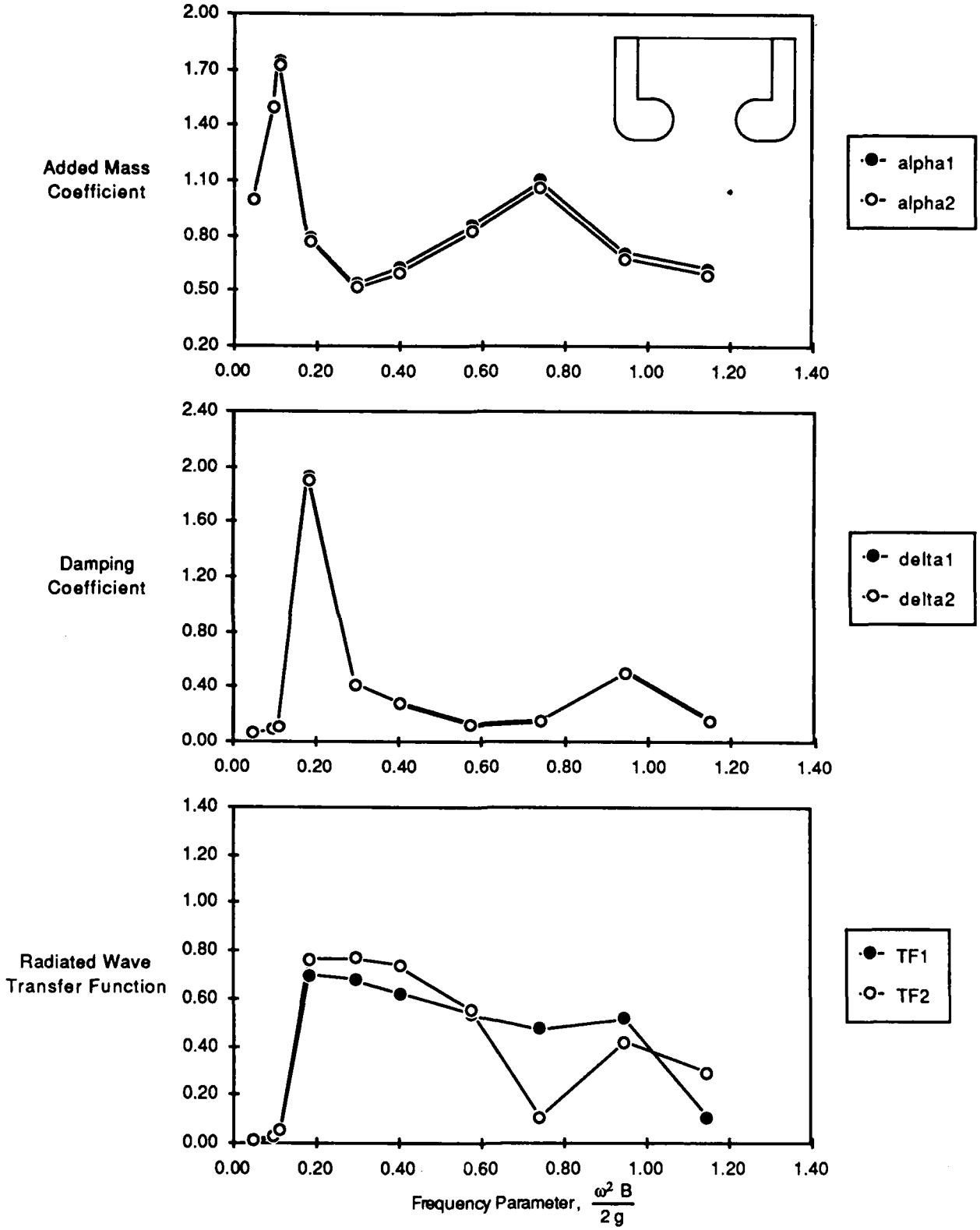

Fig. K2. Data for model K, 3-D twin hull golf club at design draft, for 1 inch (2.54 cm) oscillation amplitude.

Table K1. Data for model K, 3-D twin hull golf club at design draft, for 0.5 inch (1.27 cm) oscillation amplitude.

Model Configuration :	K. Twin Golf Club	
Model Displacement, (lbs.)	361.24	M = 11.23
Gage Wt. Z1, (lbs.)	352.47	M'1 = 10.96
Gage Wt. Z2, (lbs.)	347.43	M'2 = 10.80
Model Draft, (inches)	9.90	
C33, (lbs./ft)	211.71	

Run #	Frequency rad / sec model scale	kB/2	alpha1	delta1	alpha2	delta2
571	1.07	0.01	-0.04	0.24	0.01	0.25
572	1.98	0.05	1.00	0.08	0.98	0.08
573	3.14	0.11	1.75	0.10	1.74	0.10
574	4.05	0.19	0.68	1.74	0.67	1.73
575	5.02	0.29	0.54	0.44	0.53	0.43
576	5.99	0.42	0.65	0.23	0.63	0.22
577	6.92	0.56	0.84	0.11	0.81	0.10
578	8.06	0.76	1.13	0.10	1.09	0.10
579	9.29	1.01	0.23	0.43	0.21	0.42
580	10.00	1.17	0.55	0.14	0.52	0.13
581	14.21	2.35	1.00	0.11	0.96	0.10

Table K2. Data for model K, 3-D twin hull golf club at design draft, for 1 inch (2.54 cm) oscillation amplitude.

Model Configuration :	K. Twin Golf Club	
Model Displacement, (lbs.)	361.24	M = 11.23
Gage Wt. Z1, (lbs.)	352.47	M'1 = 10.96
Gage Wt. Z2, (lbs.)	347.43	M'2 = 10.80
Model Draft, (inches)	9.90	
C33, (lbs./ft)	211.71	

Run #	Frequency rad / sec model scale	kB/2	alpha1	delta1	alpha2	delta2
558	1.24	0.02	0.24	0.14	0.37	0.14
559	1.99	0.05	0.99	0.06	1.00	0.07
560	2.88	0.10	1.51	0.10	1.50	0.10
561	3.08	0.11	1.74	0.11	1.73	0.11
562	3.96	0.18	0.79	1.93	0.77	1.90
563	5.03	0.29	0.54	0.42	0.52	0.42
564	5.87	0.40	0.63	0.28	0.60	0.28
565	7.01	0.57	0.86	0.13	0.82	0.12
566	7.97	0.74	1.10	0.17	1.06	0.16
567	9.01	0.95	0.71	0.52	0.67	0.51
568	9.91	1.15	0.62	0.17	0.58	0.16

APPENDIX L

EXPERIMENTAL DATA FOR MODEL L

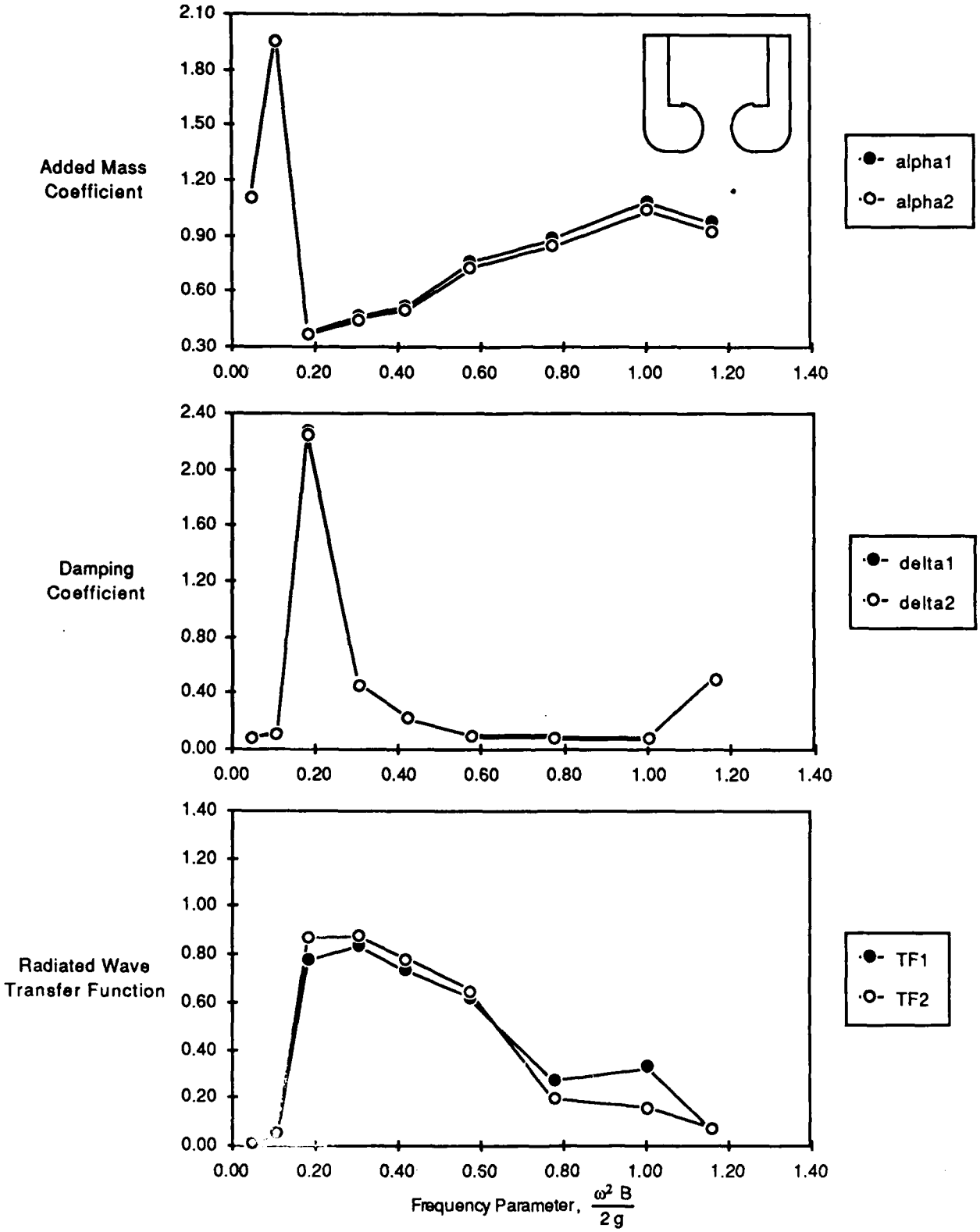

Fig. L1. Data for model L, 3-D narrow spaced twin hull golf club at design draft, for 0.5 inch (1.27 cm) oscillation amplitude.

Table L1. Data for model L, 3-D narrow spaced twin hull golf club at design draft, for 0.5 inch (1.27 cm) oscillation amplitude.

Model Configuration :	L. Twin Golf Club,narrow spaced	
Model Displacement, (lbs.)	361.24	M = 11.23
Gage Wt. Z1, (lbs.)	352.47	M'1 = 10.96
Gage Wt. Z2, (lbs.)	347.43	M'2 = 10.80
Model Draft, (inches)	9.90	
C33, (lbs./ft)	211.71	

Run #	Frequency rad / sec model scale	kB/2	alpha1	delta1	alpha2	delta2
583	1.09	0.01	0.01	0.20	0.07	0.22
584	1.98	0.05	1.11	0.08	1.10	0.09
585	3.04	0.11	1.96	0.11	1.95	0.11
586	3.96	0.18	0.38	2.27	0.37	2.25
587	5.12	0.31	0.46	0.46	0.45	0.46
588	6.00	0.42	0.52	0.22	0.50	0.22
589	7.01	0.57	0.76	0.10	0.72	0.09
590	8.16	0.78	0.89	0.09	0.85	0.08
591	9.27	1.00	1.08	0.09	1.04	0.08
592	9.97	1.16	0.97	0.52	0.93	0.50
593	13.95	2.27	0.99	0.10	0.95	0.09